BIELEFELDER ÖKOLOGISCHE BEITRÄGE

Beiträge zur Ökologie und
Geobotanik
und zu
Natur- und Umweltschutz

BAND 8 (1995)

Beiträge aus dem workshop "Structure and function on all levels" (from the molecular to the ecosystems level)

Abteilung Ökologie/Department Ecology
Universität Bielefeld

Herausgegeben von Breckle, S.-W. und Waisel, Y.

Bielefelder Ökologische Beiträge (BÖB) Band 8 (1995)

Nachdruck 2018

Herausgegeben von der
Abteilung Ökologie
Fakultät für Biologie
Universität Bielefeld
Postfach 8640
D-4800 Bielefeld 1

ISSN 0178-0698

BIELEFELDER ÖKOLOGISCHE BEITRÄGE

Beiträge zur Ökologie und
Geobotanik
und zu
Natur- und Umweltschutz

BAND 8 (1995)

Beiträge aus dem workshop "Structure and function on all levels" (from the molecular to the ecosystems level)

Referat-Beiträge im Rahmen der Deutsch-Israelischen Begegnung zwischen der George Wise Life Science Faculty / Tel Aviv und der Fakultät für Biologie / Univ. Bielefeld im Rahmen der Universitäts-Partnerschaft im April 1994 in Tel Aviv.

Contributions from the workshop held in April 1994 at George Wise Life Science Faculty / Tel Aviv within the German-Israeli-Cooperation between the Universities of Tel Aviv and Bielefeld

Abteilung Ökologie/Department Ecology
Universität Bielefeld

Herausgegeben von Breckle, S.-W. und Waisel, Y.

ISSN 0178-0698

Bielefelder Ökol. Beitr. 8 (1995)

Content / Inhaltsübersicht

Beiträge aus dem workshop "Structure and functions on all levels – from the molecular to the ecosystems level" (Hg.: Breckle, S.-W. & Waisel, Y.) 111pp., April 1994, Tel Aviv

Übersicht über die Beiträge / Contents
[in brackets: only orally delivered papers, no manuscripts available, not included in BÖB 8]

Bielefelder Ökologische Beiträge, vol. 8, (1995) p. 3 -

ALTERNATIVE MECHANISMS OF HEAT SHOCK RESPONSE IN GRAM NEGATIVE BACTERIA

Gil Segal and Eliora Z. Ron
Department of Molecular Microbiology and Biotechnology
Tel-Aviv University, Tel-Aviv, ISRAEL.

The heat shock response is a widespread phenomenon that involves the induction of a large number of proteins following stress conditions, such as a shift to high temperature. In *Escherichia coli*, the heat shock response is mediated by a positive regulator protein - σ32 - that recognizes specific promoter sequences, different from the σ70 promotes. The cellular level of σ32 is increased following heat shock, resulting in the preferential transcription of heat shock genes several of which code for chaperons (*groES, groEL, dnaK, grpE*) and σ70 - the vegetative sigma factor.

We were interested in studying the heat shock response of *Agrobacterium tumefaciens* , a gram negative bacterium that infects plants and brings about the formation of tumors ("crown gall"). Although phylogenetically close to *E. coli*, both are members of the purple bacteria, and although its factor σ70 showed a high degree of homology to that of *E. coli*, there was no evidence for the existence of factor σ32. In order to find out if there was a heat shock response in *A. tumefaciens* and characterize it we started by looking at transcriptional activation of the *groE* operon. The results indicated that the heat shock response in this bacterium appears to be different from that of *E . coli* in several aspects.

Northern analysis results indicated that transcription is significantly induced by heat shock. However, in contrast to the situation in the σ32-mediated heat shock transcription that starts from a special heat shock promoter, the heat shock transcription of *A. tumefaciens* starts from the same promoter at 25 C and at 42 C. This result was obtained by primer-extension analysis, to locate the 5'-end of the mRNA, and showed identical transcripts in the two temperatures. Sequence analysis indicated that the upstream region of the *groE* operon contains an inverted repeat, at the starting site of transcription. It was interesting to find that this inverted repeat is conserved in microbial evolution, and was found upstream of heat shock genes of gram positive bacteria and cyanobacteria. The data suggest that there is an additional mechanism for heat shock response in bacteria - one that recognizes the stem loop structure and may function instead of, or in addition to, the σ32-mediated control system. Moreover, the inverted repeat was found in all the bacterial groups except for the γ–purple bacteria, the group that includes *E. coli*.

THE USE OF GENE DISRUPTION FOR EVALUATION OF PLANT GROWTH REGULATORS ROLE IN GALL FORMATION BY *Erwinia herbicola*

I. Barash[1], A. Lichter[1], Y. Gafni[2] and S. Manulis[2]

[1]Dept. of Botany, Tel Aviv University and [2]ARO, The Volcani Center

Erwinia herbicola is widespread in nature as an epiphytic-saphrophytic bacterium. However, certain strains of *E. herbicola* have evolved to become a potent pathogen of gypsophila and induce gall formation at wound site particularly at the crown region of the stem. Gypsophila (*Gypsophila paniculata* L.) also known as "baby's breath" is an ornamental used in commercial cut-flower production in Israel, Europe and the U.S.A. The basic question that we are concerned with is what are the genes which are responsible for the transformation of this epiphytic bacterium into a pathogen and how they operate. Since gall formation in plants is known to develop by an excessive secretion of the phytohormons indole-3-acetic acid (IAA) and cytokinins by the pathogens (7), the hormon-encoding genes have been initially characterized.

Our working hyposthesis was that similar to *Pseudomonas syringae* pv. *savastanoi*, the gall-forming pathogen of olive and oleander (2), the genes for IAA and cytokinins are present in pathogenic but not in non-pathogenic strains. However, when production of IAA in culture was examined, no difference could be detected between pathogenic and non-pathogenic strains of *E. herbicola* and both produced excessive amount of IAA either in rich medium or in minimal medium supplemented with tryptophan (5). These results lead us to investigate the biosynthetic pathways of IAA in *E. herbicola*. It was found that pathogenic strains possess 2 routes for IAA biosynthesis from tryptophan (Fig.1): a) the indolephyruvate pathway and b) the indoleacetamide pathway (6). However, in contrast to the indolepyruvate pathway which was present in all pathogenic and non-pathogenic strains, the indoleacetamide pathway was exclusively present in pathogenic strains. These results lead us to assume that the indole-3-acetamide

pathway may have a role in pathogenicity and its contribution to gall formation has been investigated by its inactivation through gene disruption.

A 7.5 kb *Eco*RI fragment which hybridized to a DNA probe harboring the IAA operon of P. *syringae* pv. *savastanoi* was subcloned from lambda (EMBL3) library of plasmid from a pathogenic strain of *E. herbicola* (1). This 7.5 Kb *Eco*RI DNA fragment was cloned into pUC118 in both orientations to generate pEG101 and pEG102. *Escherichia* coli DH5α cells transformed with either pEG101 or pEG102 produced IAA when cultured in medium supplemented with L-tryptophan. Permealized transformed cells also directed the synthesis of IAA from indole-3-acetamide. The IAA biosynthetic capacity was localized to a 4kb *Hind*III-*Eco*RI fragment through subcloning and insertional inactivation. The IAA biosynthetic genes of *E.h.* pv. *gypsophilae* were designated as *iaa*M and *iaa*H because of their structural and functional similarity to *iaa*M and *iaa*H of *P. syringae* pv. *savastanoi* which encode tryptophan-2-monooxygenase and indoleacetamide hydrolase, respectively (1).

Insertional mutations were generated in *E.h.* pv. *gypsophilae iaa*M and *iaa*H. Marker exchange mutants of *E.h. gypsophilae*, generated using insertional inactivated constructs, produced the same amount of IAA in culture as the wild type. The marker-exchange mutants which exhibited either reduction or elimination of *iaa*H activity, induced smaller galls than the unmodified *E.h.* pv. *gypsophilae* (1). Results obtained suggest that, as in other gall-forming pathogens, *iaa*M and *iaa*H may be required for virulence in *E.h.* pv. *gypsophilae*. However, while expression of iaaH contributes to virulence, insertional inactivation does not severely attenuate virulence in a manner analogous to that observed in other pathogens (7).

In contrast to IAA, cytokinins production was in accordance to our working hypothesis. Thus analysis of cytokinins produced in culture by *E. herbicola* pv. *gypsophilae* indicated that pathogenic but not non-pathogenic strains secreted a significant amount of cytokinins (3). Chemical identification of cytokinins was performed by immunoaffinity chromatography followed by HPLC and GC-MS. The cytokinins were quantified by either radioimmunoassay (RIA) or ELISA using anti-cytokinin monoclonal antibodies. Zeatin, zeatin riboside, iso-pentenyladenine and two immunoreactive zeatin-type compounds were the predominant cytokinins identified in the supernatant.

A cytokinin biosynthetic gene was cloned from a cosmid library derived from plasmids of a pathogenic strain (Eh824-1). Expression was achieved following mobilization of the cosmid clones into either the non-pathogenic strain (Eh3-1) or the deletion non-pathogenic mutant (Eh3-106) but not in *E. coli*. Eh3-106 contained a deletion in the pathogenicity associated plasmid and lacked cytokinin production. A 3.9kb *Sma*I DNA fragment from a cosmid clone pLA150 was subcloned into a wide host range plasmid (pCPP50) to yield pCPP3.9 (3). This plasmid could restore production of all previously detected cytokinins following its mobilization into the deletion mutant (Eh 3-106). This 3.9 kb *Sma*I DNA fragment overlapped with the 3' end of the IAA biosynthetic operon previously cloned from this plasmid, demonstrating that IAA and the cytokinin biosynthetic genes are clustered on the pathogenicity-associated plasmid (Fig. 2).

The cloned cytokinin biosynthetic gene encoding the enzyme iso-pentenyl transferase designated as *etz* (4). Comparative analysis of deduced amino acid of *etz* with all known cytokinin biosynthetic genes indicated a maximal homology of 40.3% with the *tzs* gene of *Pseudomonas solanacearum*. The *etz* gene was preceded by another ORF designated as *Pre-etz*. It was composed of 170 amino acids and the 2 genes may constitute an operon. Insertional inactivation of the *etz* eliminated cytokinin production and substantially reduced the gall size. Insertional inactivation or a frame shift mutation within the pre-*etz* markedly reduced cytokinin production but the virulence was only slightly reduced. Complementation *in trans* of the defective *etz* gene with a construct containing an intact *etz* in the multicopy plasmid pCPP50 (i.e. PCPP3.9) resulted in restoration and over-expression of cytokinin production. It increased gall size and altered gall morphology. Results obtained indicate that cytokinins produced by *E.h.* pv. *gypsophilae* affect gall size but are not mandatory for gall formation.

Northern hybridization studies with DNA probes constructed from *etz* and pre-etz demonstrated a common transcript which fits the size of the 2 genes. The latter result suggests that the 2 genes constitute an operon. An additional transcript of 1.0 kb could be detected only with the *etz* probe. The latter finding indicates that the *etz* can also be independently transcribed. Insertional inactivation of the pre-*etz* markedly reduced the transcription of both *etz* and pre-*etz* suggesting

a regulatory role for the pre-*etz*. The ratio between the 2 transcripts was dependent on the growth phase of the bacterium.

Further identification of pathogenicity genes was carried out with the Tn3-Spice reporter system. Cosmid clones of the pPATH were subjected to saturation mutagenesis by the latter system. Two regions with clustered mutants which eliminated pathogenicity have already been identified (Fig.2). These mutants were restored to pathogenicity by complementation.

Bibliography

1. Clark, E., Manulis` S., Ophir, Y., Barash, I. and Gafni, Y. 1993. Cloning and characterization of *iaa*M and *iaa*H from *Erwinia herbicola* pv. *gypsophilae*. Phytopathology 83: 234-240.

2. Comai, L. and Kosuge, T. 1982. Cloning and characterization of iaaM, a virulence determinant of *Pseudomonas savastonoi*. J. Bacteriol. 149: 40-46.

3. Lichter, A., Manulis, S., Sagee, O. Gafni, Y., Gray, J., Meilan, R., Morris, R., Barash, I. 1994. Production of cytokinins by *Erwinia herbicola* pv. *gypsophilae* and isolation of a genetic locus specifying cytokinin biosynthesis. Molecular Plant Microbe Interactions (accepted for publication).

4. Lichter, A., Barash, I., Valinsky, L. and Manulis, S. 1994. Characterization of genes involved in cytokinin biosynthesis in *Erwinia herbicola* pv. *gypsophilae* and their relation to pathogenicity (In preparation).

5. Manulis, S., Gafni, Y., Clark, E., Zutra, D., Ophir, Y. and Barash, 1991. Identification of a plasmid DNA probe for detection of strains of *Erwinia herbicola* pathogenic on *Bypsophila paniculata*. Phytopathology 81: 54-57.

6. Manulis, S., Valinsky, L., Gafni, Y. Hershenhorn, J. and Barash, I. 1991. Indole-3-acetic acid biosynthetic pathways in *Erwinia herbicola* in relation to pathogenicity on *Gypsophila paniculata*. Physiol. Mol. Plant Pathol. 39: 161-171.

7. Morris, R. 1986. Genes specifying auxin and cytokinin biosynthesis in phytopathogens. Annu. Rev. Plant Physiol. 37: 509-538.

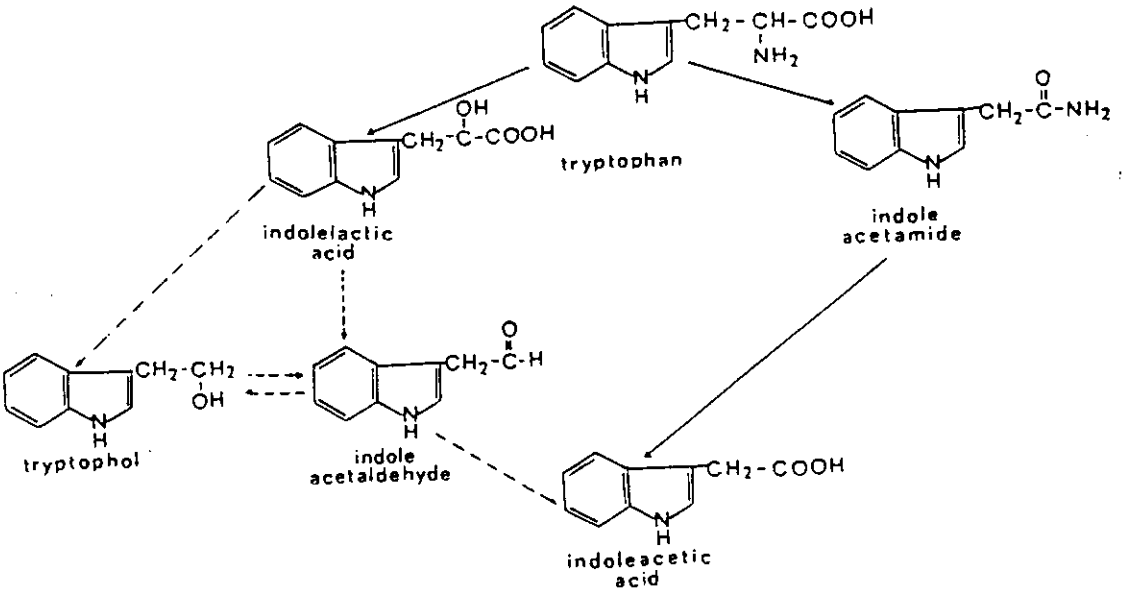

Fig.1. Biosynthetic pathways of indole-3-acetic acid (IAA) from tryptophan

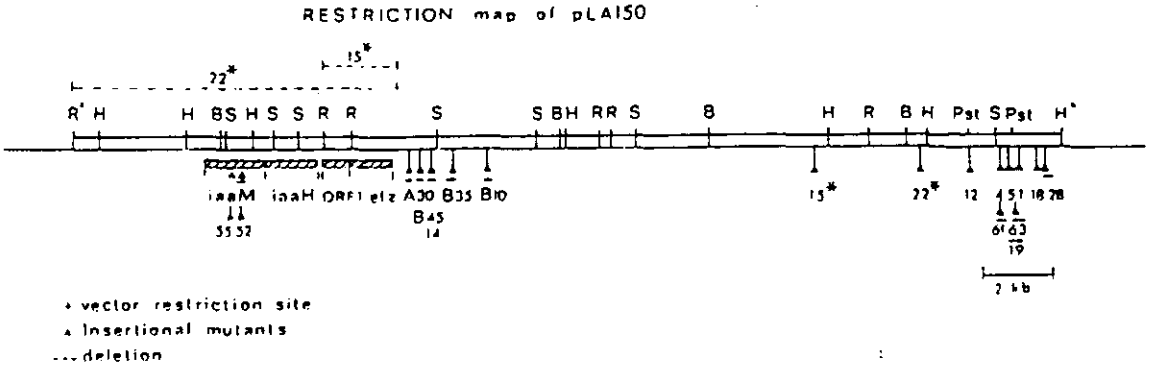

Fig.2. pLA 150 is a cosmid clone of pPATH obtained from a cosmid library of plasmids from the pathogenic strain E.h. pv. gypsophilae (Eh 824-1). The library was constructed in pLAFR3. This clone contains a cluster of 2 operons, for IAA (iaaM and iaaH) and cytokinin (ORF1 = pre-etz and etz) biosyntehesis . A transposase (not shown) was identified immedified immediately downstream to the etz. Two clusters of insertional non-pathogenic mutants were obtained by Tn3-Spice.

Mutants Eh15 and Eh22 are deletion non-pathogenic mutants which were obtained by insertions of 15^{*} and 22^{*}.

AGE-RELATED ANEUPLOIDY, SPINDLE STRUCTURE AND FORMATION AND CELL CYCLE CONTROL IN MAMMALIAN OOCYTES

U. Eichenlaub-Ritter

Univ. Bielefeld, Fakultät für Biologie IX, Gentechnologie/Mikrobiologie, 33501 Bielefeld, FRG.

INTRODUCTION

Among mammals, humans appear to have the highest rate of meiotic aneuploidy. Thus it is estimated that 18-19% of all oocytes and 3-4% of sperm have numerical chromosomal aberrations (reviewed in Eichenlaub-Ritter, 1994). The most important risk factor for nondisjunction in female meiosis is maternal age. Combined data from prenatal diagnosis, aborted embryos, stillbirths and liveborn offspring indicate that up to 60% of all oocytes are aneuploid near the end of the reproductive span in the human female (Hassold and Jacobs, 1984). Tracing of the origin of extra chromosomes in trisomies imply that chromosome malsegregation predominantly occurs during first meiotic division (reviewed in: Eichenlaub-Ritter, 1994). Mechanisms leading to nondisjunction at the cellular level are still unknown. It has been suggested that structural and functional alterations in either chromosome configuration or the oocyte spindle are responsible for the loss of fidelity in chromosome segregation with advanced maternal age (e.g. Gaulden, 1992). Thus, reduced recombination during early oogenesis and absence of chiasmata in maturing oocytes could result in the presence of randomly segregating univalents (Henderson and Edwards, 1968). Adverse influences from the environment, during the long period an oocyte rests in the ovary before resumption of maturation (in the human decades), could affect the oocyte physiological state such that no functional spindle apparatus can be formed, and homologues cannot correctly orient or migrate to opposite spindle poles during anaphase I. Besides, hormonal imbalance in an aged female associated with alterations in the pH of the follicular fluid, elevated temperature, reduced oxygen supply or other adverse conditions might affect spindle formation (reviewed by: Gaulden, 1992).

RESULTS OF OUR STUDIES

After isolation from the follicle and removal of adhering follicle cells mouse oocytes sponaneously resume maturation when cultured under appropriate conditions. We used such *in vitro* maturing oocytes of the CBA mouse as a model to directly monitor spindle structure and

formation, chromosome behaviour, cell cycle progression and chromosome configuration of the oocyte to elucidate the mechanisms of maternal age-related as well as drug-induced aneuploidy in meiosis I of mammals (Eichenlaub-Ritter et al., 1988). Previous studies have indicated that this strain of mice exhibits moderate increases in aneuploidy of oocytes/embryos with advanced age of the female although the effect is much less pronounced in this species compared to the human (Brook et al., 1984).

Initially we did not observe differences in spindle structure between maturing oocytes from young or aged female mice when they were processed for indirect antitubulin immunofluorescence after defined times of *in vitro* maturation (Eichenlaub-Ritter et al., 1988). Bivalents appeared normally aligned at the spindle equator at metaphase I. Homologues segregated sequentially in both age groups during first anaphase. However, oocytes from aged females progressed faster through first meiosis compared to those of young females although they were cultured under identical conditions (Eichenlaub-Ritter and Boll, 1989). This was correlated with elevated levels of numerical chromosomal aberrations as evident from spread, C-banded chromosome preparations of the *in vitro* matured, metaphase II-arrested oocytes of both age groups. Since the difference in aneuploidy levels between age groups was evident even after *in vitro* culture, disturbances in the milieu of the oocyte during the final stages of maturation *in vivo* such as elevated pH, high temperature or reduced oxygen supply do not appear responsible for the increases in nondisjunction. The high risk for chromosome malsegregation rather seems an intrinsic feature of "aged" oocytes and must be based on the condition of oocytes prior to resumption of maturation.

Treatment of prometaphase I oocytes for 1h with nocodazole, a microtubule-depolymerizing agent, induced rises in aneuploidy in oocytes of young and aged females as expected from an anti-mitotic drug (Eichenlaub-Ritter and Boll, 1989). However, this brief treatment also eliminated the age-related differences in cell cycle progression and, in addition, those in aneuploidy levels. From these observations we deduced that oocytes of aged females are not particularly sensitive to disturbances in spindle formation, as might be expected when their spindle is already more fragile due to age-related, environmentally-induced damage to the cell. Rather they appear progammed to undergo first meiosis with altered kinetics. Concomitant with the loss of control of cell cycle progression chromosome segregation becomes disturbed (Eichenlaub-Ritter and Boll, 1989; Eichenlaub-Ritter and Sobek-Klocke, 1993).

That alterations in maturation kinetics can induce chromosome malsegregation without visibly affecting spindle structure became evi-

dent from experiments in which oocytes of both age groups were transiently blocked in dictyate stage by drugs i) affecting the expression of genes whose products are potentially cell cycle regulating, and ii) inducing alterations in the phosphorylation of proteins (Eichenlaub-Ritter, 1993; Eichenlaub-Ritter & Sobek-Klocke, 1993). After release from such a block with a tumor promoting phorbol ester, oocytes from aged females progressed with a phenotypically similar pattern through first meiosis as untreated oocytes from aged females. Concomittantly they showed similar levels of nondisjunction. In addition, when oocytes from aged females were subjected to the same treatment, there was no additional rise in aneuploidy as compared to controls of the same age group When oocytes from young mice were simultaneously exposed to the tumor promoter and retinoic acid, the alterations in cell cycle progression were less pronounced compared to treatment with the phorbol ester alone. This resulted in decreased levels of aneuploidy (Eichenlaub-Ritter, 1993). Therefore, these observations together with those from the nocodazole experiments indicate that the loss of control of cell cycle progression is responsible for the high risk for aneuploidy.

Recently other groups have obtained evidence that extra chromosomes in trisomies derived from nondisjunction during first meiosis in the oocyte have a reduced recombination map but may still have at least one chiasma (Hassold and Sherman, 1993). Together with our observations on the disturbed kinetics of cell cycle progression of "aged" oocytes these data suggest to us that a production line (Henderson and Edwards, 1968) may exist. Thus, there may be a group of oocytes which does not find optimal conditions for development during early meiotic phases in the embryonal ovary. It may be characterized by delayed progression through S-phase, altered conformation of chromatin and a reduced frequency and altered sites of recombination. If these oocytes are destined to resume maturation only near the end of the reproductive period of the female, disturbances in cell cycle progression already manifest during the early stages of development may become once more expressed during the final stages of maturation, leading to shortening of the cell cycle in general and asynchrony in anaphase I trigger and resolution of chiasmata (Eichenlaub-Ritter, 1994). Some homologues may disjoin precociously before the proper orientation of homologues is achieved, other homologues may separate too late such that lagging and trapping of homologues in the interpolar space occurs, still others may disjoin their chromatids before chiasmata have resolved or homologues have aligned on the metahase spindle (Soewarto et al., submitted for publication). This will ultimately lead to malsegregation of chromosomes and chromosomal imbalance of the mammalian oocyte.

CONCLUSIONS AND OUTLOOK

Tumorigenesis of somatic cells appears often to be associated with loss of cell cycle control, overriding or aberrations in cell cycle checkpoints and concomittant genomic instability. We obtained evidence that loss of cell cycle progression may also be a critical factor in maternal age-related and drug-induced aneuploidy, not only of mouse, but also of human oocytes (Eichenlaub-Ritter et al., submitted for publication). In the future it will be important to identify risk factors or such conditions positivly influencing the surveillance system checking cell cycle progression in oocytes. Further studies on the order of segregation of homologous and chromatids and the mechanisms mediating spatio-temporal control of these events with respect to the cell cycle, and presence and distribution of chismata may help to prevent nondisjunction.

REFERENCES

Brook, D., Gosden, R.G. & Chandley, A.C. (1984) Maternal ageing and aneuploid embryos: evidence from the mouse that biological and not chronological age is important. Hum. Genet. 66: 41-45.

Eichenlaub-Ritter, U. (1993) Studies on maternal age-related aneuploidy in mammalian oocytes and cell cycle control. In: "Chromosomes Today" (A. Sumner & A.C. Chandley, eds.) Vol.11, pp323-337. Chapman & Hall, London.

Eichenlaub-Ritter, U. (1994) Mechanisms of nondisjunction in mammalian meiosis. Curr. Topics Dev. Biol. 29: 281-324.

Eichenlaub-Ritter, U. & Boll, I. (1989) Nocodazole sensitivity, age-related aneuploidy, and alterations in the cell cycle during maturation of mouse oocytes. Cytogenet. Cell Genet. 52: 170-176.

Eichenlaub-Ritter, U. & Sobek-Klocke, I. (1993) Implications of cell cycle disturbances for meiotic aneuploidy: Studies on a mouse model system. In: "Chromosome Segregation and Aneuploidy" (B.K. Vig, ed.), pp 173-182. Springer Verl., Heidelberg.

Eichenlaub-Ritter, U., Chandley, A.C. & Gosden, R.G. (1988) The CBA mouse as a model for maternal age-related increases in aneuploidy in man: Studies on oocyte maturation, spindle formation and chromosome alignment during meiosis. Chromosoma 96: 220-226.

Eichenlaub-Ritter, U. , Schmiady, H., Kentenich, H. & Soewarto, D. Recurrent failure in polar body formation and PCC in oocytes from a hu-

man patient: Indicators of asynchrony in nuclear and cytoplasmic maturation. (submitted for publication)

Gaulden, M.E. (1992) Maternal age effect: The enigma of Down syndrome and other trisomic conditions. Mut. Res. 296: 69-88.

Hassold, T. & Jacobs, P.A. (1984) Trisomy in man. Ann. Rev. Genet. 18: 69-97.

Hassold, T. & Sherman, S. (1993) The origin of non-disjunction in humans. In: "Chromosomes Today" (A. Sumner & A.C. Chandley, eds.) Vol. 11, pp 313-322.

Henderson, S.A. & Edwards, R.G. (1968) Chiasma frequency and maternal age in mammals. Nature 218: 22-28.

Soewarto, D, Schmiady, H. & Eichenlaub-Ritter, U. Consequences of non-extrusion of the polar body and control of sequential segregation of homologues and chromatids in mammalian oocytes. (submitted for publication).

Generic modelling of cooperative growth patterns in bacterial colonies

Eshel BEN-JACOB, Ofer SCHOCHET, Adam TENENBAUM, Inon COHEN, Andreas CZIROK & Tamas VICSEK *)

School of Physics and Astronomy, Raymond & Beverly Sackler Faculty of Exact Sciences, Tel Aviv University, Tel Aviv 69978 Israel;
*) Department of Atomic Physics, Eötvös University, Budapest, Puskin u5-7, HU-1088 Hungary

Abstract

BACTERIAL colonies must often cope with unfavourable environmental conditions[1,2]. To do so, they have developed sophisticated modes of cooperative behaviour[3-10]. It has been found that such behaviour can cause bacterial colonies to exhibit complex growth patterns similar to those observed during non-equilibrium growth processes in non-living systems[11]; some of the qualitative features of the latter may be invoked to account for the complex patterns of bacterial growth[12-18]. Here we show that a simple model of bacterial growth can reproduce the salient features of the observed growth patterns. The model incorporates random walkers, representing aggregates of bacteria, which move in response to gradients in nutrient concentration and communicate with each other by means of chemotactic 'feedback'. These simple features allow the colony to respond efficiently to adverse growth conditions, and generate self-organization over a wide range of length scales.

We have grown bacterial colonies under different growth conditions[12,13] ranging from a very low level of nutrient (0.1 g peptone per litre) to a very rich mixture (10 g peptone per litre), and from a soft substrate (~1% agar concentration) to a hard substrate (4% agar concentration). Growth was started with a droplet (5 μl containing ~10^5 bacteria) inoculation at the centre of Petri dishes incubated at 37 °C and 30% humidity. The growth pattern we describe are of bacteria derived from *Bacillus subtilis* strain 168 (refs 12, 13). The colonies adopt various shapes as growth conditions are varied (Fig. 1): patterns are compact at high peptone concentrations and become more ramified at low peptone concentrations (0.5 g l^{-1}), in agreement with results reported in refs 12-18. Surprisingly, at < ~0.25 g peptone per litre, colonies adopt a more organized (well defined circular envelope), dense structure (Fig. 1*d*).

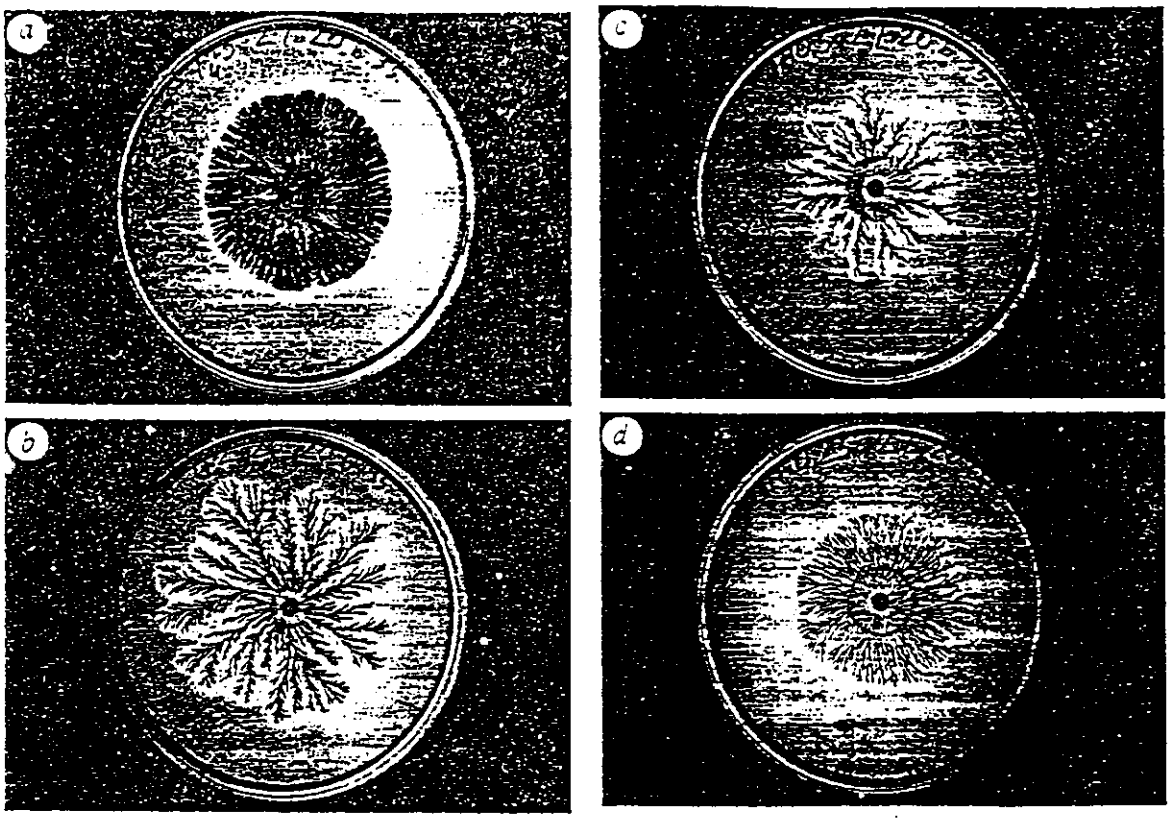

FIG. 1 Observed patterns of colonies grown on a substrate with 2% agar concentration. The peptone level is 5, 2, 0.5 and 0.25 g l^{-1} for *a*, *b*, *c* and *d* respectively. At high peptone levels the branches are wide, the pattern is very reminiscent of Hele–Shaw patterns[11] and the fractal dimension is close to two. As the peptone level is decreased, the patterns become more ramified (*b* and *c*), reminiscent of patterns observed during electrochemical deposition[11] (*b*) and diffusion limited aggregation (DLA)[22] simulations (*c*). At even lower peptone levels the patterns become denser again (*d*). As explained in the text, we expect this phenomenon to result from chemotaxis signalling.

Optical microscopy reveals that the bacteria perform a random walk-like movement within a well defined envelope. The latter (Fig. 2) is formed presumably by chemicals that are excreted by the bacteria and/or by fluid drawn by the bacteria from the agar. The envelope propagates slowly as if by the action of effective internal pressure produced by the collective movement of the bacteria. At very low peptone concentrations the density of bacteria is low—the distance between bacteria is up to several times the size of an individual bacterium. In this range, the bacteria are longer (~5 μm) (Fig. 2*e*) and the movement seems to be more organized. At high agar concentration there is a boundary layer of high bacterial density at the leading tips of the growing branches (Fig. 2*f*). In this range, colonies display a pronounced structure in the perpendicular direction as well (Fig. 2*c*).

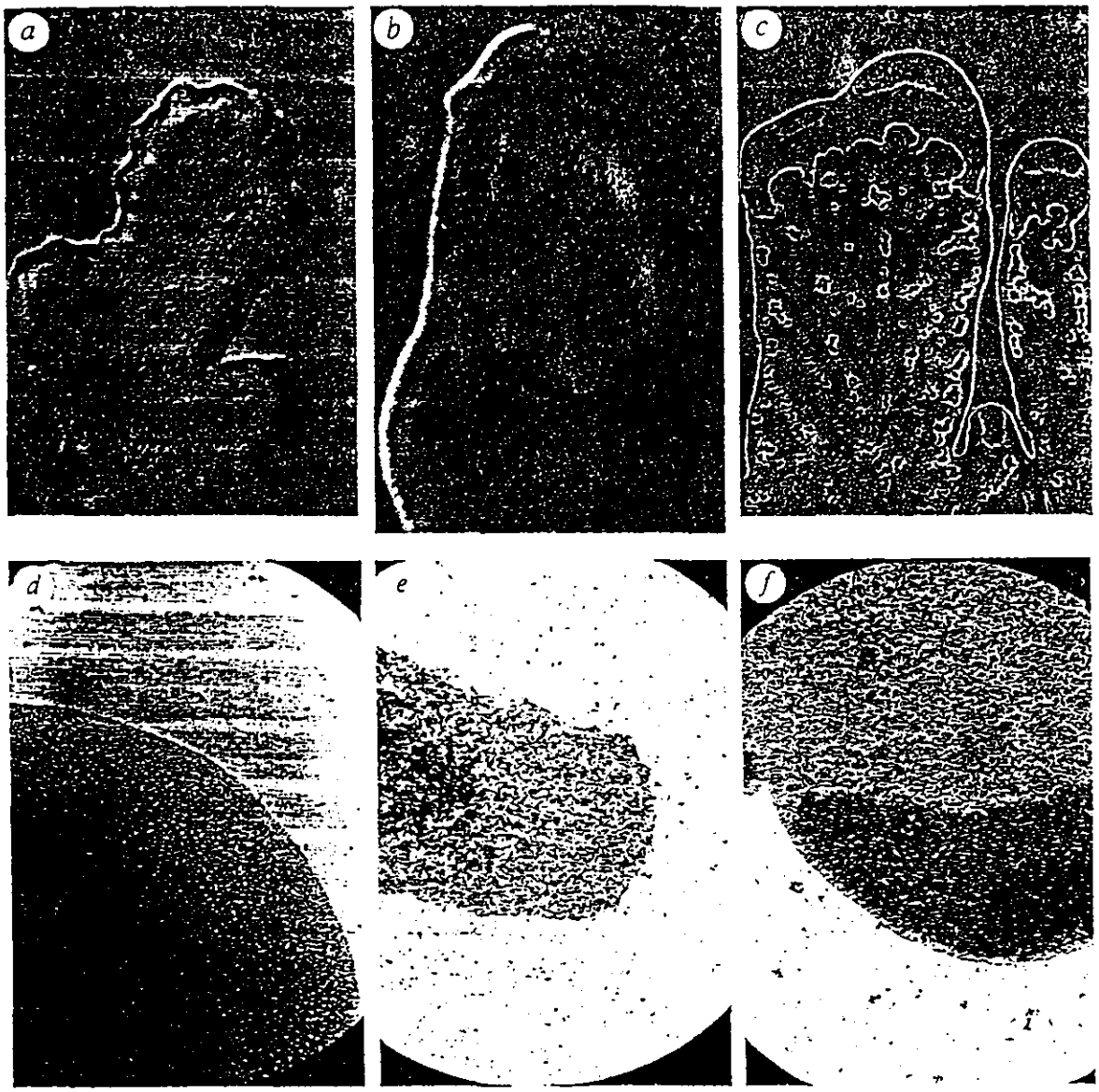

FIG. 2 Optical microscope observations of the colonies. *a* and *b*, Using a Numarski prism to indicate the sharpness of the envelopes. In *a* the envelope is rougher in the horizontal direction. *c*, Using transmitted light to show the complex three-dimensional structure of growth on substrates with a high agar concentration (2.5%). *d*, *e*, *f*, Micrographs of stained colonies. *d*, Intermediate values of peptone level and agar concentration. *e*, Low peptone level. *f*, High agar concentration: note the higher bacteria density at the tip in this case. Magnifications: *a*, *b*, *c*, ×28; *d*, *e*, *f*, ×280.

The growth of bacterial colonies presents an inherent additional level of complexity compared to non-living systems, as the building blocks themselves are living systems[15,19,20], each having its own autonomous (at times 'selfish') self-interest and internal degrees of freedom. To model the growth, we included the following generic features: (1) diffusion of nutrients; (2) movement of the bacteria; (3) reproduction and sporulation; (4) local communication. Diffusion of nutrients is handled by solving the

diffusion equation for the nutrient concentration c on a triangular lattice. The bacteria are represented by walkers, each of which should be viewed as a mesoscopic unit (coarse graining of the colony) and not as an individual bacterium.

Each walker is described by its location $\vec{r}_i$ and an internal degree of freedom ('internal energy' W_i), which affects its activity. The walker loses 'internal energy' at a rate e. To increase the internal energy it consumes nutrients at a fixed rate c_r, if sufficient food is available. Otherwise, it consumes the available amount. When there is not enough food for an interval of time (causing W_i to drop to zero), the walker becomes stationary (sporulation). When food is sufficient, W_i increases, and when it reaches some threshold t_r, the walker divides into two (reproduction).

The walkers perform off-lattice random walk within a well defined envelope (defined on the triangular lattice in Fig. 3*a*). Each segment of the envelope moves after it has been hit N_c times by the walkers. This requirement represents the local communication or cooperation in the behaviour of the bacteria. Note that, to a first approximation, the level of N_c represents the agar concentration, as more 'collisions' are needed to push the envelope on a harder substrate.

The model equations are:

$$\frac{\partial c(\vec{r}, t)}{\partial t} = D_c \nabla^2 c(\vec{r}, t) - \sum_{\text{active walkers}} \delta(\vec{r} - \vec{r}_i) \min (c_r, c(\vec{r}, t)) \quad (1)$$

This is the diffusion equation for the nutrients (D_c is the diffusion constant) which includes the consumption of food by the walkers (last term). The time evolution of W_i is given by:

$$\frac{dW_i}{dt} = \min (c_r, c(\vec{r}_i, t)) - e \quad (2)$$

At each time step, each of the active random walkers performs a random walk of step size d at an angle Θ, uniformly chosen from the interval $[0, 2\pi]$. Thus the new location $\vec{r}_i'$ is given by:

$$\vec{r}_i' = \vec{r}_i + d(\cos \Theta, \sin \Theta) \quad (3)$$

If the step $\vec{r}_i \rightarrow \vec{r}_i'$ crosses the envelope, the step is not performed and a counter on the appropriate segment of the envelope is increased by one. When a segment counter reaches N_c, the envelope segment is shifted by one lattice step.

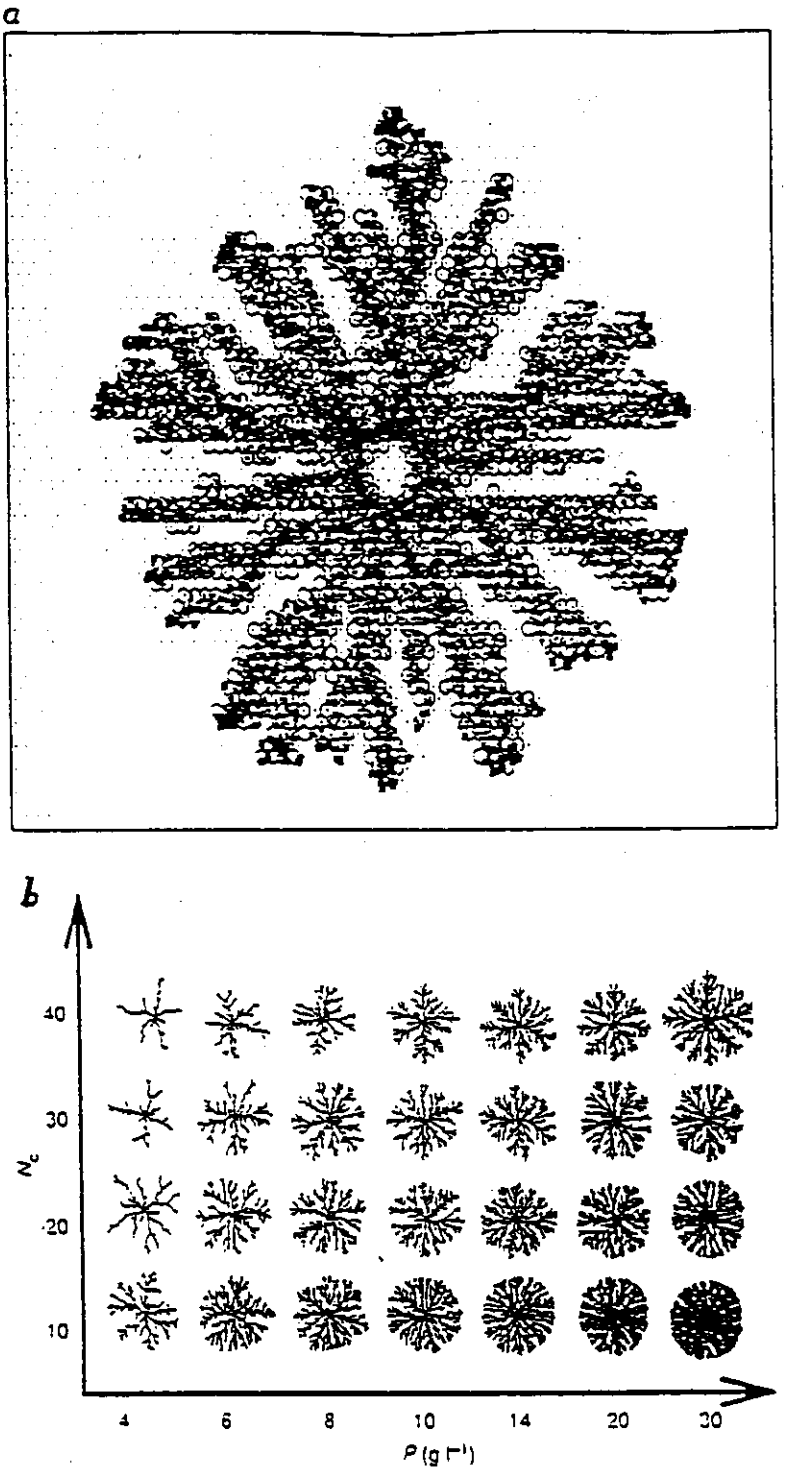

FIG. 3 The communicating walkers model. *a*, Close-up view of the model. The solid squares are the active walkers and the heavy dots are the stationary ones. Equation (1) is solved on the underlying triangular lattice. The hexagons mark the envelope. *b*, Results of numerical simulations of the communicating walkers model. The patterns are organized as function of peptone level P (the initial value of c) and N_c (corresponds to the agar concentration). The typical system size is 600×600 and the typical number of the walkers is 10^5. Hence each walker represents $\sim 10^4$ bacteria. The observed patterns are compact for high peptone levels and become ramified for low peptone levels. For the same peptone level, the patterns are more branched for higher N_c. Both are consistent with experimental observations. Note that the fractal dimension becomes much smaller than the DLA fractal dimension[22]. It reflects the fact that the envelope propagation has non-trivial dependence on the gradient of the nutrients diffusion field.

Results of numerical simulations of the model are shown in Fig. 3*b*. As in the growth of bacterial colonies, the patterns are compact at high peptone levels and become fractal with decreasing food level. For a given peptone level, the patterns are more ramified as the agar concentration increases. Clearly, the results shown in Fig. 3 are very encouraging and do capture features of the observed patterns. However, there are some crucial qualitative differences. The most dramatic one is the ability of the bacteria to develop organized patterns at very low peptone levels (Fig. 1*d*), a feature which is not captured by this version of the model.

As the environmental conditions become more hostile (low peptone concentration or hard surface), a higher level of cooperation is required for a more efficient response of the colony. Non-local communication and transfer of information between each of the individuals and the colony might be needed. Can chemotactic signalling provide the colony with the means to do so? Generally, chemotaxis means movement of the microorganisms in response to a concentration gradient of certain chemicals[6-10]. Ordinarily, the movement is along the gradient, either in the direction of the gradient or the opposite direction. The chemotactic response may be to an external chemical field or to one produced by the microorganisms; the latter may be called chemotactic signalling or communication. Moreover, it is well known[4] that excretion of the signal can be triggered by an external stress. Such non-local communication enables each bacterium to obtain information about the state of the colony as a whole and to respond to it. For example, the migration of *Dictyostelium* under low nutrient conditions depends on chemotactic signalling via cyclic adenosine monophosphate (cAMP)[11]. In this case, each of the microoooorganisms may excrete and consume cAMP and move according to its concentration gradient.

Here we include a simple version of chemotactic communication in the hope of identifying the generic features that it induces. Each of the stationary walkers (or alternatively, walkers which have been exposed to a low level of food) produces a communication chemical at a fixed rate s_r (in an attempt to drive other bacteria away), and each of the active walkers consumes the chemical at a fixed rate c_c. As we show below, this simplified version is sufficient to capture the qualitative features of the growth. A more realistic model would include a dependence of these rates on the concentrations of nutrients and chemotactic

signalling compounds. The equation of the communication field in the present model is given by:

$$\frac{\partial s(\vec{r}, t)}{\partial t} = D_s \nabla^2 (\vec{r}, t) + \sum_{\text{stationary walkers}} \delta(\vec{r} - \vec{r}_i) s_r - \sum_{\text{active walkers}} \delta(\vec{r} - \vec{r}_i) \min (c_c, s(\vec{r}, t)) \qquad (4)$$

The movement of the active bacteria changes from pure random walk (equal probability to move along any direction) to a random walk with a bias along the gradient of the communication field (high probability to move in the direction of the signalling material).

In Fig. 4 we show that the inclusion of such chemotaxis signalling indeed produces the desired phenomena. The pattern changes from fractal to a dense structure with thin branches and a well defined circular envelope. Moreover, the number of walkers (bacteria density) in the colony is much lower than in the absence of chemotaxis. We find that a chemotactic response to gradients of nutrient concentration does not reproduce this effect. Here we have simply introduced chemotactic signalling when the peptone level becomes low; in reality, there might be additional control mechanisms which change the intensity of the chemotaxis communication as the bacteria go through phenotypic transformations. We suspect that the observed perpendicular growth at high agar concentration also results from chemotactic signalling.

Our goal in this work is to demonstrate that apparently complex behaviour in biological systems can be elucidated by relatively simple, generic modelling in conjunction with a close comparison to experimental observations.

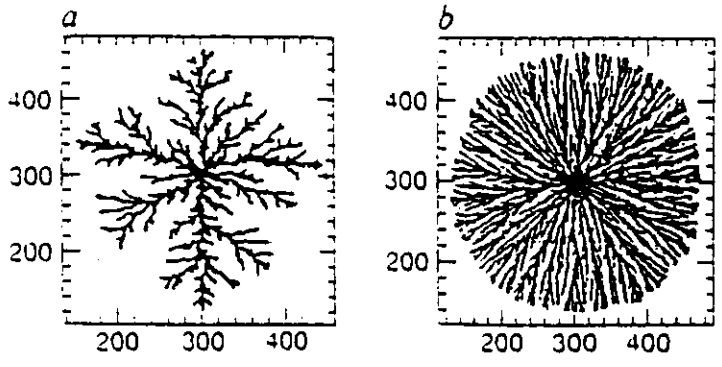

FIG. 4 Effect of chemotaxis signalling on the communicating walkers model. *a*, In the absence of the chemotaxis for $P = 10\ g\ l^{-1}$ and $N_c = 40$. *b*, In the presence of chemotaxis (for the same values of P and N_c). The pattern becomes denser with radial thin branches and well defined circular envelope, in aggreement with experimental observations. The numbers on the axes represent the trigonal lattice sites to indicate the system size.

Cited Literature

1. Stainer, R. Y., Doudoroff, M. & Adelberg, E. A. *The Microbial World* (Prentice-Hall, New Jersey, 1957).
2. Shapiro, J. A. *Scientific American* **258** (6) 62–69 (1988).
3. Shapiro, J. A. & Trubatch, O. *Physica* **D49**, 214–223 (1991).
4. Budrene, E. O. & Berg, H. C. *Nature* **349**, 630–633 (1991).
5. Kessler, J. O. *Contemp. Phys.* **26**, 147–166 (1985).
6. Adler, J. *Science* **166**, 1588–1597 (1969).
7. Lackie, J. M. (ed.) *Biology of the Chemotactic Response* (Cambridge Univ. Press, 1981).
8. Devreotes, P. *Science* **245**, 1054–1058 (1989).
9. Berg, H. C. & Purcell, E. M. *Biophys. J.* **20**, 193–219 (1977).
10. Nossal, R. *Exp. Cell Res.* **75**, 138–142 (1972).
11. Ben-Jacob, E. & Garik, P. *Nature* **343**, 523–530 (1990).
12. Ben-Jacob, E., Shmueli, H., Shochet, O. & Tenenbaum, A. *Physica* **A187**, 378–424 (1992).
13. Ben-Jacob, E., Tenenbaum, A., Shochet, O. & Avidan, O. *Physica* **A202**, 1–47 (1994).
14. Henrici, T. H. *The Biology of Bacteria* 3rd edn (Heath, Boston, 1948).
15. Cooper, A. L. *Proc. R. Soc. B* **171**, 175–199 (1968).
16. Fujikawa, H. & Matsushita, M. *J. phys. Soc. Japan* **58**, 3875–3878 (1989).
17. Matsuyama, T. & Matsushita, M. *Crit. Rev. Bact.* **19**, 117–135 (1993).
18. Schindler, J. & Rataj, T. *Binary* **4**, 65–72 (1992).
19. Allison, C. & Hughes, C. *Sci. Prog.* **75**, 403–422 (1991).
20. Hennchsen, J. *Bacter. Rev.* **36**, 478–503 (1972).
21. Kessler, D. & Levine, H. *Phys. Rev. E* (in the press).
22. Sander, L. M. *Nature* **322**, 789–795 (1986).

Acknowledgements

We thank I. Brainis, D. Weiss and H. Leibovich for technical assistance. We have benefited from conversations with J. Shapiro, E. Ron, D. Gutnik, D. Kessler, H. Levine and P. Garik. This research was supported in part by the German–Israeli Foundation for Scientific Research and Development, the Hungarian Research Foundation and the Program for Alternative Thinking at Tel-Aviv University.

taken from:
Nature (1994), vol.368 p.46-49 -
"used for the BOB, as it is"

Bielefelder Ökologische Beiträge, vol. 8, (1995) p. 25

ALPHA SCORPION NEUROTOXINS AND BACULOVIRUSES: A WORKING MODEL FOR THE DESIGN OF NOVEL SELECTIVE INSECTICIDES

Michael Gurevitz[1*], Noam Zilberberg[1], Daniel Urbach[1], Dalia Gordon[2], Eliahu Zlotkin[2], Nor Chejanovsky[3]

[1]Department of Botany, Life Sciences Institute, Tel-Aviv University, Ramat-Aviv 69978, Tel-Aviv; [2]Department of Cell and Animal Biology, Institute of Life Sciences, The Hebrew University, Jerusalem 91904; [3]Institute for Plant Protection, Volcani Center, ARO, Bet-Dagan 50250; Israel

*Corresponding author

NATURAL TOXINS SUITABLE FOR INSECT PEST CONTROL:

Public concern over the risks associated with widespread use of insecticidal chemicals has motivated our efforts to develop safer and more effective approaches to pest control. Thus, natural insecticidal compounds may serve as rational alternatives. In this respect, polypeptide scorpion toxins show promise when incorporated into insect pathogens by enhancing their killing efficacy (1-4). These toxins bind to insect sodium channels (5) and modify their properties. This results in a disruption of normal neuromuscular functions, paralysis and death. Thus, the incorporation of anti-insect selective scorpion toxins into insecticidal microorganisms, offers an opportunity to improve and augment current crop protection strategies (1-3). In order to minimize biological hazards which may be associated with such a genetic approach and to avoid the possibility of resistance build-up of insect pests, the molecular basis for anti-insect selectivity of these toxins should be clarified.

Among the scorpion toxins that show selectivity for insect sodium channels over their vertebrate counterparts, are the excitatory (6) and the depressant (7) toxins. However, α-toxins show activity against both insects and mammals. This class constitute a family of structurally and functionally related polypeptides, each containing 62-65 amino acid residues cross-linked by four disulfide bridges (8; Fig. 1). Alpha mammal toxins from the scorpion Androctonus australis Hector (such as AaH1 and AaH2) or from Leiurus quinquestriatus quinquestriatus (such as Lqq4 and Lqq5) bind in a voltage dependent manner to the receptor site of vertebrate voltage sensitive sodium channels (9-11). Their toxic effect is due to a modification of the channel activity by slowing inactivation

and altering its voltage dependence (12-14). As specific modifiers of the inactivation process, they are practically used as tools for the clarification of the molecular mechanism of ion channel gating. Thus, the introduction to this research of new natural or genetically engineered alpha toxins, is useful for the identification, characterization and discrimination between sodium channels in different organisms, tissues, and even in different locations within the same tissue (15).

Recently, a new α-toxin, LqhαIT, with significant similarity in sequence and in mode of action to the anti-mammal alpha scorpion toxins, was characterized in the venom of the scorpion Leiurus quinquestriatus hebraeus (16). This toxin is active against both insect and mammalian sodium channels and its binding site does not overlap with those of either the excitatory or depressant anti-insect selective toxins in reciprocal radioligand binding experiments (16,17). LqhαIT thus recognizes a binding site on the sodium channel that may be common to insects and to mamamls, while at the same time having an apparent higher affinity for the insect channel.

On this basis, our molecular genetic study of the basis for the anti-insect selectivity of scorpion neurotoxins is focused, in its initial stages, on LqhαIT as a representative of the α-toxins class. Furthermore, there are several advantages in persuing this study with α-toxin:

a) Alpha scorpion toxins comprise a large group of the most studied scorpion neurotoxins displaying natural variability with respect to primary sequences, binding sites and displacability characteristics, potency and effectiveness, and the ratio of their anti-insect/mammal toxicity.

b) Biological assays, including radioligand binding and neurophysiological

assays for insect and mammalian sodium channel function are available.

c) Several cDNAs encoding α-scorpion neurotoxins were cloned by us and their sequences determined. Furthermore, we established a reliable system for ex-vivo functional expression of LqhαIT (18) which is most suitable for site-directed modificational analysis and determination of its 3-D structure.

d) Alpha scorpion toxins display different binding capabilities to various sodium channels of the same organism or in different animals. For example, AaH2 and Bom3 (Buthus occitanus mardochei) do not displace each other from the receptor site in rat brain synaptosomes (19); Lqq4 hardly affects insects when compared to the strong anti-insect toxicity of LqhαIT (18); We show that the anti-insect/mammal toxicity ratio can be altered (18). These data suggest that the binding ratio of alpha toxins to various channels could be modified by genetic means.

e) The three-dimensional structure of three alpha scorpion toxins, AaH2, AaH3 and BeM9 (Buthus eupeus), have been solved by x-ray crystallography and ^{1}H 2D-NMR (20-23). By using molecular modelling of LqhαIT based on the crystal structure of AaH2, our mutagenesis program is now based on a combination of comparative analyses of alpha toxin sequences and 3-D putative structures.

f) LqhαIT-cDNA was placed by us under a strong promoter (polyhedrin) in the genome of the insect pathogen Autographa californica Nuclear polyhedrosis virus (AcMNPV) and viral isolates with enhanced insecticidal properties were obtained (4).

STRUCTURE-ACTIVITY RELATIONSHIP OF ALPHA SCORPION TOXINS:

Several approaches have been undertaken in studying structure-function relationship of scorpion toxins: chemical modifications introduced to isolated toxins (24-26); immunochemical studies to identify regions participating in binding to the receptor site in sodium channels (27); a biophysical approach to determine the three-dimensional structure (20-23); and, a genetic approach using isolated cDNA clones and ex-vivo expression systems (28-30,2-4,18).

Chemical modifications: A number of chemical modifications of various toxins have been carried out for localizing residues involved in the binding to the receptor or in their pharmacological properties. Biotinylation of Lys56 in AaHl and Lys58 in AaH2 of A. australis Hector or in Lqq5 of L. q. quinquestriatus reduced the toxicity by 80-99% (24). Arg 2 and Arg60 were modified in the toxin AaHl by p-hydroxyphenylglyoxal causing a reduction of 60-70% in toxicity (25). Arg2 modified by 1,2-cyclohexanedione in AaH3 reduced the binding to the receptor site by 99% (25). Similar treatment of Lys60 in Lqq5 caused 40% loss of activity (24). Nitration of Tyr residues in AaH3 by tetranitromethane caused reduction of 50% in the activity when either Tyrl4 or Tyr60 were affected. Nitration of both residues reduced the activity by 68%. When Tyr5, Tyrl4 and Tyr60 were nitrated, the remaining activity was 10% (25). Sulfenylation of Trp38 in AaH2 decreased the activity to 9% (25). The same treatment of Trp45 in AaH3 did not affect the toxicity (25). Proteolytic cleavage of the N-terminal pentapeptide of Bom3 of Buthus occitanus mardochei, reduced its activity to 10% (26). All of these residues are located in or near a conserved hydrophobic region proposed by Fontecilla-Camps (31) to carry

the "toxic site". A conclusion drawn out of these studies was that all important residues are clustered on one face of the α-mammal toxin, suggesting a multipoint interaction with the proteins of the mammalian sodium channel.

Immunochemical studies: An immunochemical approach using five antibody populations specific toward various regions of the toxin AaH2, was conducted to probe the interaction of the toxin with its receptor site. The results obtained, revealed two antigenic sites around the disulfide bridge 12-63 and one encompassing residues 50-59 whose blocking avoided binding to the receptor site (27). Monoclonal antibody that recognized an epitope that included Lys58, Val10 and His64, had similar effects. However, antibodies directed against stretches 19-28 and 28-39 did not affect the capability of the toxin to bind to its receptor site.

Determination of 3-D structure: The 3-D structures of the α-anti mammal toxins AaH2 and AaH3 from Androctonus australis Hector (20-22), and BeM9, an α-anti mammal toxin from Buthus eupeus (23), have been determined by x-ray crystallography and ^{1}H 2D NMR. These data confirmed the hypothesis that these toxins share a very similar carbon backbone structure. This fact is important when structure-activity relationship of such a toxin is being studied by a comparative approach.

Genetic approach: Several cDNA clones encoding scorpion neurotoxins have been cloned and in some cases expressed either in COS cells (28) or insect cultured cells using a baculovirus vector (2-4). However, genetic modifications using these expression systems have not been reported. We have established an expression system that is most suitable for genetic alteration studies. We first isolated (Fig. 1) and characterized several cDNAs encoding different alpha toxins from the Israeli yellow scorpion (L.

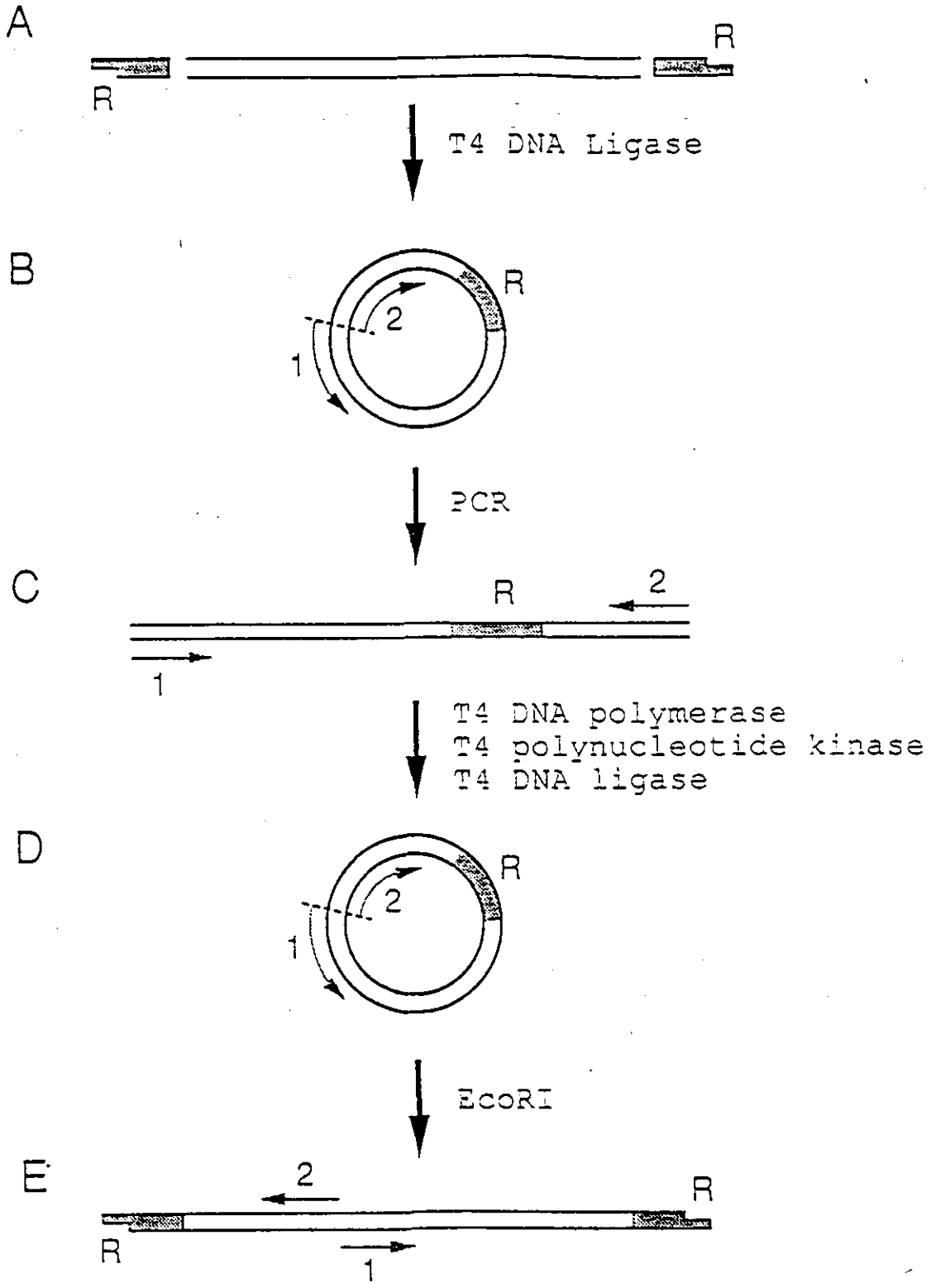

Fig. 1 : Isolation of cDNA clones. A: Molecular adaptors containing unique restriction sites, are ligated to the cDNA mixture; B: Circularization of the cDNA by T4 DNA ligase followed by inverse-PCR (the "back to back" primers are indicated); C: the PCR product (note the central position of the adaptor and former positions of the primers); D: The linear PCR product is circularized by T4 DNA ligase after "fill-in" and 5'-phosphorylation; E: Digestion with EcoRI generates a linear conable PCR-product. R indicates EcoRI site: 1 and 2 designate primers.

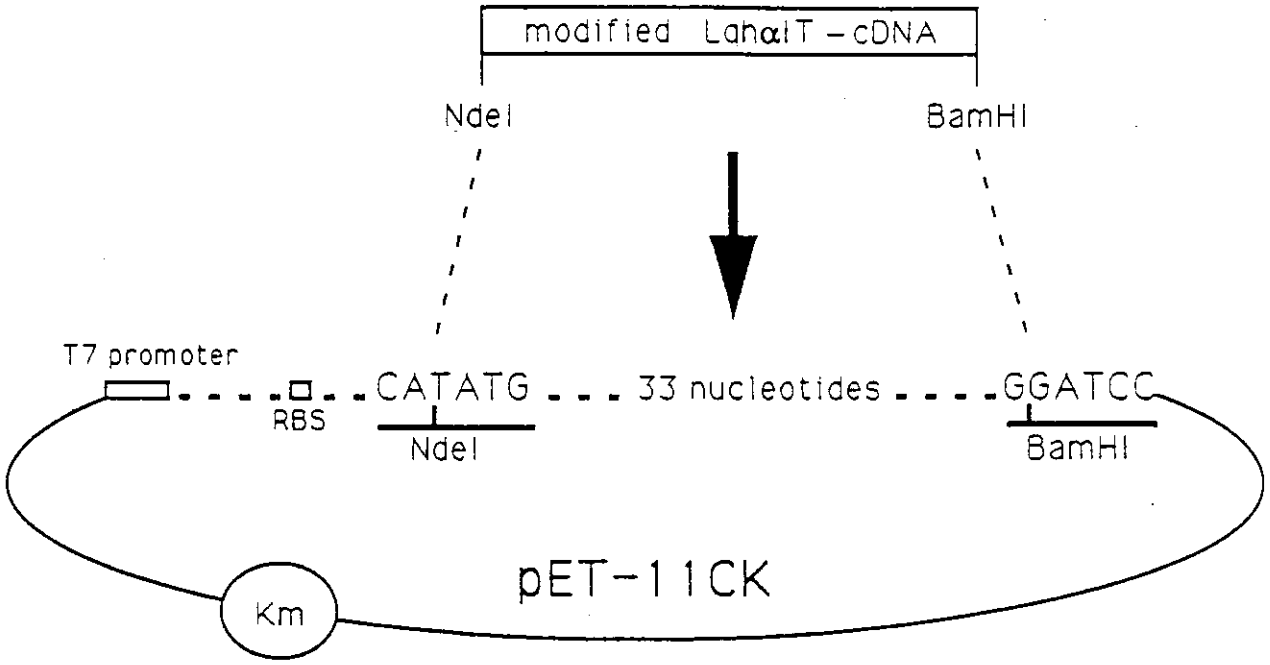

Fig. 2: Construction of the expression vector. The engineered cDNA was inserted between the NdeI and BamHI sites in the vector pET-11c, under the control of the T7 promoter.

```
                  10        20        30        40        50        60
                  :         :         :         :         :         :
LqhαIT   .VRDAYIAKNYNCVYECFRDAYCNELCTKN.GASSGYCQWAGKYGNACWCYALPDNVPIRVP..GKCR
Lqq4     G-------DDK----T-GSNS---TE---D.--E------L---------IK---K----I-..----
Bot1     G.------QPE------AQNS---D----D.--T------L---------KD--------I-..---HF
Bot11    .LK-G--VDDR--T-F-GTN-----E-V-LK-.E------V-R--------K---H-RTVQA..-R--S
BeM10    .---G---DDKD-A-F-G-N---D-E-K-..--E--K-WY--Q--------K---W---KQKVS---N
Lqq5     .LK-G--VDDK--TFF-G-N----DE-K-K.-GE------ASP--------K---R-S-KEK..-R-N
Amm5     .LK-G--I--L--TFF-------DD--K-K.-G-------ASP----------R-S-KEK..-R-N
AaH2     .---G--VDDV--T-F-G-N-----E---LK-.E------ASP-----Y--K---H-RTKG-..-R-H
```

Fig. 3: Sequence comparison between scorpion alpha neurotoxins. Identical residues with the LqhαIT sequence are designated by dashes. Lqq4 and Lqq5, Leiurus quinquestriatus quinquestriatus toxin 4 and toxin 5; Bot1 and Bot11, Buthus occitanus tunecatus toxin 1 and toxin 11; BeM10, Buthus eupeus toxin 10; LqhαIT, Leiurus quinquestriatus hebraeus alpha insect toxin; Amm5, Androctonus mauretanicus mauretanicus toxin 5; AaH2, Androctonus australis Hector toxin 2.

g. hebraeus) (29,30). The cDNA clone of LqhαIT, a unique alpha toxin with a high ratio of anti-insect/mammal activity, was successfully expressed in E. coli by using the pET-11c translational vector bearing a strong T7 promoter (Fig. 2). The toxin obtained in large insoluble amounts was completely denatured and then reoxidized under controlled conditions (18). The protein was purified by HPLC and analyzed for its activity. Toxicity was estimated by injection to blowfly larvae, electrophysiological properties were determined by current and voltage clamp experiments using a cockroach isolated axon, and, binding to the receptor was performed with a neuronal membrane preparation from locust synaptosomes. The folded recombinant toxin engineered with an additional methionine residue at its N-terminus, was found to be identical with the authentic toxin purified from the scorpion venom (16). This expression system was used for amino acid substitutions of specific C-terminal and N-terminal residues. These modifications were based on comparative analyses with other alpha toxins of high anti-mammal/insect toxicity ratio (Lqq4 and AaH2; Fig. 3). The substitutions of three residues at the C-terminal half had a minute effect on the toxicity to blowfly larvae and on the binding affinity to insect neuronal membranes. However, the ratio of anti-insect/mammalian activity (toxicity and binding to the receptor) increased several fold. Conversely, the substitution of three amino acid residues at the N-terminal half of the toxin, reduced the biological activity (ED_{50} and IC_{50}) by several orders of magnitude (Table 1).

Table 1: Biological activity of variant genetically modified LqhαIT toxins.

Toxins and modificants	ED_{50} (ng/100 mg body weight)	IC_{50} (nM)	LD_{50} (ng/gr body weight)
LqhαIT-rec	14	0.38±0.1	250
C-terminus	20	0.44±0.1	1000
N-terminus	3000	2500±1500	70000
Lqq4	950	unknown	70

ED_{50}, determined on 100-150 mg blowfly larvae.
IC_{50}, determined on locust synaptosomal membranes.
LD_{50}, determined on 20 gr ICR mice.

LqhαIT-rec stands for the nonmodified recombinant toxin.
C-terminus and N-terminus stand for the modified toxins.
Lqq4, purified toxin from the venom of L. q. quinquestriatus.

Table 2: Oral infectivity of wild-type and recombinant AcMNPV to Heliothis armigera larvae.

Time post infection (h)	Mortality (%)		Weight gain (mg)	
	WT	Recomb.	WT	Recomb.
24	0	0	9.5	7.8
48	0	0	13.1	12.0
72	0	4.5	63.2	36.1
96	11.4	72.7	125.0	43.0

First instar larvae were fed with virus-contaminated diet (4000 PIB/plug). Mortality and weight gain were determined in population samples of 48 larvae per treatment.

BACULOVIRUS-MEDIATED TARGETING OF SCORPION TOXINS:

The nervous system of insects serves as a major target for conventional efforts of insect control relied on hazardous chemicals of four groups: organochlorines, organophosphates, carbamates and pyrethroids [32]. It is our aim to develop new safer means for pest control by utilizing natural anti-insect agents. Insecticidal polypeptidic neurotoxins from scorpion venoms targeted to insect sodium channels of excitable tissues can be used for this purpose. However, in order to be efficiently utilized, they require a delivery system to reach their target sites. In this respect, an insect pathogen which naturally infects and spreads within the insect host and is amenable for genetic engineering, should be an ideal vector.

Baculoviruses infect insects and do not infect mammals (33). They were registered in the past as bioinsecticides despite their slow killing rates (6-10 days post infection) of insect pest larvae. During this period of time, an extensive damage to the crop, is already obtained (33). The availability of insect cell cultures used for the engineering of recombinant baculoviruses (for a comprehensive review see 34), has motivated us and others (1-4) to attempt the expression of scorpion cDNAs encoding insecticidal toxins in insect pests. We engineered a recombinant AcMNPV with the LqhαIT-cDNA under the control of the potent polyhedrin promoter (35) and obtained expression of the toxin in Spodoptera frugiperda culture cells. A recombinant LqhαIT functional toxin was processed (leader peptide removed) and secreted by the cells. Toxicity of the recombinant toxin was demonstrated on blowfly and on lepidopterous (Spodoptera littoralis) larvae. The bioinsecticidal effect of the recombinant baculovirus was assayed on Heliothis armigera larvae. A

significant reduction in the time of killing and in the mean weight gained by the larval population were obtained when compared to wild-type viruses (Table 2).

CONCLUSIONS AND FUTURE PROSPECTS:

The results of the chemical, immunochemical and genetic approaches in studying alpha scorpion toxins, can be interpreted according to the 3-D structure published for AaHII and our 3-D model of LqhαIT. The "conserved hydrophobic surface" (CHS) suggested previously to be involved in binding to the receptor site, is in fact located away of the putative binding surface. However, the outstanding impact of the substitutions at the N-terminal region of LqhαIT and their position in the 3-D putative structure of LqhαIT suggests that these residues are involved in binding. Thus, the genetic system has become a powerful tool in determining the structural motifs participating in binding and conferring insecticidity.

The ability to design molecules capable to distinguish between insect and mammalian nerves is of a major academic as well as applicative value. The potency and pharmacological specificity of the anti-insect neurotoxins prompt us to clarify their structure-function relationship and toxin-receptor interactions at the molecular level. The fact that the selective neurotoxin interacts with a well conserved membranal structure serving a defined neuronal function, enables its utilization as a specific marker of the above structure and a key for clarifying its function. As such, the anti-insect specific scorpion toxins and their modificants serve as valuable tools in comparative neurochemistry, neuropharmacology, and

developmental neurobiology.

From an applicative point of view, these toxins are able first to distinguish between the nervous system of an insect and another animal, and second to identify in the former a functionally critical target. As such, they can be used as models for the design of insect-selective insecticides. The industrial and agricultural significance of the insect-selective peptide neurotoxins can be appreciated on the background of recent advances in developing baculovirus vectors bearing scorpion toxin genes for plant protection, or, for their alteration via recombinant DNA techniques in order to clarify structural elements that may help to design non-peptide agents active specifically against insect pests (36).

BIBLIOGRAPHY:

1. Tomalski MD, Miller LK (1991) Insect paralysis by baculovirus-medieted expression of a mite neurotoxin gene. Nature 352:82-85.
2. Stewart LMD, Hirst M, Ferber ML, Merryweather AT, Cayley PJ, Possee RD (1991) Construction of an improved baculovirus insecticide containing an insect-specific toxin gene. Nature 352:85-88.
3. Maeda S, Volrath SL, Hanzlik TN, Harper SA, Majuma K, Maddox DW, Hammock BD, Fowler E (1991) Insecticidal effects of an insect-specific neurotoxin expressed by a recombinant baculovirus. Virology 164:777-780.
4. Chejanovsky N, Zilberberg N, Zlotkin E, Gurevitz M (1994) Baculovirus directed expression of a functional alpha scorpion neurotoxin specific against insects in Spodoptera frugiperda insect cells. In preparation.

5. Gordon D, Moskowitz H, Eitan M, Warner C, Catterall WA, Zlotkin E (1992) Localization of receptor sites for insect selective toxins on sodium channels by site directed antibodies. Biochemistry 31:7622-7628.

6. Zlotkin E (1983) Insect selective toxins derived from scorpion venoms: an approach to insect neuropharmacology. Insect Biochem 13:219-236.

7. Zlotkin E, Gurevitz M, Fowler E, Adams M (1993) Depressant insect selective neurotoxins from scorpion venom: Chemistry, action and gene cloning. Arch Insect Biochem Physiol 22:55-73.

8. Rochat H, Bernard P, Couraud F (1979) Scorpion toxins: Chemistry and mode of action. In: Advances in Cytopharmacology (B Ceccarelli, F Clementi, Eds) 3:325-334, Raven Press, New York.

9. Catterral WA (1977) Membrane potential dependent binding of scorpion toxin to the action potential sodium ionophore. Studies with a toxin derivative prepared by lactoperoxidase catalyzed iodination. J Biol Chem 252:8660-8668.

10. Ray R, Catterral WA (1978) Membrane potential dependent binding of scorpion toxin to the action potential sodium ionophore. Studies with a 3(4-hydroxy 3-[^{125}]iodophenyl) propionyl derivative. J Neurochem 31:397-407.

11. Couraud F, Rochat H, Lissitzky S (1978) Binding of scorpion and sea anemone neurotoxins to a common site related to the action potential Na^+ ionophore in neuroblastoma cells. Biochem Biophys Res Commun 83:1525-1530.

12. Catterall WA (1980) Neurotoxins that act on voltage-sensitive sodium channels in excitable membranes. Annu Rev Pharmacol Toxicol 20:15-43.

13. Gordon D (1990) Ion channels in nerve and muscle cells. Current

Opinion in Cell Biology 2:695-707.

14. Catterall WA (1986) Molecular properties of voltage-sensitive sodium channels. Annu Rev Biochem 55:953-985.

15. Barchi RL (1987) Sodium channel diversity: subtle variations on a complex theme. TINS 10:221-223.

16. Eitan M, Fowler E, Herrman R, Duval A, Pelhate M, Zlotkin E (1990) A scorpion venom neurotoxin paralytic to insects that affects sodium current inactivation: Purification, primary structure, and mode of action. Biochemistry 29:5941-5947.

17. Gordon D and Zlotkin E (1993) Binding of an α scorpion toxin to insect sodium channels is not dependent on membrane potential.FEBS Lett 315:125-128.

18. Zilberberg N, Gordon D, Zlotkin E, Pelhate M, Gurevitz M (1994) Reconstitution of an active alpha scorpion neurotoxin expressed in Escherichia coli: Site directed mutagenesis identifies residues important for biological activity. Mol Pharmacol. Submitted.

19. Vargas O, Martin MF, Rochat H (1987) Characterization of six toxins from the venom of the Morrocan scorpion Buthus occitanus mardochei. Eur J Biochem 162:589-599.

20. Fontecilla-Camps JC, Almassy RJ, Suddath FL, Bugg CE (1982) The three-dimentional structure of scorpion neurotoxins. Toxicon 20:1-7.

21. Fontecilla-Camps JC, Habersetzer-Rochat C, Rochat H (1988) Orthorhombic crystals and three-dimentional structure of the potent toxin II from the scorpion Androctonus australis Hector. Proc Natl Acad Sci USA 85:7443-7447.

22. Mikou A, Laplante SR, Guittet E, Lallemand JY, Martin-EauClaire MF, Rochat H (1992) Toxin III of the scorpion Androctonus australis

Hector: Proton nuclear magnetic resonance assignments and secondary structure. J Biomolec NMR 2:57-70.

23. Pashkov VS, Maiorov VN, Bystrov VF, Hoang AN, Volkova TM, Grishin EV (1988) Biophys Chem 31:121-133.

24. Darbon H, Jover E, Couraud F, Rochat H (1983) α-Scorpion neurotoxin derivatives sutable as potential markersof sodium channels. Int J Pept Protein Res 22:179-186.

25. Kharrat R, Darbon H, Rochat H, Granier C (1989) Structure/activity relationships of scorpion α-toxins. Eur J Biochem 181:381-390.

26. El Ayeb M, Darbon H, Bahraoui EM, Vargas O, Rochat H (1986) Differential effect of defined chemical modifications of antigenic and pharmacological activities of scorpion α and ß toxins. Eur J Biochem 155:289-294.

27. El Ayeb M, Bahraoui EM, Granier C, Rochat H (1986) Use of antibodies specific to define regions of scorpion α-toxin to study its interaction with its receptor site on the sodium channel. Biochemistry 25:6671-6678.

28. Bougis PE, Rochat H, smith LA (1989) Precursors of Androctonus australis scorpion neurotoxins: Structures of precursors, processing outcomes, and expression of functional recombinant toxin II. J Biol Chem 264:19259-19265.

29. Zilberberg N, Gurevitz M (1993) Rapid isolation of full length cDNA clones by "inverse PCR". Purification of a scorpion cDNA family encoding α-neurotoxins. Anal Biochem 209:203-205.

30. Gurevitz M, Urbach D, Zlotkin E, Zilberberg N (1991) Nucleotide sequence and structure analysis of a cDNA encoding an alpha insect toxin from the scorpion Leiurus quinquestriatus hebraeus. Toxicon

29:1270-1272.

31. Fontecilla-Camps JC, Almassy RJ, Suddath FL, Bugg CE (1982) The three-dimentional structure of scorpion neurotoxins. Toxicon 20:1-7.
32. Elliot M (1986) In: Neuropharmacology and Pesticide Action (MG Ford, GG Lunt, RC Reay, PNR Usherwood, Eds) pp 498-500, Ellis Horwood. UK.
33. Huber J (1986) Use of baculoviruse in pest management programs. In: In: The Biology of Baculoviruses. (RR Granados, BA Federici, Eds) Vol II, pp 181-202, CRC Press, Boca Raton, FL.
34. Luckow VA, Summers MD (1988) Trends in the development of baculovirus expression vectors. Bio/Technology 6:47-55.
35. Smith GE, Summers MD, Fraser MJ (1983) Production of human beta interferon in insect cells infected with a baculovirus expression vector. Mol Cell Biol 3:2156-2165.
36. Gurevitz M, zilberebrg N (1994) Advances in molecular genetics of scorpion neurotoxins. J Toxicol - Toxin Rev 13:65-100.

Bielefelder Ökologische Beiträge, vol. 8, (1995) p. 43 - 49

The Enzyme Malate Dehydrogenase of the Extremely Halophilic Archaebacterium *Haloarcula marismortui.*

Moshe Mevarech

Dept. of Molecular Microbiology and Biotechnology
George S. Wise Faculty of Life Sciences
Tel Aviv University, Tel Aviv 69978 Israel

In general, living organisms are adapted to function in a rather limited set of physiological conditions: chemical and ionic composition of the medium, pH, temperature and pressure. Significant deviations from physiological conditions will lead to disaggregation of complex biological structures, denaturation of protein and DNA molecules and consequently to cell death. Most living organisms are able to maintain metabolic activity and viability only within narrow limits of external physical conditions. It is however possible to find organisms that were adapted to survive, grow and multiply under the most extreme environmental conditions. Adaptation of microorganisms to extreme salinity, as can be found for instance in the Dead Sea or the Great Salt Lake in Utah, is possible by one of several mechanisms. There are microorganisms that overcome the extreme salinity of the external environment by having a membrane that is impermeable to salt. The osmotic pressure balance is maintained, in these organisms, by accumulation, in the cytoplasm, of low molecular weight metabolites. The extremely halophilic archaebacteria on the other hand, are adapted to external salinity by a different mechanism. In these bacteria the internal salt concentration is equal to or even higher than that of the external one (2). The entire biochemical machinery is thus adapted to function at very high salt concentrations.

Very little is known on the molecular basis for halophilic properties. The most general difference between the halophilic enzymes and their non-halophilic homologues are their amino acid compositions. It was found that when amino acid compositions are determined for whole halobacterium proteins, the amount of acidic amino acids exceeds the amount of basic amino acids by about 10 mole % compared to equimolar amounts in *E. coli* (5). The same picture is obtained when the amino acid composition of purified halobacterial proteins is compared to the composition of similar non-halobacterial proteins. It is however unclear how this excess negative charge in halophilic proteins contributes to their response to salt concentration.

For our studies we have use the enzyme malate dehydrogenase of the extremely halophilic archaebacterium *Haloarcula marismortui* (h-MDH). This enzyme can be purified to homogeneity in a rather simple way using methods there were entirely adapted to high salt concentrations (4). In order to gain a better understanding of the molecular basis of adaptation of enzymes to function at high salt concentrations various methodologies were used. First, the effect of salt concentration on the biochemical properties of the enzyme was determined. It was found that salts stabilize the enzyme (see Figure 1).

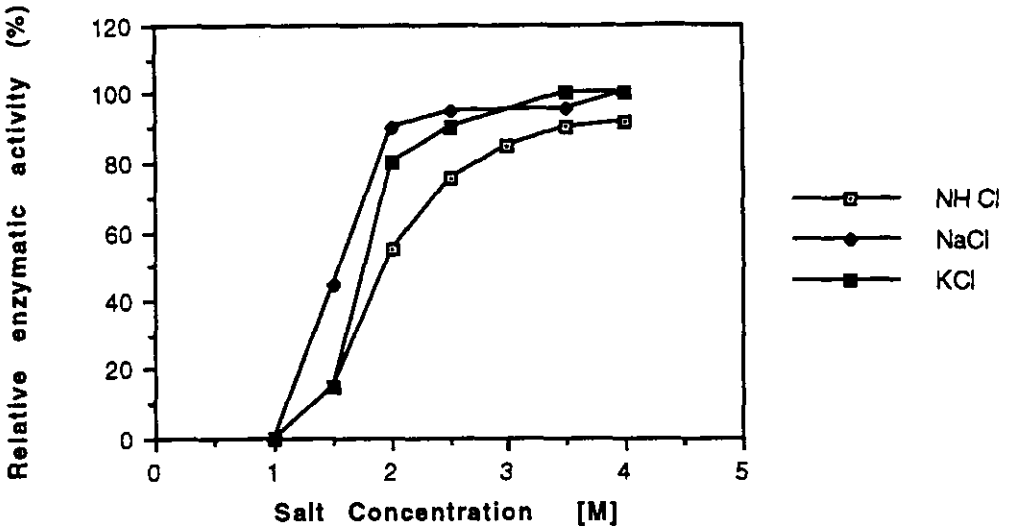

Figure 1. The dependence of the stability of hMDH on salt concentration. The enzyme was exposed to the indicated salt solutions for 9 hours at 30 ^{0}C and then the activity was measured at standard conditions.

At salt concentrations lower than 2M the enzyme is unstable and loses activity in a first order kinetics (data not shown). Different salts have different stabilization capacities.

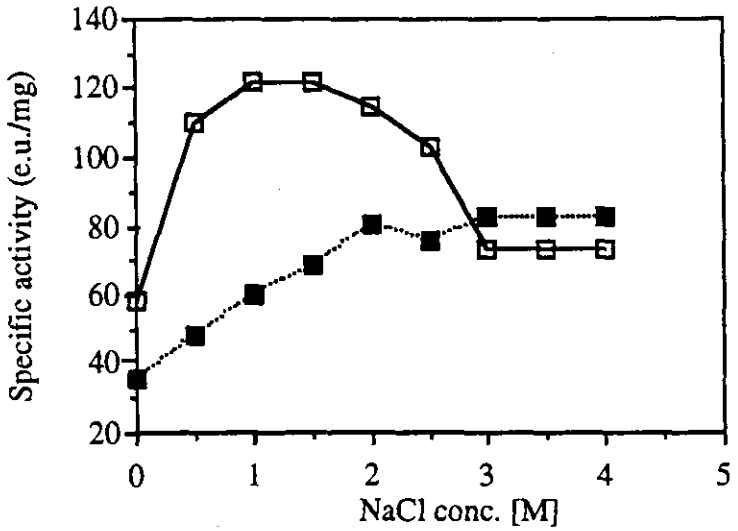

Figure 2. The effect of salt concentration on the enzymatic activity of hMDH. Assays were performed using oxaloacetate concentrations of 0.1 mM ( ) or 10 mM ( ).

The effect of salt concentration on the enzymatic activity of hMDH is more complicated (see Figure 2). At low oxaloacetate concentration maximum activity is achieved at about 1.2 M NaCl and activity is inhibited at higher salt. At high oxaloacetate concentration the specific activity is lower than at low oxaloacetate concentration but always increases with salt concentration.

In order to be able to compare the halophilic enzyme to its non halophilic counterparts, the primary structure of hMDH was determined by isolating and sequencing the gene coding for this enzyme. The gene was isolated by probing genomic library of *Haloarcula marismortui* by a synthetic oligodeoxynucleotide probe made according to the amino acid sequence of the N-terminal region of the protein (1). The sequence of the gene is given in Figure 3.

```
CCCCGCTTCA GGTGGAGCGG TCGAGTCGTC GTCGTGTCCG GCGCACTCGC AGCCGCCTCG TCACCTACGC CGAACTGGAC
TCGGGCCTCG TCGCTGGGGT CGGCAACCTC GATCTGGTCA CCGTCGTCGG TCTGGCCCTC CTGTTCGTCA GCATCCGACG
GGTCCGCCCC GCTGGCCTGT GTATCGCGAG CGACCGGCTC TTGGCAGGTG GGGCAGAACT CCTGACCGTC ATGCCGGAAG
ATGGGGTCGC CACACTCGCT GCAGTGGGCG TTCGTCATCG TCGCGCCCTT CAACCAGGGG TTCGCTCATT TGCTCGGTCG
CGCCCGGTTG TCCTCCTCTT GCTCGAACTT CTCGCGGAGT TTCTCGCGTT CGGCTTCCTT GTCGAAGTCG CTCATACGAG
TCACAACGCC ACGGGGCTGA AAACAGTTTA CGGGTGCGAG ATGTCGATAT CGCCTGAACG ATATCCGTCG GAATTGGGGT
TTCGACACGT TTAACGTTCG CGCCCGAGCC TTTTCGAATG GT

 M   T   K   V   S   V   V   G   A   A   G   T   V   G   A   A   A
ATG ACA AAG GTA AGC GTA GTC GGC GCA GCC GGA ACG GTC GGC GCA GCC GCA

 G   Y   N   I   A   V   R   D   I   A   D   E   V   V   F   V   D
GGG TAC AAC ATC GCG CTC CGT GAC ATC GCT GAC GAG GTC GTC TTC GTG GAC

 I   P   D   K   E   D   D   T   V   G   E   A   A   D   T   N   H
ATC CCG GAC AAG GAA GAC GAC ACG GTC GGG CAG GCC GCT GAC ACG AAC CAC

 G   I   A   Y   D   S   N   T   R   V   R   Q   G   G   Y   E   D
GGC ATC GCC TAC GAT TCG AAC ACG CGC GTC CGC CAG GGC GGC TAC GAG GAT

 T   A   G   S   D   V   V   V   I   T   A   G   I   P   R   Q   P
ACT GCC GGC TCA GAC GTG GTA GTC ATC ACG GCC GGG ATT CCT CGC CAG CCC

 G   Q   T   R   I   D   L   A   G   D   N   A   P   I   M   E   D
GGC CAG ACA CGT ATC GAC CTC GCG GGC GAC AAC GCG CCC ATC ATG GAG GAC

 I   Q   S   S   L   D   E   H   N   D   D   Y   I   S   L   T   T
ATC CAG TCC TCA CTG GAC GAA CAC AAC GAC GAC TAC ATC TCG CTG ACC ACC

 S   N   P   V   D   L   L   N   R   H   L   Y   E   A   G   D   R
TCG AAC CCC GTC GAC CTG CTC AAC CGC CAC CTC TAC GAG GCC GGC GAC CGC

 S   R   E   Q   V   I   G   F   G   G   R   L   D   S   A   R   F
TCG CGC GAG CAG GTC ATC GGC TTC GGC GGC CGA CTG GAC TCC GCG CGG TTC

 R   Y   V   L   S   E   E   F   D   A   P   V   Q   N   V   E   G
CGT TAC GTC CTG AGC GAG GAG TTC GAC GCC CCG GTT CAG AAC GTC GAA GGA

 T   I   L   G   E   N   G   D   A   Q   V   P   V   F   S   K   V
ACG ATC CTC GGG GAA CAC GGC GAC GCA CAG GTT CCC GTG TTC TCG AAG GTC

 R   V   D   G   T   D   P   E   F   S   G   D   E   K   E   Q   L
CGC GTT GAC GGC ACC GAC CCC GAA TTC AGC GGG GAC GAG AAA GAG CAG CTG

 L   G   D   L   Q   E   S   A   M   D   V   I   E   R   K   G   A
CTC GGC GAC CTG CAG GAA TCG GCG ATG GAC GTC ATC GAG CGC AAG GGC GCG
```

```
 T   E   W   G   P   A   R   G   V   A   H   M   V   E   A   I   L
ACC GAG TGG GGG CCA GCC CGC GGT GTC GCA CAT ATG GTC GAA GCC ATC CTC

 H   D   T   G   E   V   L   P   A   S   V   K   L   E   G   E   F
CAC GAC ACC GGT GAA GTA CTG CCG GCT TCG GTC AAG CTA GAG GGT GAG TTC

 G   H   E   D   T   A   F   G   V   P   V   R   L   G   S   N   G
GGG CAC GAG GAC ACT GCC TTC GGT GTC CCG GTC CGT CTC GGG AGC AAC GGC

 V   E   E   I   V   E   W   D   L   D   D   Y   E   Q   D   L   M
GTC GAA GAG ATC GTC GAG TGG GAT CTT GAC GAC TAC GAG CAG GAC CTG ATG

 A   D   A   A   E   K   L   S   D   Q   F   D   K   I   S
GCC GAC GCT GCC GAG AAG CTC TCG GAC CAG TAC GAC AAA ATC TCG taa

CCAGATATTA CTCGCGGTCG GCAGGGTCCG GGACGGCACC CGTCCCGAAT ATTATTTTGC CTCGCCAGCG GTGTGAAGAC
GCGGCTGTCA CTGCGAGGAG CGCTCTCTGA CAAACAGTGG CCGTTACGCG GGCTCGTCCT GCTCGTCAAG CAAGTCGCTA
TCGCGTCCGT CGTCATCGAT ATCAGCACCG AGGAGTGATG CCCACTCTTC GAGGTGTGAG TCCGATGTCG AGAGTTCTCG
GTGGTTCATG GCGTTATCCG AAGCATCCAC GGCATATTAT ATAATGGTTG TGCCGCATTG
ATACATAATG CTGTATGCAG CGGTTCTACG GGGTAATCCG GGATTGGCGA TCACAAA
```

Figure 3. Nucleotide sequence of the gene coding for hMDH and the derived amino acid sequence of the encoded protein.

This sequence shows that the enzyme contains a large excess of acidic groups versus basic groups (62 asapartic and glutamic residues versus 23 arginine and lysine residues). Aligning the amino acid sequence of hMDH with the amino acid sequences of non-halophilic MDHs and L-LDHs is shown in Figure 4. As can be seen, hMDH is more similar to L-LDHs than to MDHs.

The ability to study structure-function relationships by modifying the primary structure of any enzyme is largely dependent on the ability of producing large amounts of the enzyme by cloning its coding gene in a high expression vector. The gene coding for hMDH was cloned into the *Escherichia coli* expression vector pET11d. Large amounts of hMDH polypeptide were produced upon induction (1). However, being an halophilic enzyme, the polypeptides could not assembled in *E. coli* into an active enzyme. Activation of hMDH could be easily achieved by increasing the salt concentration of the *E. coli* extracts to 4 M NaCl.

```
                  10        20        30        40        50
                   |         |         |         |         |
PmM                            AKVAVLGASGGIGQPLSLLLK-NSPLVSRLTLYDIA-HTP
EcM                           M-KVAVLGAAGGIGQALALLLKTQLPSGSELSLYDIAPVTP
HmM                           MTKVSVVGAAGTVGAAAGYNIALRDIADEVVFV-DIPDKED
DfL     ATLKDKLIGHLATSQEPRSYNKITVVGV-GAVGMACAISILMKDLADEVALV-DV--MED
BsL                     MKNNGGARVVVIGA-GFVGASYVFALMNQGIADEIVLI-DANESK-

           60        70        80        90        100       110
            |         |         |         |         |         |
PmM     GVAADLSHIETRATVKGYLGPEQLPDCLK--GCDVVVIPAGVPRKPGMTRDDLFNINATI
EcM     GVAVDLSHIPTAVKIKGFSGEDATP-ALE--GADVVLISAGVRRKPGMDRSDLFNVNAGI
HmM     DTVGQAADINHGIAYDSNTRVRQGG-YEDTAGSDVVVITAGIPRQPGQTRIDLAGDNAPI
DfL     KLKGEMMDLQHGSLFLHTAKIVSGKDYSVSAGSKLVVITAGARQQEGESRLNLVQRNVNI
BsL     -AIGDAMDFNHGKVFAPKPVDIWHGDYDDCRDADLVVICAGANQKPGETRLDLVDKNIAI
```

```
          120       130       140       150       160       170
           |         |         |         |         |         |
PmM   VATLTAACAQHCPDAMICIISNPVNSTIPITAEVLKKHGVYNPNKIFGVTTLDIVRANAF
EcM   VKNLVQQVAKTCPKACIGIITNPVNTTVAIAAEVLKKAGVYDKNKLFGVTTLDIIRSNTF
HmM   MEDIQSSLDEHNDDYISLTTSNPVDLLNRHLYE--AGDRSREQVIGFGGR-LDSARFRYV
DfL   FKFIIPNIVKHSPDCIILVVSNPVDVLTYVAKK--LSGLPMHRIIGSGCN-LDSARFRYL
BsL   FRSIVSEVMAHGFQGLFLVATNPVDILTYATWK--FSGLPHERVIGSGTI-LDTARFRFL

          180       190       200       210       220       230
           |         |         |         |         |         |
PmM   VAELKGLDPARVSVPVIGGHAGKTIIPLISQCTPKVD--FP--QDQ---LSTLTGRIQEA
EcM   VAELKGKQPGEVEVPVIGGHSGVTILPLLSQ-VPGVS--FT--EQE---VADLTKRIQNA
HmM   LSEEFDAPVQNVEGTILGEHGDAQVPVFSKVRVDGTDPEFSGDEKE-----QL---LGDL
DfL   MGERLGVHSCSCHGWVIGEHGDSVPSVWSGMNVSIELHPLDGTNKDKQDWKKL---HKDV
BsL   LGYFSVAPQ-NVHAYIIGEHGDTELPVWSQAYIGVMPIRKLVESKGEEAQKDLERIFVNV

          240       250       260       270       280
           |         |         |         |         |
PmM   GTEVVKAKAGAGSATLSMAYAGARFVFSLVDAMNGKEGVVECSFVK-SQETDCPYFSTPL
EcM   GTEVVEAKAGGGSATLSMGQAAARFGLSLVRALQGEQGVVECAYVE-GDGQYARFFSQPL
HmM   QESAMDVIERKGATEWGPARGVAHMVEAILHDTGEVLPASVKLEGEFGHEDTA-FG-VPV
DfL   VDSAYEVIKLKGYTSWAIGLSVADLAETIMKHLCRVHPVSTMVKDFIGIKDNV-FLSLPC
BsL   RDAAYQIIEKKGATYYGIAMGLARVTRAILHNENAILTVSAYLDGLYGERDVY-IG-VPA

          290       300       310       320
           |         |         |         |
PmM   LLGKKGIEKNLGIGKISPFEEKMIAEAIPELKASIKKGEEFVKNM
EcM   LLGKNGVEERKSIGTLSAFEQNALEGMLDTLKKDIALGQEFVNK
HmM   RLGSNGVEEIVEWD-LDDYEQDLMADAAEKLSDQYDKIS
DfL   VLNDHGISNIVKMK-LKPDEEQQLQKSATTLWDIQKDLKF
BsL   VINRNGIREVIEIE-LNDDEKNRFHHSAATLKSVLARAFTR
```

Figure 4. Multiple alignment of hMDH (HmM) with pig mitochondrial MDH (PmM), *Escherichia coli* MDH (EcM), Dog fish L-LDH (DfL), and *Bacillus stearothermophilus* L-LDH (BsL).

It was previously shown that *Bacillus stearothermophilus* L-LDH can become MDH by one mutation that will convert Gln 100 into Arg (Q100R) (6). Having an *E. coli* expression system of hMDH, we were able to mutate Arg 100 of hMDH into Gln (R100Q). As a result of this mutation the specificity of hMDH was higher for pyruvate (the substrate of L-LDH) than for oxaloacetate (the substrate of MDH). The dependence of the activity of the mutated hMDH on salt concentration was dramatically changed as can be seen in Figure 5. First, the reduction of pyruvate by the mutated hMDH did not show substrate inhibition. The specific activity was higher at higher pyruvate concentrations. The specific activity decrease, however with salt concentration. The molecular basis for the differences between the dependence of the activity wild hMDH on salt concentration and that of the mutated hMDH is not clear yet. It seems, however, that these differences are due to the interaction of Arg 100 with the carboxylic group of oxaloacetate. In the mutated hMDH this Arg was replaced by Gln and the substrate pyruvate

has no more this carboxylic group.

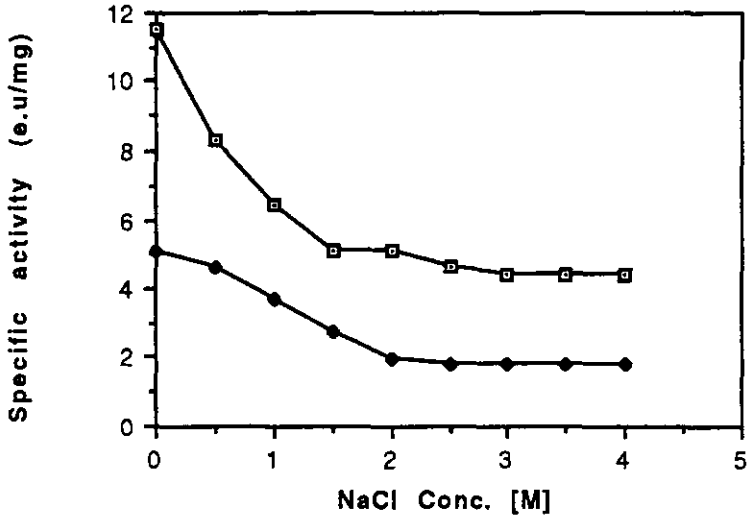

Figure 5. The effect of salt concentration on the enzymatic activity of mutated hMDH. Assays were performed using pyruvate concentrations of 1 mM ( ) or 10 mM ( ).

It seems that salt has effect on both, the enzymatic activity of hMDH and on its stability. In order to explain halophilic adaptation of enzymes, one has to ask first what is the main problem for enzymes at high salt concentration. It seems that the low water activities at high salt concentrations enhance intermolecular hydrophobic interaction which eventually cause aggregation of the proteins. In order to prevent this unspecific aggregation, halophilic enzymes acquired in the course of evolution high negative surface charge. Due to this surface charge, which is important to prevent unspecific aggregation, the halophilic proteins became dependent on salt for their stability. At low salt concentrations, the charges repel each other causing disruption of the secondary, tertiary and quartenary structures. It is still unclear why such high salt concentrations are needed to mask the surface charge. In principle, at 0.5 M salt most of the electrical potential must be masked. It is, therefore, possible that salt plays another role in the stabilization beyond mare masking of excess negative charge. Recently the three-dimensional structure of hMDH was determined (3) at a resolution of 3.2 Å. It is hoped that information obtained by the structure will provide a better understanding on the type of interactions are involved in the stabilization of the protein and what is role of salt.

References

Cendrin, F., Chroboczek, J., Zaccai, G., Eisenberg, H. and Mevarech, M. (1993) Cloning, sequencing, and expression in *Escherichia coli* of the gene coding for malate dehydrogenase of extremely halophilic archaebacterium *Haloarcula marismortui*. Biochemistry 32: 4308-4313.

Christian , J.H.B. and Waltho, J.A. (1962) Solute concentrationswithin cells of halophilic and non-halophilic bacteria. Biochim. Biophys. Acta 65: 506-508.

Dym, O., Mevarech, M. and Sussman, J.L. Structural features stabilizing halophilic malate dehydrogenase from an archaebacterium. Science (in Press).

Mevarech, M., Eisenberg, H, and Neumann, E. (1977) Malate dehydrogenase isolated from extremely halophilic bacteria of the Dead Sea. 1. Purification and molecular characterization. Biochemistry 16: 3781-3785.

Reistad, R. (1970) On the composition and nature of the bulk protein of extremely halophilic bacteria. Arch. Mikrobiol. 71: 353-360.

Wilks, H.M., Hart, K.W., Feeney, R., Dunn, C.R., Muirhead, H., Chia, W.N., Bartlow, D.A., Atkinson, T., Clarke, A.R. and Holbrook, J.J. (1988) A specific highly active malate dehydrogenase by redisign of a lactate dehydrogenase framework. Science 242: 1541-1544.

The function of a putative HCO_3^--transporter in the marine macroalga Ulva

Sven Beer
Department of Botany, Tel Aviv University
Tel Aviv 69978, Israel

ABSTRACT

Seawater contains HCO_3^- as its principal inorganic carbon (Ci) source, and marine macroalgae such as Ulva can use this carbon form in two ways: either via extracellular, carbonic anhydrase (CA)- mediated, dehydration followed by uptake of CO_2, or by direct HCO_3^- uptake. A model is presented in which these two systems operate alternatively in response to environmental conditions in various, or in the same, Ulva species. It is viewed that extracellular HCO_3^- dehydration is of relevance under conditions of low to medium photosynthetic rates while an inducible system of HCO_3^- transport, via a putative HCO_3^- transporter in the plasmalemma, is of importance under conditions conducive to high photosynthetic rates.

INTRODUCTION

Since the diffusion of solutes is orders of magnitude slower in liquids than in air, plants surrounded by water may face constraints in their uptake of major nutrients. This is especially true with regard to CO_2; if this nutrient is limiting for many terrestrial plants (mainly those of the C_3 type), then it should be suspected that also submerged macrophytes would be CO_2-limited. Another form of inorganic carbon, namely HCO_3^-, is present at much higher concentrations than CO_2 in water bodies of high enough pH to sustain submerged macrophyte life. However, although it is known that this ionic Ci form can be utilised by submerged plants, it has been shown that the mechanism(s) for its utilization in freshwater angiosperms restricts their photosynthetic yield (Beer et al. 1990). On the other hand marine macrophytes, and especially algae, showed a much higher efficiency of HCO_3^- utilization, and photosynthetic rates of this plant group seemed not to be limited by Ci acquisition (but rather by their carboxylating activity of ribulose-1,5-bisphosphate carboxylase/oxygenase (Rubisco) (Beer et al. 1990).

There are two recognised ways in which marine algae can utilize HCO_3^- (which at the seawater pH of 8.2 is present at a concentration 200 times higher than that of CO_2, i.e. 2 mM vs. 10 μM). The first way is by extracellular dehydration of the ionic carbon form so as to produce CO_2 adjacent to the photosynthesising cells (first suggested by Smith and Bidwell 1987). Since the dehydration of HCO_3^- is a slow process, there is a need for

extracellular/surface-bound CA to be active near the cell membranes. In addition, since the rate of HCO_3^- dehydration is strongly pH-dependent, such a system would contribute feasibly to the plants' Ci acquisition only if the surface-pH were not too high. Thus, it was shown that extracellular CA-mediated HCO_3^- dehydration could supply CO_2 for photosynthesis in several species of the common marine chlorophyte Ulva (Bjork et al. 1992, 1993). Contrary to this, it was found that the pH within the unstirred (diffusion-limited) boundary layer of another Ulva species was around 10 during steady-state photosynthesis (Beer and Israel 1990), and it was implied that extracellular HCO_3^- dehydration could at the most yield extremely low (in the nM range) CO_2 concentrations close to the plasmalemmae. Therefore, and since another Ulva form was found to lack activity of extracellular/surface-bound CA (Drechsler and Beer 1991), it was suggested that Ulva might transport HCO_3^- into its cells as a means of supporting high photosynthetic rates. Considerations regarding the two main possible ways of Ci acquisition in marine algae have been elaborated upon extensively in a recent review (Beer 1994), to which the interested reader is referred. The following is a summary of results which support the novel notion of a HCO_3^- uptake system in Ulva, while not disregarding HCO_3^- dehydration via extracellular/surface-bound CA under certain conditions. As will be shown, it is thus likely that this marine chlorophyte can support its Ci acquisition from seawater by both, or alternative, extracellular HCO_3^- dehydration and direct HCO_3^- uptake, and that there may be advantages of each system under different ecological conditions. A model for Ci acquisition in Ulva, taking both alternatives into consideration, will also be presented here for the first time.

A HCO_3^- TRANSPORTER IN ULVA?

In contrast to CO_2, HCO_3^- is a charged anion which does not diffuse easily through lipid bilayer membranes (Gutknecht 1977). Therefore, its uptake into cells would probably require facilitation by some type of membrane protein. As it was realised that Ulva fasciata lacked extracellular/surface-bound CA, it could be calculated that spontaneous HCO_3^- dehydration could not support photosynthesis in this plant, and that HCO_3^- uptake was in effect (Drechsler and Beer 1991). Inhibition of photosynthesis by other anions when HCO_3^-, but not when CO_2, was taken up indicated distinct uptake sites, and the inhibition by 4,4'-diisothiocyanostilbene-2,2'-disulphonate (DIDS) pointed specifically to an anion transporter (AE) which shared functional resemblances with the AE conveying HCO_3^- transport in red blood cells (there called AE1) (Cabantchik and Greger 1992). So far, the main physiological evidence for HCO_3^- transport in Ulva fasciata via an AE1-like anion transporter are based on 1) Inhibition of HCO_3^- uptake by DIDS (Drechsler and Beer 1991), as well as by other disulphonic stilbenes (Drechsler et al. 1993) which are known to inhibit HCO_3^- transport in red blood cells; 2) Inhibition of HCO_3^- uptake by pyridoxal phosphate and trypsin treatments, indicating the involvement of

lysine groups in the transport of HCO_3^- and the location of the putative transporter to the plasmalemma, respectively (Drechsler et al. 1993); 3) Inhibition of HCO_3^- uptake by phenylglyoxal and 1,2-butanedione, indicating the involvement of arginine groups in the collection and transport of HCO_3^- (Drechsler et al. 1994) and 4) A decrease in the photosynthetic affinity to Ci (measured as $1/K_{1/2}(Ci)$) with pH which parallelled the expected decrease in protonicity of an (amino) acid with a pK of 10 (Drechsler et al. 1994). In all, these responses indicated the function of an AE1-like protein within the plasmalemma which, via the high-pK amino acids lysine and arginine, could transport HCO_3^- into the cells.

In addition to the functional resemblances between HCO_3^- transport in Ulva fasciata and in red blood cells, structural similarities were indicated as well. It was found that three different antibodies raised against the human AE1 immuno-reacted with a light-membrane polypeptide of ca. 95 kDa (which is the same molecular weight as the human protein) extracted from Ulva fasciata (Sharkia et al. 1994). In spite of these positive results, a recent trial to hybridise cDNA from the human AE1 gene with genomic DNA from Ulva fasciata failed. Therefore, the degree of structural resemblance between the human and putative algal HCO_3^- transporter needs yet to be established (once the algal gene has been identified).

TWO SYSTEMS OF HCO_3^- ACQUISITION IN ULVA?

It emanates from the above that two system of HCO_3^- utilization can be present in Ulva, and that at least different species possess specific systems. However, in recent work in cooperation with Axelsson and his group in Sweden, we have also found that the ubiquitous Ulva lactuca could alter its mode of HCO_3^- utilization from extracellular HCO_3^- dehydration to HCO_3^- uptake in response to growth at high pH. It was found that this Ulva species, when taken from normal field conditions, possessed the activity of extracellular/surface-bound CA (implied by its sensitivity to the inhibitor acetazolamide), but showed no signs of an operating HCO_3^- transporter (as indicated by its insensitivity to DIDS). However, growing such thalli for 24 h in a flow-through system at pH 9.4 (thus limiting the availability of both CO_2 and HCO_3^-), completely reversed the response to the CA- and putative AE1- transporter inhibitors, and it seemed that the algae had thus switched from the extracellular CA-system to that of HCO_3^- transport. Simultaneously, the affinity for Ci at high pH (i.e. the affinity to HCO_3^-) had increased more than 6-fold, while the high affinity for CO_2 (at lower pH) was much less affected (Axelsson et al. 1994). In addition, recent results from a COST-48 workshop on Ulva carbon and light utilization (Kristineberg, Sweden, 1993) showed a similar transition from extracellular CA-mediated HCO_3^- dehydration to direct HCO_3^- uptake via the putative transporter following the addition of nutrients to the growth medium. These results are in conformation with the novel thought that Ulva can alter its ways of acquiring HCO_3^- according to its needs: Under

conditions of low light and low temperature, and possibly during nitrogen depletion, the dehydration of HCO_3^- via extracellular/surface-bound CA is enough to support its photosynthetic production rates. However, under condition conducive to high growth rates (i.e. high light and temperature and high nitrogen concentrations), the AE1-like transporter would be needed so as to support high photosynthetic rates. Under such conditions the unstirred boundary layer would acquire a high pH, and CO_2 concentrations would be extremely low in the vicinity of the plasmalemma while HCO_3^- concentrations would still be in the 0.1 mM range. While such a transition between extracellular-CA and AE1-like states has not been observed in nature, it is tempting to assume that the reason that Ulva lactuca in Sweden is often in its extracellular-CA state is related to the low temperature and light availability there, while in Israel Ulva fasciata is naturally in its AE1-like state because of the higher light and temperature regimes and the high nitrogen load in its coastal waters.

The following model is proposed for Ci acquisition in Ulva (Fig. 1). It is based on the findings that Ulva fasciata often lacks the activity of extracellular/surface-bound CA (depicted within the unstirred boundary layer, UBL, including the cell wall) and transports most of its HCO_3^- into the cells (1), apparently via the putative AE1-like protein, while Ulva lactuca can either transport HCO_3^- (1) or dehydrate it extracellularly CA (2) (depending on growth conditions). Subsequent events involve transport of Ci (probably HCO_3^-) at the chloroplast level (3). This transport is proposed to be present irrespective of the Ci form penetrating the cell membrane since a) both "extracellular-CA" and "AE1-like" Ulva lactuca have a high affinity for CO_2 (Axelsson et al. 1994) and b) there is no evidence that AE1-like-mediated HCO_3^- transport is an active process - in red blood cells, the EA1 transports HCO_3^- via facilitated anion exchange. Both types of Ci acquisition are seen as a first step in Ulva's CO_2 concentrating system, causing CO_2 to be concentrated to the site of Rubisco in the chloroplast (possibly within the pyrenoid), thus rendering Ulva efficient photosynthetic rates in which photorespiration is suppressed (as evidenced by Ulva's O_2-insensitive photosynthetic rates and low CO_2 compensation concentrations) (cf. Beer 1994). As said, it is proposed that the AE1-like system is of importance especially under conditions conducive to high photosynthetic rates in which the CO_2 (and HCO_3^-?) close to the plasmalemma would be "sensed" by the plant.

REFERENCES

Axelsson, L., Ryberg, H. & Beer, S. Two modes of bicarbonate acquisition in Ulva lactuca. Plant Cell and Environ. (in press) 1994.

Beer, S. Mechanism of Inorganic Carbon Acquisition in Marine Macroalgae (with Special Reference to the Chlorophyta) In: Progress in Phycological Research, Biopress Ltd., Bristol, England, 1994 (in press).

Beer, S. & Israel, A. Photosynthesis of Ulva fasciata. IV. pH, carbonic anhydrase and inorganic carbon conversions in the unstirred layer. Plant Cell Environ. 13: 555-560, 1990.

Beer, S., Sand-Jensen, K., Vindbaek Madsen, T. & Nielsen, S.L. The carboxylase activity of Rubisco and the photosynthetic performance in aquatic plants. Oecologia 87: 429-434, 1991.

Bjork, M., Haglund, K., Ramazanov, Z., Garcia-Reina, G. & Pedersen, M. Inorganic-carbon assimilation in the green seaweed Ulva rigida C. Ag. (Chlorophyta). Planta 187: 152-156, 1992.

Bjork, M., Haglund, K., Ramazanov, Z. and Pedersen, M. Inducible mechanisms for HCO_3^- utilization and repression of photorespiration in protoplasts and thalli of three species of Ulva (Chlorophyta). J. Phycol. 29: 166-173, 1993.

Cabantchik, Z.I. & Greger, R. Chemical probes for anion transport in mammalian cell membranes. Am. J. Physiol. 262: C803-C827, 1992.

Drechsler, Z. & Beer, S. The utilization of inorganic carbon by Ulva lactuca. Plant Physiol. 97: 1439-1444, 1991.

Drechsler, Z., Sharkia, R., Cabantchik, Z.I. & Beer, S. Bicarbonate uptake in the marine macroalga Ulva sp. is inhibited by classical probes of anion exchange by red blood cells. Planta 191: 34-40, 1993.

Drechsler, Z., Sharkia, R., Cabantchik, Z.I. & Beer, S. The relationship of arginine groups to photosynthetic HCO_3^- uptake in Ulva sp. mediated by a putative anion exchanger. Planta 1994 (in press).

Gutknecht, J., Bisson, M.A. & Tostesson, F.C. Diffusion of carbon dioxide through lipid bilayer membranes: Effects of carbonic anhydrase, bicarbonate and unstirred layers. J. Gen. Physiol. 69: 779-794, 1977.

Sharkia, R., Cabantchik, Z.I. & Beer, S. A membrane-located polypeptide which may be involved in the HCO_3^- transport of Ulva sp. is recognized by antibodies raised against the red blood cell anion exchange protein. Planta 1994 (in press).

Smith, R.G. & Bidwell, R.G.S. Carbonic anhydrase-dependent inorganic carbon uptake by the red macroalga, Chondrus crispus. Plant Physiol. 83: 735-738, 1987.

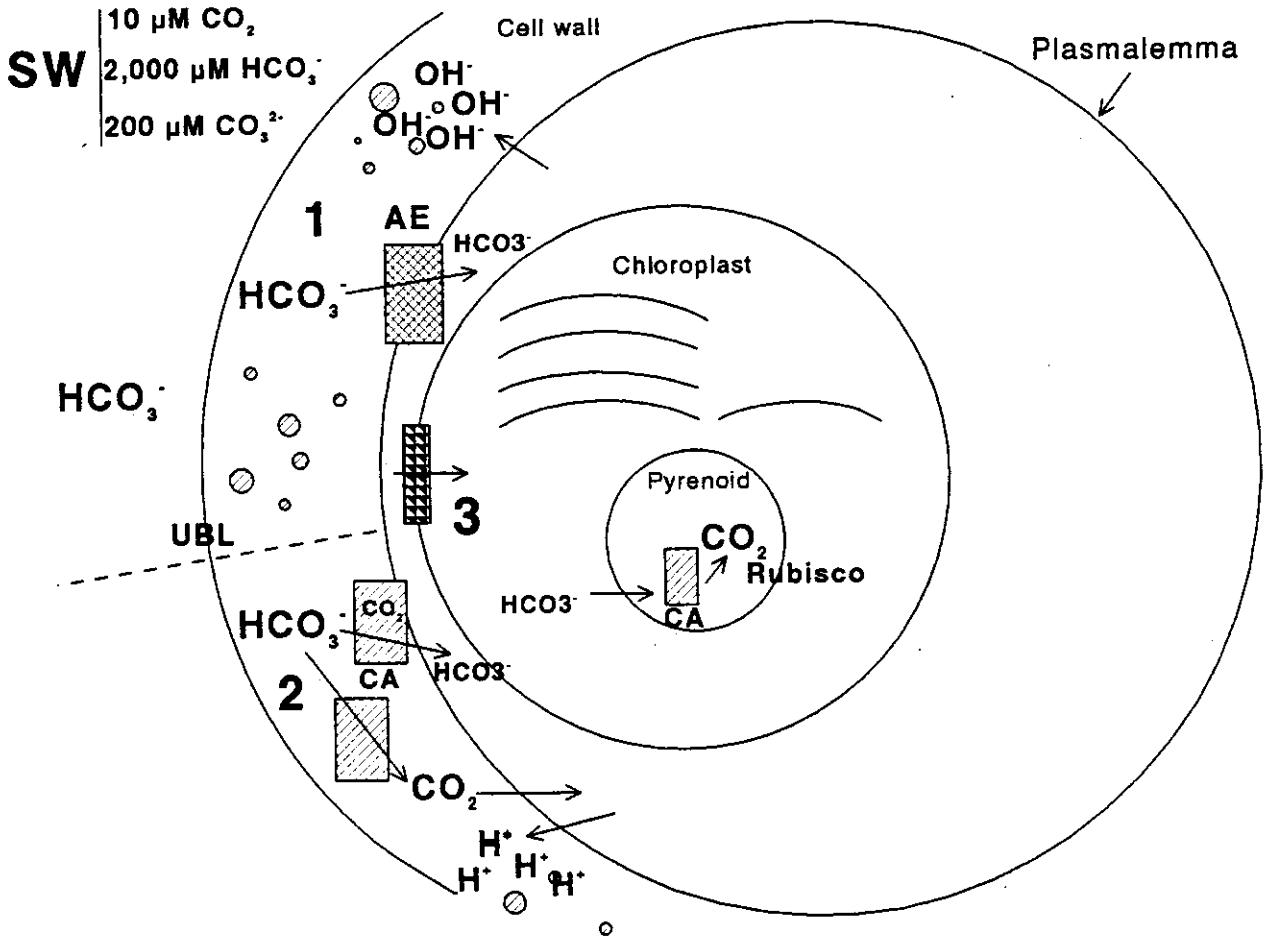

Fig. 1: A model of HCO_3^- utilization in Ulva (see text for explanations).

Bielefelder Ökologische Beiträge, vol. 8, (1995) p. 57 -6

ERETMOCERUS-BEMISIA TABACI ASSOCIATION, a case of morphological manipulation.

Dan Gerling[1], and Tamar Orion[1]
Dept. of Zoology, The George S. Wise Faculty of Life Sciences,
Tel Aviv University, Ramat Aviv, 69978 Israel;

Abstract

Eretmocerus species oviposit under their hosts and develop first as ectoparasitoids and later as endoparasitoids. Instars one and two are typified by a cellular vital capsule that envelops the developing parasitoid larva. We tried to answer two questions: What is the origin of the capsule cells, and what are the stages involved in larval engulfment in the capsule?

We found that the capsule originates in the epidermal cells of the host. They first proliferate *in situ.* then form a dome-shaped structure that later seem to develop into a spherical capsule. The very young *Eretmocerus* larva move actively into the capsule, squeezing its body through into the narrow entrance. The hatching first instar larva probably injects growth-regulating materials through a hole that it pierces in the venter of the host. These redirect the normal host tissues into capsule formation. We think that developing within a capsule that is produced by host epidermis, permits *Eretmocerus* to exploit the internal environment of the host without eliciting its internal defense reactions. Until the present time, this is the only parasitoid known to induce the formation of a hypodermal capsule in the host and exploit it for its development.

Key words: *Eretmocerus* - encapsulation - host-parasite interaction - host immunity - endoparasitism - parasitoid penetration.

Introduction

The genus *Eretmocerus* (Hymenoptera, Aphelinidae) contains exclusively parasitoids of whiteflies. All known developmental biologies are similar, inasmuch as the eggs are laid under whitefly nymphs and larvae after hatching, penetrate the host and develop as internal parasitoids (Gerling, 1990). Gerling *et al.* (1990) have shown that the whitefly host forms a cellular capsule around the parasitoid and that the parasitoid develops therein during its first two instars. The capsule does not melanize or harden but remains cellular and viable, and the larvae were never observed to develop without a capsule. During the third instar, the capsule tears and the parasitoid larva lives freely among the remnants of the

host.

Once the general pattern of events has been determined, we set out to establish the origin of the capsule. This is especially pertinent since, except for the findings of Matz *et al.* (1971), encapsulation has been attributed only to mesodermal cells, e.g., Nappi (1975) and Salt (1970).

Another intriguing question in this association is the mode of parasitoid penetration into the host. The mandibles of first instar *Eretmocerus* are lancet-shaped (Gerling, 1966) and, therefore, seem incapable of forming a round 47 x 55 μm hole (Gerling *et al.*, 1990). Thus, it seemed appropriate to investigate the mechanism by which the hole and capsule are formed.

Materials and methods

We used *Bemisia tabaci* as the host insect and *Eretmocerus* sp. from Arizona and California as the parasitoid. Whiteflies were grown on cotton plants in a growth chamber a about 27°C. They were parasitized by placing a leaf under a microscope and releasing an *Eretmocerus* female on them . All of the hosts under which oviposition was noted were mapped. The leaf was then incubated and the whitefly nymphs were examined as the experiments prescribed.

Examination was performed on whole mounts of parasitized *B. tabaci* nymphs fixed in 70% alcohol, stained in Acid Fuchsin and mounted in Euparal, and by examining 8 μm thick microtome sections that had been fixed in Brazil's fixative, embedded in paraffin, and stained in Delafield's eosin or Mallory's triple stain (Barbosa, 1974). In order to follow early penetration stages we fixed the parasitized whitefly with the leaf section on which it had been developing. Later stages were examined by using detached whitefly nymphs.

Results

Three days after oviposition the *Eretmocerus* larva was visible between the leaf and the whitefly nymph. Concurrently, the host's epidermal region immediately above the larva showed extensive cell growth and multiplication, causing it to grow in thickness and to fold inwards . Within a few hours, parasitoid larvae were observed partly engulfed within the growing epidermal proliferation. A constriction was often observed in the body of the parasitoid larva (Figs.1, 2), which suggested that while the epidermal cells form the future capsule, the larva actively moves upward into the capsule through a narrowing entrance hole. Finally, the larva can be seen within the complete capsule, where it molts into the second instar (Fig 3).

The first and second parasitoid larvae have extremely large (salivary?) glands (Figs. 2, 3), that open through ducts to the mouth. We assume that they provide secretory materials that serve in the first instar to regulate the capsule

formation, and to prevent normal host development. In both instars they probably redirect the host's metabolism to provide nutrients for the parasitoid inside the capsule.

Once the first and second instar larvae are within the capsule, they are surrounded by a non-cellular matrix that separates them from the wall of the capsule (Fig. 3). No mechanism by which the entrance hole of the capsule is plugged has been observed.

The lancet-shaped mandibles of the first instar are replaced in the second instar by triangular ones (Gerling, 1966), which can be seen moving up and down about the oral orifice in live preparations.

Discussion

Using our observations, we can reconstruct the following apparent sequence of events, leading to the establishment of the parasitoid in the host: The hatching larva resides with its posterior part in the chorion while its lancet-shaped mandibles penetrate the whitefly venter and host-regulating materials are injected. These materials probably originate in the very large glands that were observed (Fig. 3). As a result, epidermal cells of the host grow, form a dome-shaped structure, and engulf the *Eretmocerus* larva which, at the same time, moves actively into the forming capsule (Figs. 1, 2). The entrance hole and its proximity remain covered with cuticle; however, the anterior, particularly around the parasitoid's head is devoid of a cuticle. Shortly after penetration, the larva molts into the second instar.

References

Barbosa, P. 1974. Manual of Basic Techniques in Insect Histology. Autumn Publishers, P.O. Box 42, Amherst, Mass., 245 pp.

Clausen, C.P. and Berry, P.A. 1932. The citrus blackfly in Asia, and the importation of its natural enemies into tropical America. USDA Tech. Bull. 330: 1-58, Washington, D.C.

Foltyn, S. and Gerling, D. 1985. The parasitoids of the aleyrodid *Bemisia tabaci* in Israel: Development, host preference and discrimination of the aphelinid *Eretmocerus mundus*. Entomol. Exper. Appl. 38: 255-260..pa.pa

Gerling, D. 1966. Studies with whitefly parasites of southern California. 2. *Eretmocerus californicus* Howard (Hym.: Aphelinidae). Can. Entomol. 98: 1316-1329.

Gerling, D. 1990. Natural enemies of whiteflies, predators and parasitoids. In D. Gerling (ed.) Whiteflies, their Bionomics, Pest Status and Management. Intercept, Andover, UK. pp. 147-185.

Gerling, D., Orion, T. and Delarea, Y. 1990. *Eretmocerus* penetration and

immature development: A novel approach to overcome host immunity. Arch. Insect Biochem. Physiol. 13: 247–253.

Matz, G., Monier, Y. and Vago, C. 1971. Une réaction de défense cellulaire chez les insectes: l'enkystement epityhelial. Bull. Soc. Zool. France 96: 209–215.
Nappi, A.J. 1975. Parasite encapsulation in insects. In K. Maramorosch and R.E. Shope (eds.) Invertebrate Immunity, Mechanisms of Invertebrate Vector–parasite Relations. Academic Press, New York, pp. 293–326.
Salt, G. 1970. The Cellular Defense Reactions of Insects. Cambridge Univ. Press, Cambridge, England.

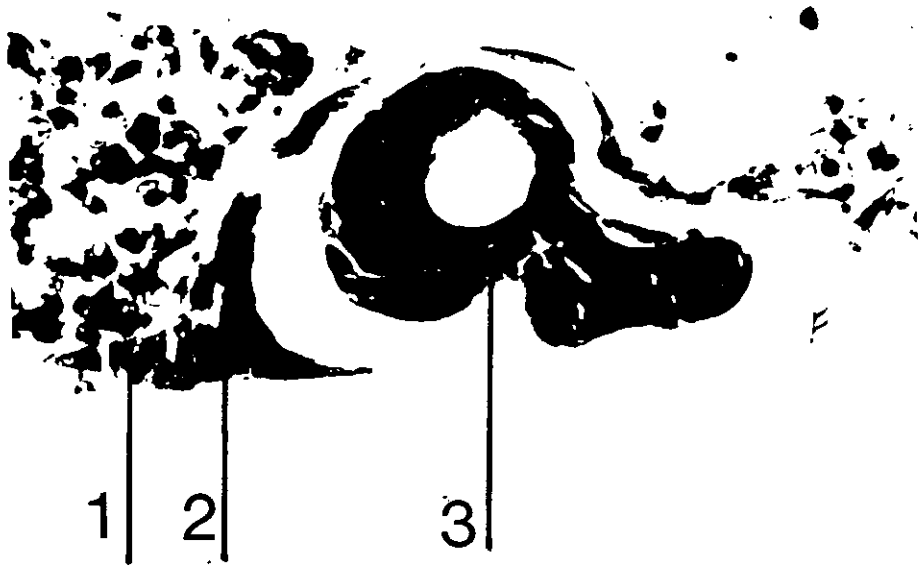

1. A first instar larva of *Eretmocerus* penetrating its whitefly host. 1– host tissue, 2– capsule being formed, 3– larva.

2. A first instar larva of *Eretmocerus* penetrating its whitefly host. A somewhat more advanced stage than in Fig. 1. 1- host tissue, 2- capsule, 3- larva, 4- salivary glands

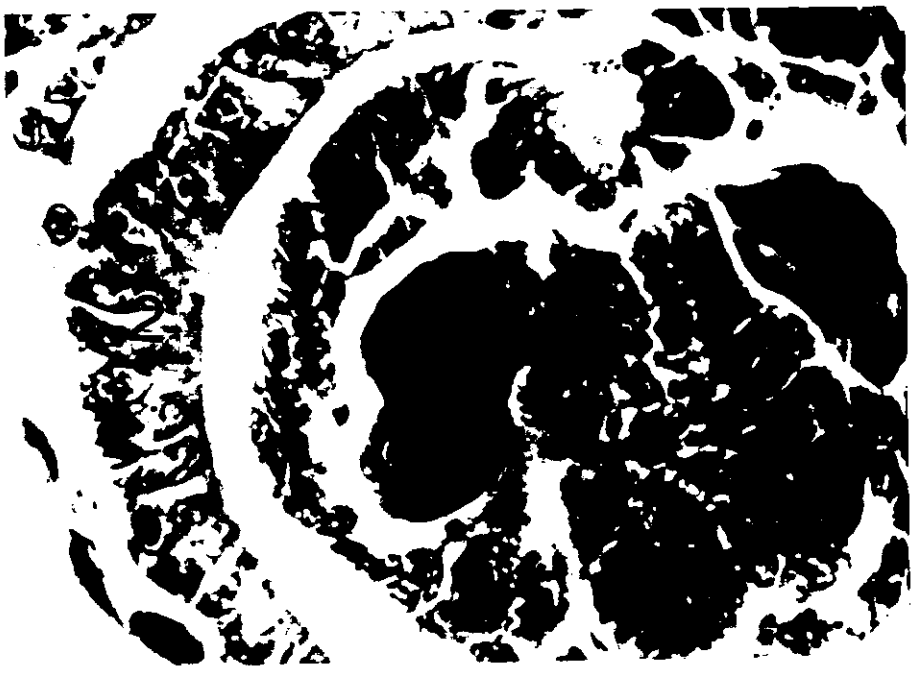

3. A second instar larva within the capsule. 1- larva, 2 capsule, 3 salivary glands.

Structural adaptations contributing to the biological function of the lateral line system of the clawed toad *Xenopus laevis*.

Peter Görner

Fakultät für Biologie der Universität, D - 33615 Bielefeld, Germany

Introduction

For a long time the lateral line system of lower vertebrates has been of great interest for both morphologists and physiologists because of its biological relevance, its great structural and functional diversity, and its close relationship to the organs of the inner ear. Its basic unit is the hair cell with a single kinocilium and numerous stereovilli. In the lateral line organ the hair cells are surrounded by supporting cells and mantle cells which secrete a cupula of jelly-like consistency. Together they form the neuromast. In fish most neuromasts are innervated by several afferent (and a few efferent) nerve fibers, in amphibians only by a few afferent (and up to three efferent) fibers. Several neuromasts may be innervated by the same afferent nerve fibers.

While in amphibians all neuromasts of the lateral line system are on the body surface, in fish part of the lateral line system is submerged in canals. The cells of the neuromast are embedded in the epidermis while the kinocilia and the stereovilli of the hair cells as well as the cupula protrude into the water. Thus, water movements parallel to the skin cause a displacement of the cupula together the kinocilia and the stereovilli. Theoretical considerations (Kalmijn 1989) and experimental evidence in surface feeding fishes (Bleckmann and Topp 1981) reveal that the adequate stimulus to the lateral line organ is not the displacement amplitude of the cupula, but the acceleration of its movement.

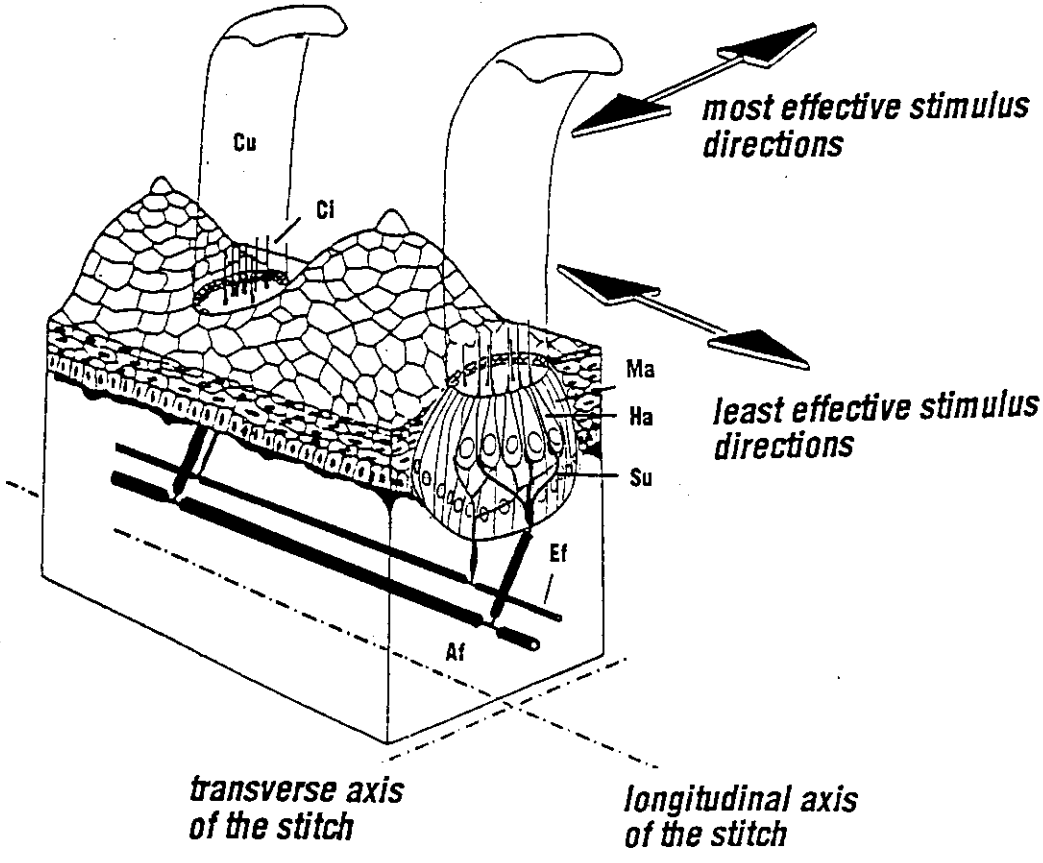

Fig. 1 Cross section through a neuromast of a stitch in the skin of *Xenopus laevis*. Only one of the afferent fibers is shown. Af afferent fiber, Ef efferent fiber, Ci kinocilium, Cu cupula, Ha hair cell, Ma mantle cell, Su supporting cell (From Görner 1963, redrawn by B. Claas).

Morphological adaptations in *Xenopus* to increase sensitivity

The lateral line system of the lower vertebrates shows several morphological adaptations to its function which shall be demonstrated in the clawed toad *Xenopus laevis*. Typical for a lateral line organ of *Xenopus* is the linear arrangement of groups of neuromasts, called stitches. Most stitches of the trunk lateral lines are innervated by two afferent and one to three efferent nerve fibers (Fig. 1). Each of the two afferents is connected to one of the two sets of hair cells which differ in the insertion of their kinocilium on the rim of the apical surface of the hair cell: in each of the sets they insert in two opposite directions, such that the axis of maximal sensitivity is perpendicular to the long axis of the stitch (see insert of Fig. 2). If stimulus angles other than 90° occur, the afferent response decreases with the cosine of the stimulus angle. At stimulus angles of 0° or 180° the fiber's activity does not change from its spontaneous rate. Angles from more than 180° to less than 360° suppress the activity (see Fig. 2).

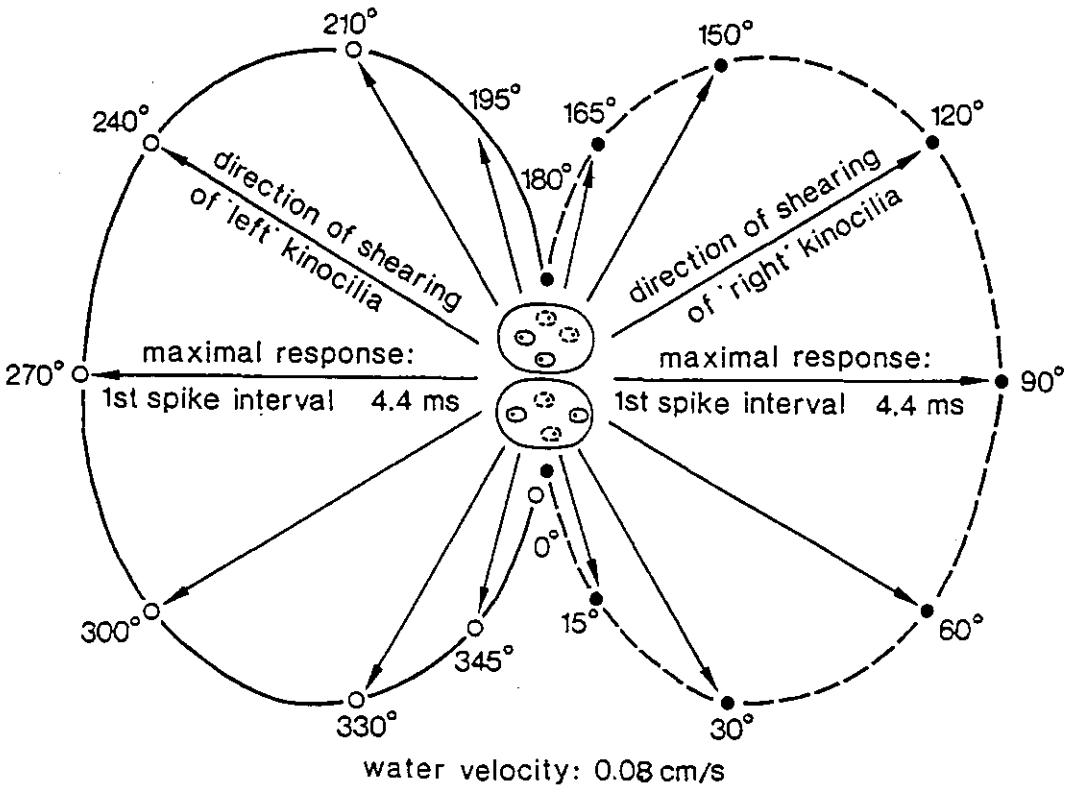

Fig. 2. Directional sensitivity of two afferent nerve fibers of a stitch of *Xenopus laevis* stimulated with a laminar water current. Two neuromasts (large ovals) with the apical surface of four hair cells each (small ovals) are shown schematically. The black dots within the sensory cells indicate the insertion of the kinocilium. The hair cells drawn with solid lines are depolarized by a water current from the right side; those drawn with dashed lines are depolarized by a water current from the left side. The lengths of the arrows express the amount of excitation of the correspondent afferent nerve fiber (from Görner and Mohr 1989).

The structure of the lateral line stitch in *Xenopus* seems to indicate that morphological adaptations evolved at several levels which all led to an increase in sensitivity. i) Since the kinocilium faces in the same direction in all hair cells innervated by the same afferent nerve fiber, all of them are stimulated with the same intensity. ii) The cupula acts as a lever arm to the sensory hairs whereby water moving parallel to the wide side of the ribbon-like cupula is the most efficient stimulus. This may also enhance the directional sensitivity. Moreover, while the cupula will easily be bent by forces acting on its wide side, it is less flexible to forces acting against its narrow side. Thereby the stimulus will most efficiently be transmitted to the basal part of the cupula, i.e. to the

kinocilia and stereovilli. iii) Between two adjacent neuromasts the epidermis folds into a hillock. The groove between two hillocks allows the water flow to hit the basal part of the cupula from the most effective direction. Another effect of the hillocks is to protect part of the cupula and the kinocilia from mechanical damage.

Does the directional sensitivity of a stitch explain the directional response of *Xenopus*?

The arrangement of the stitches on the epidermis of *Xenopus* indicates that almost all stimulus directions can be analyzed with optimal sensitivity: on the head up to 20 stitches of the preorbital and supraorbital line surround the eye, thus facing in many different directions; on the trunk the upper and middle lateral line stitches are arranged orthogonally. At stimulus angles between the orthogonal rows of neuromasts the response of these stitches will be at least 70% of the maximal response (cosine 45° and cosine 135° = 0.7). One may conclude that the directional sensitivity of the stitches explains the excellent directional responses of clawed toads in behavioral experiments (e.g. Elepfandt 1982, Görner et al 1984). We tested this hypothesis and stimulated single stitches of a clawed toad with a water jet (Görner and Mohr 1989). These experiments revealed that it is not the direction of the stimulus which is essential for the turning response of *Xenopus*, but the side where the stitch is located on the body: toads whose lateral line system was completely lesioned on the left side turned predominantly towards the right side, irrespective of the direction from which the water jet hit the stitch. Similar results were obtained by Müller and Schwartz (1982) in the surface feeding fish *Aplocheilus lineatus*.

But if the directional sensitivity of a stitch obviously does not give the toad information about the stimulus direction, how can the toad's well-directed behavioral response be explained when it is stimulated with surface waves? When a surface wave passes over a clawed toad in shallow water the stitches of the lateral line system are stimulated one after the other with different intensities (according to their location on the body surface, and to what extend the cupulae are accelerated). Obviously the toad is able to evaluate the direction of the surface wave from the time-intensity pattern of the stimulated stitches. This can be deduced from the same experimental series described above, in which we stimulated the toads (with an intact lateral line system only on one side) with surface waves from different directions. In this case they turned correctly towards all stimulus directions, as completely intact toads do.

What is the functional significance of the directional sensitivity of a stitch?

The results of the experiments lead to the question of the functional significance of the directional sensitivity. I presented arguments that the complex structure of a stitch has evolved to increase its sensitivity. Although a single stitch is maximally sensitive in only two opposite directions (see above), this is no disadvantage for the toad: as mentioned before, the axes of the stitches on the skin of *Xenopus* vary in orientation direction. That means, most stimuli elicit a maximal or nearly maximal response in at least some of the stitches. Obviously, it is of greater advantage for the toad to develop a limited number of stitches, each optimized for sensitivity, than to arrange the sensory cells irregularly. The latter configuration would result in the system gaining a large set of different directional responses but losing sensitivity.

The meaning of an increase in number of neuromasts in a stitch: redundancy or enhancement of sensitivity?

In a stitch of *Xenopus* up to 12 or more neuromasts are arranged in a line (see Mohr 1994). What is the functional significance of the evolution of so many identical units if they are innervated by the same afferent fiber? There is evidence that the sensitivity of a stitch increases with an

increasing number of neuromasts (Mohr 1994). In electrophysiological experiments the activity of an afferent nerve fiber of a stitch of *Xenopus* was recorded while the toad was stimulated with surface waves. The number of spikes increased significantly from stitches with one to those with five neuromasts (Fig. 3). A different interpretation is that numerous neuromasts in a stitch may have been evolved to increase the signal-to-noise ratio, or simply to provide redundant information. This possibility is not unlikely since the fragile cupula of a neuromast may easily be damaged when the skin of the toad contacts obstacles in the water. There is also evidence for this interpretation. As mentioned above, stitches with five or six neuromasts are more sensitive than those with only a few neuromasts. A further increase of sensitivity with an increasing number of neuromasts, however, could not be observed. Obviously additional neuromasts above six provide only redundant information.

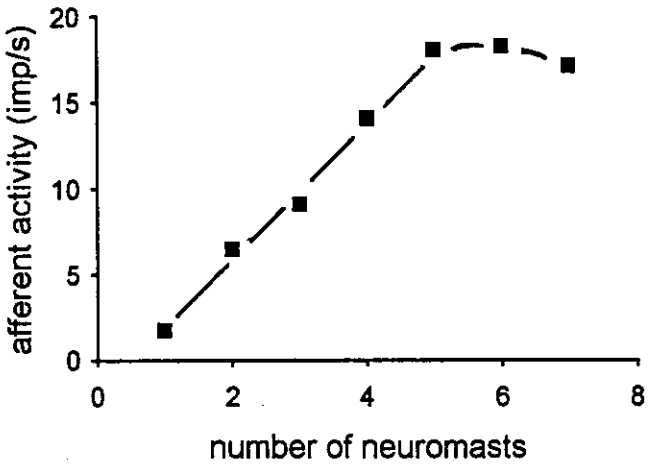

Fig. 3 Median values of the evoked activity of the afferent nerve fibers in *Xenopus laevis* (ordinate) and number of active neuromasts in stitches in which the neuromasts were successively destroyed (abscisse) (From Mohr 1994).

The afferent innervation pattern of stitches on the head and on the trunk: increase in spatial resolution or increase in sensitivity?

Many questions still have to be solved. E.g. the occipital and the auditory lateral line seem to play a predominant role in *Xenopus* for the localization of a surface wave (Görner et al 1984; Schmitz 1991; Claas 1994). Most stitches of these lines are innervated by more than two nerve fibers (Mohr 1994). This may indicate an enhanced spatial resolution. Although the number of stitches is less in the head area than in the trunk area, the number of nerve fibers is approximal the same in both areas. This may lead to a greater overall sensitivity in stitches on the trunk, while in those on the head the spatial resolution may be better.

Outlook

Many further investigations on the neuroanatomy and electrophysiology of the central pathways, the central neuronal data processing, as well as behavioral experiments, have to be done in *Xenopus*. These may help us to approach an understanding of the biological relevance of the lateral line system in only one of the many lower vertebrates provided with this multi-functional sense organ. With the knowledge of the structure and function of the periphery alone - the lateral line stitches - we have (perhaps) solved a fraction of all the questions on its biological significance.

Acknowledgments. My thanks are due to my wife, Dr. Ursula Görner, to Dr. Axel Schmid and to Dr. Mike Landolfa for critical reading the manuscript. Dr. Barbara Claas kindly improved Fig. 1.

References

Bleckmann H., Topp, G. (1981) Surface waves sensitivity of the lateral line organs of the topminnow *Aplocheilus lineatus*.-Naturwissenschaften 68:624-625.

Claas B. (1994) Wie analysiert das Seitenliniensystem die Laufrichtung von Oberflächenwellen? Untersuchungen am Krallenfrosch *Xenopus laevis* D.-Habilitationsschrift an der Fakultät für Biologie der Universität Bielefeld.

Elepfandt A. (1982) Accuracy of taxis response to water waves in the clawed toad (*Xenopus laevis* Daudin) with intact or with lesioned lateral line system.-J. Comp. Physiol. 148:535-545.

Görner P., Mohr C. (1989) Stimulus localization in *Xenopus*: Role of directional sensitivity of lateral line stitches. In: Coombs S., Görner P., Münz H. (Eds.): The Mechanosensory Lateral Line: Neurobiology and Evolution. Springer-Verlag New York, Berlin, Heidelberg. p 543-560

Görner P., Moller P., Weber W. (1984) Lateral-line input and stimulus localization the African clawed toad *Xenopus sp*.-J. Exp. Biol. 108:315-328.

Kalmijn A. (1989) Functional evolution of the lateral line and inner ear sensory systems. In: Coombs S., Görner P., Münz H. (Eds): The Mechanosensory Lateral Line: Neurobiology and Evolution. Springer-Verlag New York, Berlin, Heidelberg. p 187-215.

Mohr C. (1994) Innervationsmuster des Steitenliniensystems des Krallenfrosches *Xenopus laevis* und die funktionelle Bedeutung der Neuromastenzahl in einer physiologischen Einheit.-Dissertation an der Fakultät für Biologie Bielefeld der Universität Bielfeld.

Mohr C., Görner P., Münz H. (1989) Relation between the afferent activity and the number of neuromasts in a stitch of the lateral line system of *Xenopus laevis*. Proc. 18th Göttingen Neurobiol. Conf. G. Thieme Stuttgart, New York. p 164.

Müller U., Schwartz E. (1982) Influence of single neuromasts on prey localizing behavior of the surface-feeding fish, *Aplocheilus lineatus*.-J. Comp. Physiol. 149:399-408.

Schmitz A. (1991) Temporäre, partielle Läsionen am Seitenliniensystem des Krallenfrosches *Xenopus laevis*.-Diplomarbeit an der Fakultät für Biologie der Universität Bielefeld.

Structure and function of the prefrontal cortex in Gerbils (Meriones unguiculatus). Alteration of behavior after an early single dose of methamphetamine.

R. Czaniera, Dept. Neuroanatomy, University Bielefeld.

Structure of the prefrontal cortex

The prefrontal cortex (PFC) (Fig. 1) makes up a great portion of the frontal lobe and undergoes progressive expansion and architectonic differentiation in higher animals, reaching its greatest development in man. In mammals the PFC has been defined as the cortical projection field of the mediodorsal thalamic nucleus (MD) and of the ventral tegmental area (VTA; neurons of the mesoprefrontal dopamine (DA) system). On the basis of the MD projection, the PFC in the rat is divided into two subregions, one occupies the medial aspect of the hemisphere anterior of the genu of the corpus callosum (medial PFC), and the other one is confined to the dorsal bank of the rhinal sulcus (orbital PFC). The subregions (Fig. 2) can be distinguished by their anatomical characteristics, cytoarchitecture, afferent and efferent connections, and by differences in involvement in certain brain functions (Groenewegen 1988, Uylings und Van Eden 1990).

Among the PFC connections, the projection from the MD and the dopaminergic projection from the VTA seem to be the most prominent ones. Destruction of either one of these connections has been found to disrupt PFC functioning dramatically, in rats as well as in humans (review in Uylings and Van Eden 1990).

Function of the PFC

The PFC is important in temporally ordering and planning actions. PFC damage in animals, of which the rat and the monkey are the most commonly studied species, also results in deficits of temporal ordering of events, expressed in cognitive behavioral tasks as delayed response and delayed alternation tasks. The PFC also has been implicated in the process of behavioral inhibition. According to this view, one of the functions of the PFC is to enable organisms to inhibit or withhold responding. Thus, interference with PFC functions removes these inhibitory control over behavior, which could lead to increased responding during passive avoidance, or increased motor activity (review in De Bruin et al. 1983).

The behavioral functions of brain DA have been the focus of intense scientific investigation for several decades. The preponderance of work has centered upon the nigrostriatal DA system and its involvement in motor function and Parkinson's disease, as well as the nucleus accumbens and its links to locomotor activity and motivational processes. Comparatively fewer studies have investigated the behavioral functions of the mesoprefrontal DA-System. Considerable evidence indicates that the DA innervation of the PFC is involved in responsiveness to stress (Deutsch und Roth 1990). DA depletions in the PFC have been demonstrated to impair performance on delayed alternation tasks in both rodents and monkeys. In addition, studies indicate that increases in spontaneous or stimulant-induced motor activity can occur after ablations of PFC-tissue or depletions of prefrontal DA (review in Kolb 1984, Kolb und Whishaw 1993)

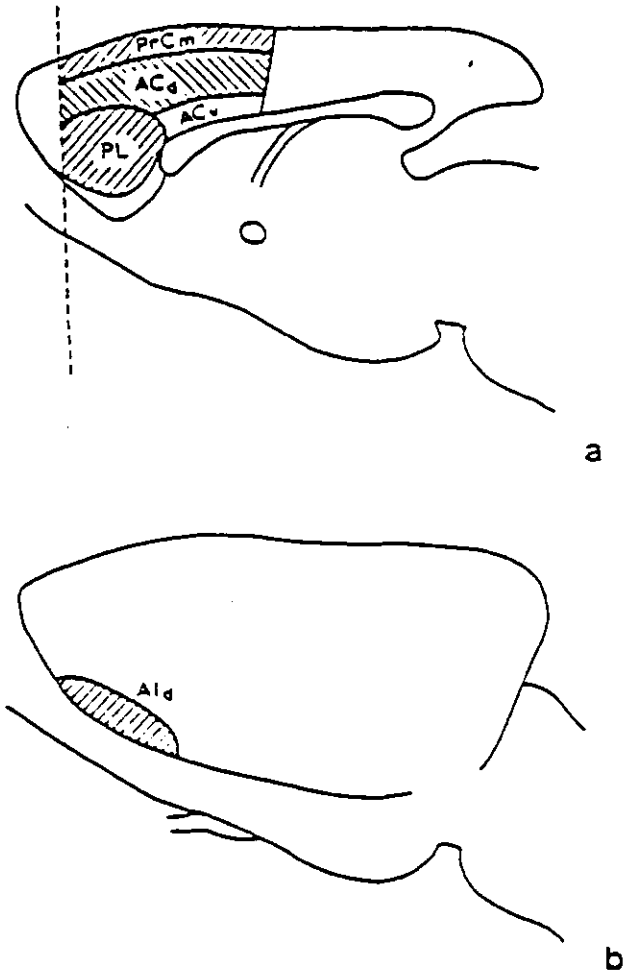

Fig. 1:
Sheme of the rostrocaudal extent of the PFC subareas (a) and the lateral surface of the cerebral hemisphere (b) (Van Eden und Uylings 1985b)

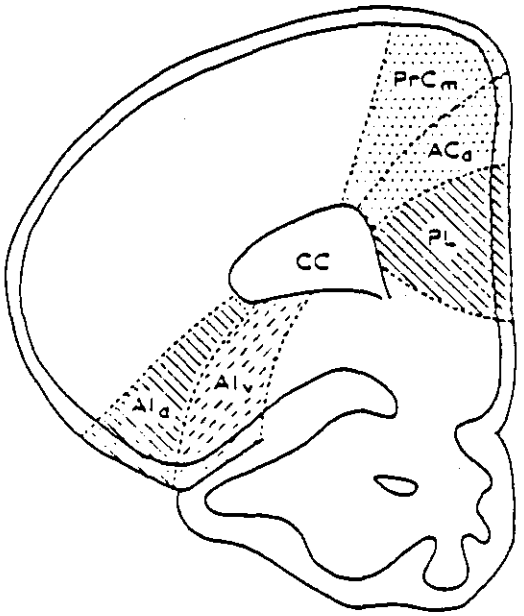

Fig. 2:
Diagram of the transsectional aspect of the left frontal pole of the gerbil brain. Hatchings indicate the relations of the cyto–architectonical subareas with the subnuclei of the mediodorsal thalamic nucleus (Van Eden und Uylings 1985a)

Abbreviations

ACd	dorsal anterior cingulate cortex (medial PFC)
ACv	ventral anterior cingulate cortex (medial PFC)
PL	prelimbic cortex (medial PFC)
PrCm	medial precentral cortex (medial PFC)
AId	dorsal agranular insular cortex (orbital PFC)
AIv	ventral agranular insular cortex (orbital PFC)

The prolonged development of the PFC

It appears that the age at which PFC lesions first produce a behavioral effect is relatively late as compared with other cortical areas. This finding was taken as an indication for a relatively late functional maturation of the PFC. The volumetric growth pattern of the PFC also points to a delayed and prolonged maturation ot the PFC, as compared with the visual cortex. The late volumetric and functional development of the PFC is related to the maturational process in the mesoprefrontal DA–System (Van Eden und Uylings 1985a).

Data of our investigations to the maturation of the DA innervation during postnatal development of the PFC in gerbils (*Meriones unguiculatus*) show that the quantitative maturation of the prefrontal DA innervation is characterised by a clearly delayed course. There is reason to argue that

mesoprefrontal DA projections may be an important determinant in the morphogenesis of the PFC. The delayed quantitative maturation of prefrontal DA innervation appears to be a valid structural correlate of the prolonged functional maturation of this brain area (Dawirs et al. 1993).

The postnatal maturation of DA innervation in the PFC is sensitive to an early single dose of Methamphetamine

At our institute DA-immunoreactivity was investigated in the PFC of 90 day old adult male gerbils after they had received a single dose of either methamphetamine (MA) (50 mg/kg; i. p.) or saline at the age of postnatal day 14. For that purpose, a selective and sensitive antibody directed against glutaraldehyde–conjugated DA was applied. All detectable fragments of DA-immunoreactive fibers were identified in consecutive frontal sections of the pregenual PFC, and their total numbers and total length were determined in the medial PFC and orbital PFC. The results indicate that a single application of MA during early postnatal development caused a significant and severe restraint of the subsequent maturation of the prefrontal DA-innervation. The solitary pharmacological challenge entailed final adult innervation densities which were about 38% (medial PFC) and 50% (orbital PFC) below those of the controls (Fig. 3) (Dawirs et al. 1994).

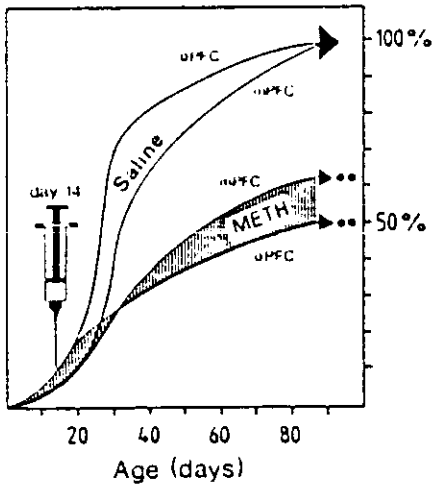

Fig. 3:
Effect of a single early dose of MA (50 mg/kg; i. p.) on the maturation of prefrontal DA-innervation considering general postnatal growth pattern of immunoreactive fibers; orbital PFC (oPFC) and medial PFC (mPFC) ; significant differences in adult innervation densities; $P \leq 0{,}01$ (**) (Dawirs et al. 1994)

The adult performance of delayed alternation tasks in gerbils is sensitive to an early single dose of MA

Most informations on MA neurotoxicity result from experiments on continuous or intermittant applications. Moreover it could be shown that a single dose of MA causes neurotoxic effects in developing and adult gerbils specifically in the PFC (Teuchert–Noodt et al. 1991, Dawirs et al. 1991). Additionally it was reported that an early single dose of MA, injected on postnatal day 14, restrains the dopaminergic innervation pattern in the PFC of adult gerbils (Dawirs et al. 1994).

Furthermore it has long been known that young immature brains are more capable than adult ones of compensating for functional disturbances induced by lesioning. Therefore sparing of function after early lesions should depend on the plastic capacity of neurons which is particular distinct during maturation of the brain. Nevertheless, these qualifications seem to be limited (Dawirs et al. 1994).

Recovery of function should be distinguished from sparing of function: The term *recovery of function* has been used in relation to the improvement, either partially or completely, of immediate behavioral impairments over time. Recovery of function is generally used to imply a regaining of functions identical to those that were impaired in response to the brain damage (Van Hof und Mohn 1981). Using this definition , recovery should be distinguished from *sparing of function*. This term is used when brain damage does not lead to the specific deficits which are expected on the basis of location and extent ot the lesions. Such a phenomenon can be observed when damage is inflicted in the developing nervous system. For example, damage to the PFC in adult rats results in an impaired performance of their spatial delayed alternation behavior. However, when a similar lesion is made in a young animal, it can perform this task as well as controls in adulthood. It would not be correct to use the term recovery in this context, since the damage occurs at a time that the function is not yet present (De Brabander et al. 1991).

Against this background, it is of particular interest to know in which way and how far early pertubation of prefrontal DA–functions might affect functional maturation of the PFC. In the present study the performance of *delayed alternation tasks* were compared between young adults, either being treated with MA or with saline as early juveniles.

Material and Methods

Subjects: 20 male gerbils: they were housed individually. On day 90 they started with the behavioral procedure.

Apparatus: The apparatus was a Y–maze (Fig. 4). Guillotine doors could be mounted at the entrance to each arm, used to directe the forced runs. Food cups, containing food pellets as reinforcers was located at the end of each arm. The guillotine–door of the start room could be opened automatically by an electromagnetic control mechanism.

Behavioral Procedure: *Habituation and Pretraining:* On 5 consecutive days the animals were habituated in the Y–maze. After this habituation period (on day 6) the animals were pretrained on 8 consecutive days. After a 2 minute stay in the start room the electromagnetic controlled guillotine door were raised automatically to give access to the choice–alley. Only one arm were baited with a food–cup, filled with pellets. The animal had to run in this baited arm and had to return with a food pellet in the start room. There the animal could consume the pellet. After this run the opposite arm were baited with, during the food–cup of the first run were taken out and the animal had to enter the new baited arm. Each animal had 20 runs on each day. The first run of each day was chosen randomly. All further runs were practiced in a closed alternated sequence.

Training: On the next 7 consecutive days the animals were trained in pairs of 10 trials of alternation training in a session. On the first (forced) run in the pair trial, a guillotine door blocked one of the arms of the Y–maze; the animal could consume the pellet and could immediately start to a free–choice run with no delay (O sec. intertrial interval). On this run, both arms were opened. The animal had to run in the arm opposite to the forced run. The forced runs of the pair trials were chosen in a random order. If the gerbil entered the same arm as on the forced run, an incorrect response was recorded and the animal was returned to the start room. The interval between the pair trials were 1 minute. During this time the animals waited in the closed start room. This alternation training was continued until all rats reached a criterion of 70% or more correct responses over the last three training sessions.

Test: On day 21 the delayed alternation test was started for 7 consecutive days. In the test a delay between the forced run and the free choice run was introduced for 15 seconds in a random order. 10 pair runs were made for the daily session. During the delay, the animals were placed in the start room.

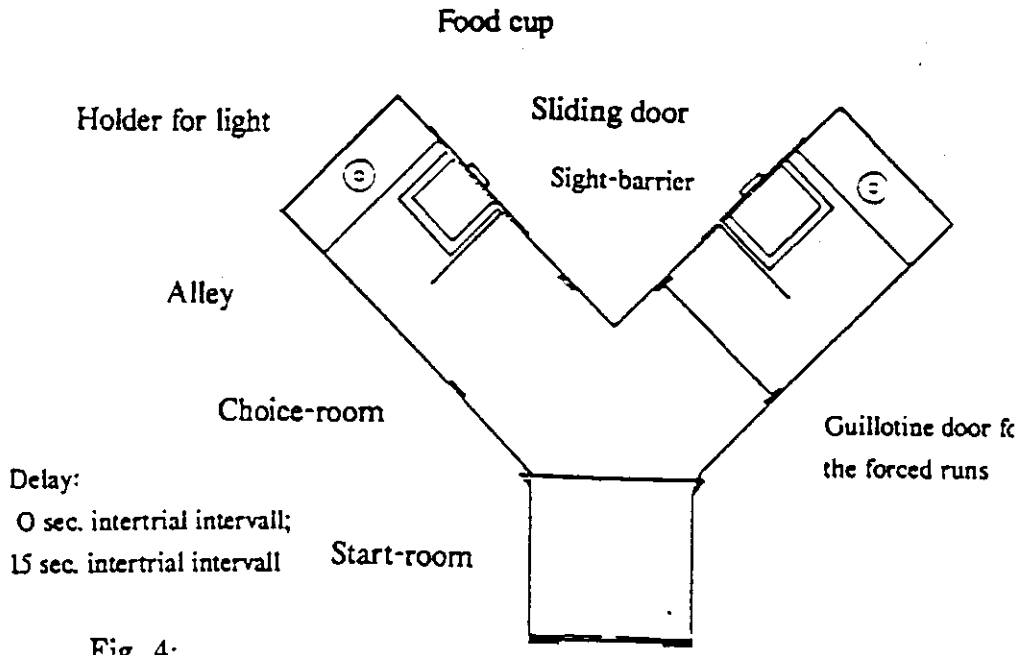

Fig. 4:
Y-maze

Results

Delay: 0 sec. intertrial interval
Means of errors in 10 choices per daily session

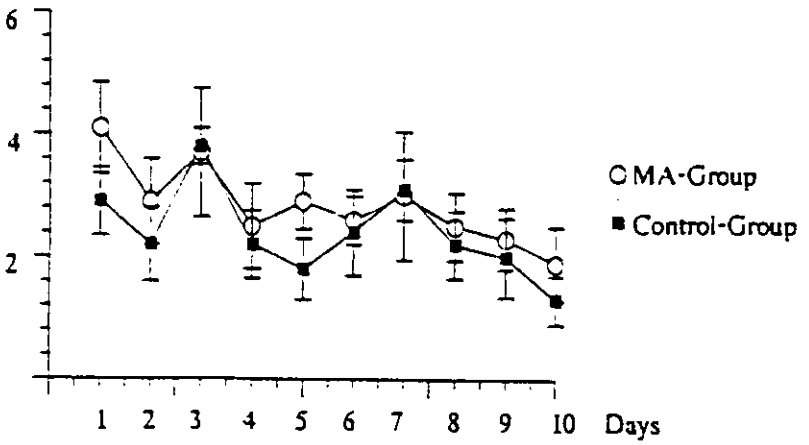

Fig. 5:
Shown are total nr. of errors (SD) per session during the 10 days with a 0-sec. intertrial interval. Two-way ANOVA with multiple measures revealed no significant effect between the MA- and the control-group

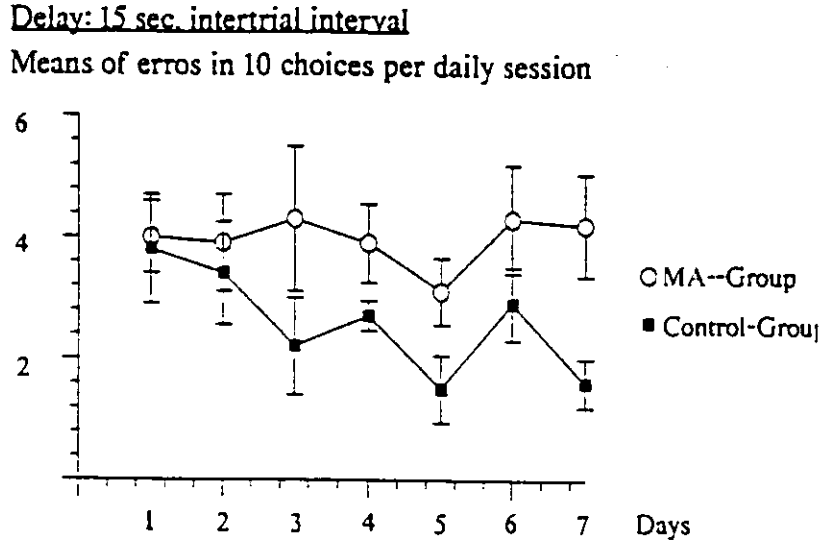

Fig. 6:
Shown are total errors (SD) per session during the 7 days with a 15 sec. intertrial interval. When a delay of 15 sec. is imposed between the trials, the MA-group make significant more errors. Two-way ANOVA with multiple measures revealed a significant effect of MA treatment ($P \leq 0{,}001$)

Conclusion

From the present studies there is now ample evidence that a single drug-induced stimulation of prefrontal DA-function in juveniles causes a significant suppression of proliferating DA-fibers and lead to severe deficits in PFC-related behavior.

It has been shown that, as a rule, after early lesioning of the PFC mammals reveal an inconspicuous behavioral development (sparing of function), whereas comparable lesions in adults lead to acute and persistant behavioral deficits (De Brabander et al. 1991). We further know that an intact mesoprefrontal DA-system is a prior condition for the normal functioning of the PFC. Therefore, lesions selectively directed to DA-terminals of adult animals, e. g. by local application of 6-hydroxydopamine (neurotoxin) or by bilateral thermal coagulation of the VTA, lead to behavioral deficits comparable to those following mechanical local ablation of prefrontal target fields, that is for instance disruption of delayed response (De Brabander et al. 1991).

Although the basic mechanisms for functional compensation (sparing of function) after early lesions are not yet understood, there are few indicati-

ons to the probable implication of ingrowing DA–afferents for the adaptive maturation of the PFC (De Brabander et al. 1991). However, in the case of a systemical MA–intoxication, one has to start from the principle that all prefrontal axon terminals of sensitive DA–neurons become equally affected, and are finally lost. Thus, we understand that a single early dose of MA not only causes an acute lesion, but can totally delete the entire prospective innervation capacity of the projection neurons concerned. From the present results we may further conclude that these increasing innervation deficits were obviously not substituted by hyperinnervation on intact ("MA–insensitive") DA–neurons.

In *conclusion*, it was demonstrated that a single intensive stimulation of the mesoprefrontal DA–system during early postnatal development may significantly interfere with the maturation of the adult behavioral repertoire.

Literature

Dawirs, R. R., Teuchert–Noodt, G., Czaniera, R. (1993) Maturation of the dopamine innervation during postnatal development of the PFC in gerbils (Meriones unguiculatus). A quantitative immunocytochemical study. J. Brain Res. 3: 281–290.

Dawirs, R. R., Teuchert–Noodt, G., Czaniera, R. (1994) The postnatal maturation of DA innervation in the PFC of gerbils (Meriones unguiculatus) is sensitive to an early single dose of MA. A quantitative immunocytochemical study. J. Brain Res. 35: 195–204.

De Brabander, J. M., De Bruin, J. P. C., Van Eden, C. G. (1991) Comparison of the effects on neonatal and adult medial prefrontal cortex lesions on food hoarding and spatial delayed alternation. Behav. Brain Res. 42: 67–75.

De Bruin, J. P. C., Van Oyen, H. G. M., Van de Poll, N. E. (1983) Behavioral changes following lesions of the orbital prefrontal cortex in male rats. Behav. Brain Res. 10: 209–232.

Deutsch, A. Y., Roth, R. H. (1990) In Uylings, H. B. M., Van Eden, C. G., De Bruin, J. P. C., Corner, M. A., Feenstra, M. G. P. (eds): The PFC: Its structure, function and pathology. Progress in Brain Research, Vol. 85, Elsevier, Amsterdam. pp. 367–403.

Groenewegen, H. J. (1988) Organization of the afferent connections of the mediodorsal thalamic nucleus in the rat, related to the mediodorsal–prefrontal topography. Neuroscience 24: 379–431.

Kolb, B. (1984) Functions of the frontal cortex of the rat: A comparative review. Brain Res. Rev. 8: 65–98.

Kolb, B., Whishaw, I. Q. (1993) Neuropsychologie, Spektrum Verlag, Heidelberg: pp. 250–278.

Teuchert–Noodt, G., Dawirs, R. R. (1991) Age–related toxicity in PFC and caudate–putamen complex of gerbils (Meriones unguiculatus) after a single dose of MA. Neuropharmacology 7: 733–743.

Uylings, H. B. M., Van Eden, C. G. (1990) Qualitative and quantitative comparison of the PFC in rat and in primates, including humans. In Uylings, H. B. M., Van Eden, C. G., De Bruin, J. P. C., Corner, M. A., Feenstra, M. G. P. (eds): The PFC: Its structure, function and pathology. Progress in Brain Research, Vol. 85, Elsevier, Amsterdam. pp. 31–62.

Van Eden, C. G., Uylings, H. B. M. (1985a) Cytoarchitectonical development of the PFC in the rat. J. Comp. Neurol. 241: 253–267.

Van Eden, C. G., Uylings, H. B. M. (1985b) Postnatal volumetric development of the PFC in the rat. J. Comp. Neurol. 241. 268–274.

Van Hof, M. W., Mohn, G. (1981) Functional recovery from brain damage. Development in Neuroscience, Vol. 13, Elsevier, North–Holland Biomedical Press, Amsterdam.

Bielefelder Ökologische Beiträge, vol. 8, (1995) p. 79 -8

Structural Aspects of Root Systems

Amram Eshel and Iris Tamir, Dept. of Botany,
The George S. Wise Faculty of Life Sciences, Tel-Aviv University

Introduction

Some of the most important functions of plant root systems namely water uptake, nutrient uptake and anchorage, which is the result of adhesion of the roots to the soil, take place at the root surface. Therefore, these processes are directly proportional to the size of the root surface area. Increase of root surface area is brought about by root branching and by root elongation. The study presented here focused on root branching which also affects hormone production by the root system and permeation of the rooting volume.

Root branching occurs by initiation of laterals along each axis, and their subsequent extension. The anatomical aspects of the extension stages have been studied in great detail but the early stages of initiation and its control are not understood yet. Laterals are initiated at the pericycle cells associated with protoxylem poles. Thus the number of these poles affects the arrangement of the laterals along the axis. Yet it is still unclear how the actual sites of lateral initiation in roots of higher plants are determined (Charlton 1991).

Riopel (1966) who studied lateral root distribution in banana, which has polyarchous roots, concluded that "...a three dimensional zone of negative influence exists near established lateral root primordia". But he failed to consider the fact that laterals are initiated in an acropetal sequence along the axis; therefore any primordia could affect the formation of other ones further down the axis or sideways only. Moreover, Mallory *et al.* (1970) who studied the same phenomenon in *Cucurbita maxima* concluded that "...little or no inhibition or competition occurs between primordia opposite adjacent protoxylem poles". Recently Newson *et al.* (1993) reached the same conclusion regarding lateral primordia initiation along tomato roots.

It was found that in a certain fern the laterals are formed in a spiral sequence (Mallory *et al.* 1970). As for Aangiosperms, the same authors concluded that the laterals are formed in groups along the main axis. A similar arrangement was thought to exist in tomatoes (Barlow & Adams 1988). However, a more critical analysis of the data by Newson *et al.* (1993) did not indicate a significant tendency towards ordered distribution of laterals along each xylem pole.

The regular sequence of lateral initiation and development is interrupted, whenever the root curves. In such a case laterals appear at the external side of the curving segment. This phenomenon was described already by Noll (1900) who named it "Exotropism of

the lateral roots". Recently Fortin *et al.* (1989) found the same phenomenon to occur in *Aarabidopsis thaliana* roots which curved as a result of gravitropic stimulation.

In this study we report findings related to the spatial arrangement of laterals along the axis, and discuss their adaptive significance.

Materials and Methods

Sunflower (*Helianthus annuus* cv. D.I.-1, Hazera Seed Co., Israel) seeds were germinated and grown on germination paper (SD7615L Anchor Paper Co. St. Paul, MN) roll for one week. The seedlings were transferred to the aeroponic chambers of the Sarah Racine Root Laboratory. This unique research facility enables free growth and development of the root system of fully grown plants. The plant roots which suspended in the air were sprayed (20 s out of every min) with nutrient solution 0.5 g/L 20-20-20 N-P-K commercial fertilizer (Deshanim Ltd., Haifa, Israel) to which 0.5 mM $CaCl_2$ and 0.3 mM $MgSO_4$ were added. Branched roots were removed from the main root system of fully developed plants, for microscopic observations and detailed measurement of lateral distribution .

Cross sections were cut manually with a razor blade, and examined in an optical microscope under x100 and x400 magnifications in order to determine the arrangement of the vascular tissues within the stele of these plants.

In other sets of roots, all laterals, which have developed on five cm segments were trimmed to less than a mm. These root segments were mounted in a fixed position over a piece of black velvet, for analysis. Analysis was done using a high contrast video recording in an image analysis system composed of a CCD color video camera (Sony DXC-151P) with a micro 1:35 55mm lens (NIKKOR), 14" video monitor (Sony KX-14CP1), and a PC-486 computer. The software was CUE-3 Image Analysis Program Ver. 4.5 (Galai Production Ltd., Migdal Haemek, Israel).

With the aid of fine (0.2 mm dia.) steel pins every root segment was turned three times exactly 90° around its axis, and recorded from all sides. All four images of every root segment were aligned one next to the other on the video screen, and the position of every lateral was identified on two images at least. The position of the lateral along the root, the position of both edges of the root at the site of every lateral (R,L), and the distance of the lateral from the edge of the root (X) were measured on the screen. Two parameters were calculated for each lateral : its distance from the end (in mm), and its direction (in degrees). The direction was determined from the measurements by the following trigonometric formula:

$D=aCos\{[(R+L)/2-X]/[(R+L)/2-L]\}*180/\pi$

where: D - direction of the lateral (in degrees)

aCos - the arcCosine function (in Radians)

R - position of the right edge of the root

L - position of the left edge of the root

X - position of the center of the lateral

Observations regarding the relationships between curve angle and lateral distributions were made on tissue culture of carrot (*Daucus carota*) Hairy roots (induced by *Agrobacterium rhizogenes* strain 8196) grown on solid MS medium. Elongating roots were bent by sterile needles and allowed to continue growing until laterals could be observed along the bent segment.

Results and Discussion

Examination of cross sections of sunflower roots revealed that in this species there are roots of two types. Some are triarchic - having three protoxylem poles, and others are tetrarchic - having protoxylem poles. Laterals always develop in the preicycle cells adjacent to a protoxylem pole. This characteristic is therefore of prime importance in determination of the architecture of the root system, since it determines the number of potential sites for lateral initiation around the root.

Several examples of the results obtained by the image analysis were presented in Fig.1. Two main features can be observed. Firstly roots differ from one another in the number of series of laterals which develop. In certain cases (Figs.1a,b) only two series of roots develop along adjacent protoxylem poles, in others three and even four series of laterals develop along the same root (Fig.1c). The study so far, did not reveal any regularities in these differences. A more comprehensive analysis will have to be done in order to reach a general conclusion in that respect.

Another feature of root architecture, revealed by this figures is the tortuosity of the vascular system. The fact that the acropetal series of laterals appear in diagonals, in length vs. direction figures, indicate that protoxylem poles change direction gradually along the root. The angle of the diagonal reveal the degree of tortuosity in degrees per mm length. Again we see that roots differ in that respect (Fig.1).

A similar phenomenon was found for root system of the fern Ceratopteris thalictroides (Mallory *et al.* 1970).However, the- anatomy and developmental pattern of these plants are different from those of higher plants, like the species that we investigate.

This is the first time that such a tortuosity is measured directly in higher plants, and it is contrary to the traditional form by which roots of higher plants are portrayed in common textbooks.

Lateral distribution along straight and curving segments of Hairy roots, grown on solid medium, was measured. The difference in lateral root density between the outside (convex) and inside (concave) of curved roots was 0.617 ± 0.281 mm^{-1}. The difference in root density between the two sides of straight root segments was 0.080 ± 0.276 mm^{-1}. It is thus demonstrated that Hairy roots exhibit the same preference for lateral root direction towards the convex side of the curving root that was demonstrated for intact roots (Noll 1900; Fortin *et al.* 1989). Attempts to affect lateral distribution by bending root tips were not successful. It is therefore suggested that the control signals which cause the root to bend, also affect the differential lateral initiation.

This characteristic of the roots will determine the distribution of the laterals in the rooting volume. It will facilitate the permeation of all parts of this rooting volume by the roots, reducing root overlap and increasing the efficiency for soil utilization.

Both structural characteristics studied reveal how root systems are adapted to efficiently utilize the soil volume they are permeating. This efficient utilization results both from reduced overlap among adjacent roots and from growing roots at all possible directions. Every root exploits a certain volume of soil around it and affects ion availability in its immediate vicinity by epidermal exudates. Adjacent roots which grow too close to one another will compete and reduce each other's capacity to perform its roles in supplying the plant with water and nutrients. Directing laterals at all directions in the soil will not only reduce their potential for mutual competition but will increase the volume of the soil exploited by the root system, giving the plant access to larger amounts of soil borne resources.

Acknowledgments

The authors' thanks are due to Dr. Eli Sahar, Dept. of Cell Biology and Biotechnology, for the use of the Image Analysis System, in his laboratory.

The Hairy root observations were done at the laboratory of Prof. J. Tempe, Inst. Sci. Veg., C.N.R.S., Gif sur Yvette, France, with the skillful supervision of Dr. N. Petit.

References

Barlow PW & Adam JS (1988) The position and growth of lateral roots on cultured root axes of tomato, *Lycopersicon esculentum* (*Solanaceae*) Plant Syst. & Evol. 158:141-15

Charlton WA (1991) Lateral root initiation. in: Plant Roots: The Hidden Half (Waisel Y, Eshel A & Kafkafi U eds.) Marcel Dekker Inc. NY, Ch.6 pp. 103-128

Fortin M-C, Pierce FJ & Poff KL (1989) The pattern of secondary root formation in curving roots of *Arabidopsis thaliana* (L.) Heynh. Plant, Cell and Environ. 12:337-339

Mallory TE, Chiang S-H, Cutter EG & Gifford EM Jr. (1970) Sequence and pattern of lateral root formation in five selected species. Amer. J. Bot. 57:800-809

Newson RB, Parker JS & Barlow PW (1993) Are lateral roots of tomato spaced by multiple of fundamental distance? Ann. Bot. 71:549-557

Noll F (1900) Uber den bestimmenden Einfluss von Wurzelkrummengen auf Enstehlung und Anordnung der Seitenwurzeln. Landwirtsch. Jahrb. 29:361-426

Riopel JL (1966) The distribution of lateral roots in *Musa acuminata* 'Gros Michel'. Amer. J. Bot. 53:403-407

Figure 1. Directional distribution of lateral roots along three segments of sunflower root axes. Every row mark a rank of laterals, along one xylem pole.

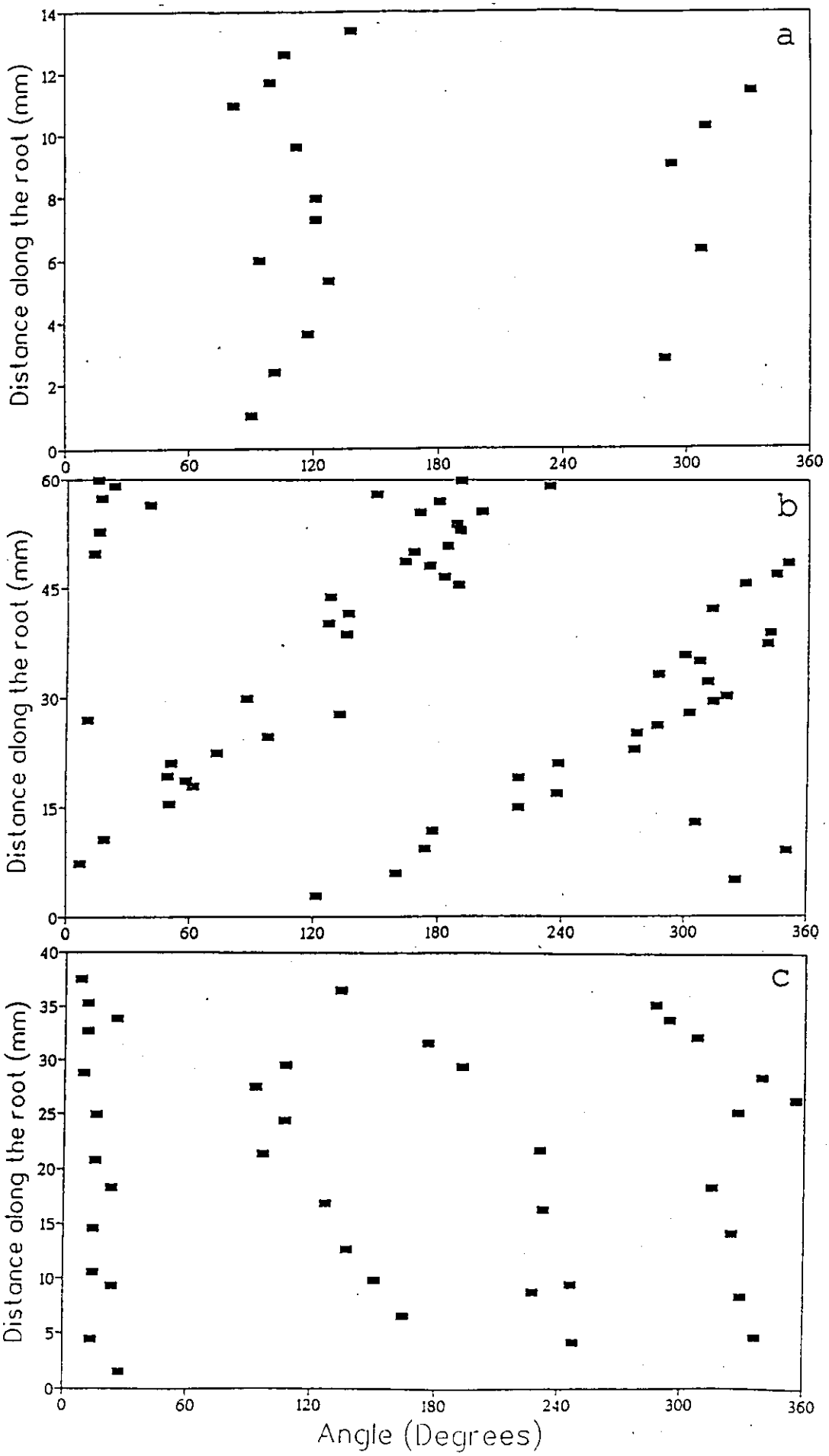

Bielefelder Ökologische Beiträge, vol. 8, (1995) p. 85 - 96

Structures of Geomorphological and Ecological Units and Ecosystem Processes in the Linear Dune System near Nizzana/Negev

Maik Veste
Department of Ecology, University of Bielefeld

Sand Dune Ecosystems

A dune is an accumulation of sand ranging between about 30 cm and 400 m in height and between 1 m and 1 km in width, whose shape has been adjusted to ambient wind conditions (Cooke et al. 1993). The dunes can be divided by their morphology into various types (Besler 1987, Thomas 1992): e.g. Barchanes, transverse dunes, star dunes, and linear dunes.

In the Negev desert sand dunes are found in the north-western parts and are the eastern extension of the Sinai continental sand fields (Fig 1). The southern part is characterized by linear dunes with a west-east trend. The Nahal (wadi) Nizzana in the east, the wadi Azariq in the north and the northern margin of the central Negev highlands in the south, mark the boundary of the Nizzana sand dune field. North of this sand field lie the sandy areas of Aguar and Haluza and which have a different morphology from the sand dunes near Nizzana. The dunes in the study site reach heights up to 18 m with an average of around 8.5 m (Allgaier 1993). The dunes are stabile and vegetated with no lateral movement (Tsoar and Moller 1986). From the viewpoint of dune morphology, this dune system is comparable with linear dunes in Australia, in the Kalahari of southern Africa and the southwestern parts of the USA (Buckley 1981, Lancaster 1982, Tsoar and Moller 1986). The sands in the ecosystem were deposited between 20.000 BP and 10.000 BP and forms the recent dune topography (Goring-Morris and Goldberg 1990, Yair 1994).
The average rainfall in Nizzana is around 90 mm (Yair 1990). Rain occurs between November - March. In 1993/94 the rainfall was around 50 mm, 1992/93 it was 136 mm (Sharon and Berkowicz 1993, Berkowicz pers. comm.)

In satellite images a sharp contrast between the Israeli and Egyptian side of the sand dunes can be observed. The Israeli side has a darker color, in comparison to the Egyptian side and the Gaza strip as a result of different albedos (Otterman and Waisel 1974, Otterman et al. 1975). The authors explained the difference in the albedo as due to differing vegetation cover. The vegetation cover on the Israeli side was between 25% and 35% of the area and on the Egyptians site was less than 25% (Otterman et al. 1975). The lower vegetation density is a result of grazing by goats and other live stock. Some of the interdune area and northern dune base have been used by Bedouin for agriculture. The dunes in Egypt also have a higher mobility and a different morphology (Otterman et al. 1975, Tsoar and Moller

1986). The stabilized dunes have a flat and round profile, whereas the unvegetated Seif-dunes have a sharp profil (Tsoar and Moller 1986, Thomas 1992).

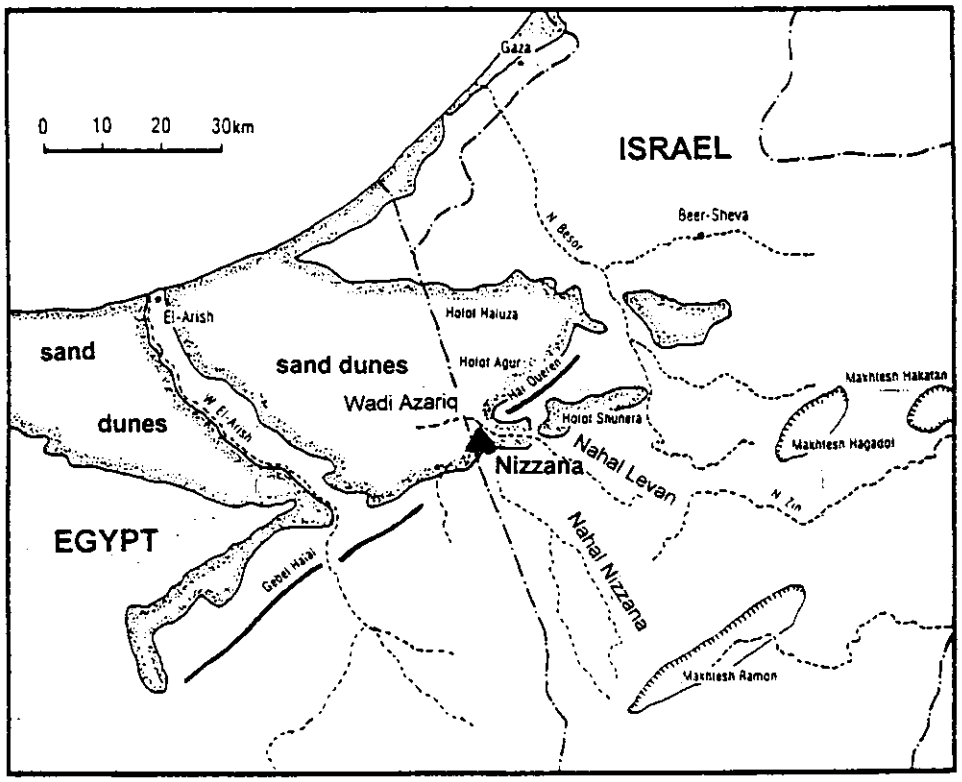

Fig 1: Location of the study site in the linear dune system, Nizzana, Israel

Structures in the sand dune systems of Nizzana

An ecosystem is a complex mosaic of various structures with different processes. These processes display temporal and spatial variations at the micro-scales. A simplified view of the ecosystem is necessary for analyzing ecosystem functions. The sand dune ecosystems of the study site can be divided into various simple units (Fig 2, see also Danin 1983, Yair 1990, Allgaier 1993). Such a definition includes geomorphological and microclimatical aspects, soil types, plant composition, ecosystem processes such as run-off, salt distribution, and sand movement and the biological crust (Table 1). These habitats are not isolated from each other, there are also linkages between them including the run-off processes along the slopes to the interdune area. Typical plant species with different ecophysiological and ecological reactions are chosen as models for the analysis of the role of plants for ecosystem processes.

1. Mobile sand on dune crest and slopes

The dune crest and part of the southern slopes and some northern slopes are mobile. The tops of the dunes are bare of vegetation because of the highly mobile sand. Plants of such a habitat need to be adapted to coverage and sometimes burial of the entire plant in sites where sand accumulation occurs, or exposure of roots in deflation sites. *Stipagrostis scoparia*, *Heliotropium digynum* and the xerohalophyte *Cornulaca monacantha* are typical species in such a habitat. *Moltkiopsis ciliata* grows in more stabilized parts of the dune top.

2. Stable dune slopes

Most of dune slopes are stabilized and vegetated by various shrubs and covered by a biological crust (see below). South and north facing slopes differ also regarding to the radiation input and the heat balance. The different microclimates of the slopes must be considered for the definition of the eco-units and the selection of investigation sites. Plant species of this unit are e.g. *Artemisia monosperma*, *Moltkiopsis ciliata*, *Convolvulus lanata* and *Noea mucronata* , *Retama raetam*. Various annuals also occur along the slopes.

3. Dune base

Along the base of the north-facing slopes a belt with dense vegetation occurs. *Artemisia monosperma*, *Moltkiopsis ciliata*, *Anabasis articulata*, *Retama raetam*, *Cornulaca monacantha* and *Thymelaea hirsuta* comprise part of this habitat. The high density could be a result of a good water and nitrogen supply from the run-off along the dune slopes.

4. Interdune area

Typical plant species of the interdune areas are e.g. *Retama raetam*, *Thymelaea hirsuta*, *Convolvulus lanata*, *Moltkiopsis cilita*, and *Anabasis articulata* and various grasses.
Old dunes occur in some parts of the interdune area and are covered by a hard abiotic crust. On some of these old dunes, *Cornulaca monacantha* is dominant.

5. Playas

Playas are flat areas rich in clay and silt (Yair 1990) with low or no vegetation cover. Accumulation of salt in the ecosystem could be found mainly in the playa areas. The salt content of a playa in comparision to the sand dune is shown in Fig 3. Blume et al. (1994) classified the soils as Solonchak and Calcisol. After rainfalls a salt crust can be observed. The dominant plant species of this unit is the xerohalophyte *Anabasis articulata* (Chenopodiaceae). Annuals grow here only on small spots having thin sand cover or in soil cracks.

Table 1: Preliminary list of dominant plant species, soil types, ecosystem processes and crust types in different ecological units in the sand dune ecosystem of Nizzana (1) for details see Blume et al. 1994)

Ecological unit	Plant species	Soil type[1)]	Ecosystem processes	Biol. crust type
Mobile sand (top and slopes)	Stipagrostis scoparia Heliotropium digyum Cornulaca monacantha Moltkiopsis ciliata	Shifting dune	- sand mobility - water infiltration - low nutrient content	no
North-facing slope	Moltkiopsis ciliata Retama raetam Artemisia monosperma	Arenosol A1	- N-fixation by crust? - run-off - micro-climate - radiation - stability	dark,thick (with mosses)
South facing slope			- N-fixation by crust? - run-off - micro-climate - radiation - stability	light, thin
Dune base	Artemisia monosperma Retama raetam Anabasis articulata Thymelaea hirsuta dense vegetation	Arenosol A1	- stability - run-off - high nutrient content - N-fixation by crust ?	dark,thick with mosses
Interdune area	Moltkiopsis ciliata Retama raetam Convolvulus lanata Thymelaea hirsuta	Arenosol A1, A2, A3	- N-fixation by Retama and crust ? - stability - deep water storage	light, thin no mosses
Old dunes	Cornulaca monacantha (Anabasis articulata)	Arenosol A1	- run-off ? - salt ? - compact soil crust	abiotic crust
Playa	Anabasis articulata	Solonchak S1,S2 Calcisol C1,C2,C3	- salt accumulation - compact soil - limited water infiltration	no

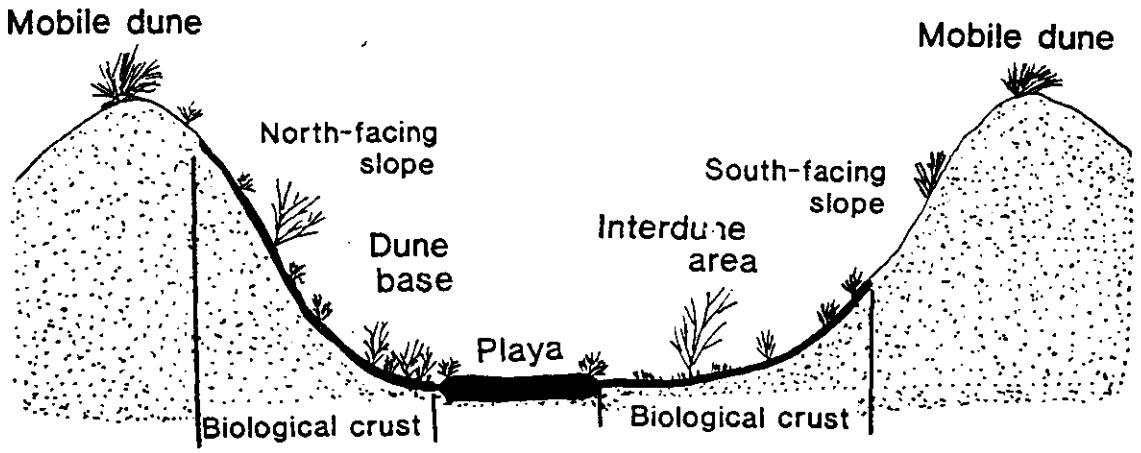

Fig 2: Schematic topographical cross-section and eco-units of the linear dune system

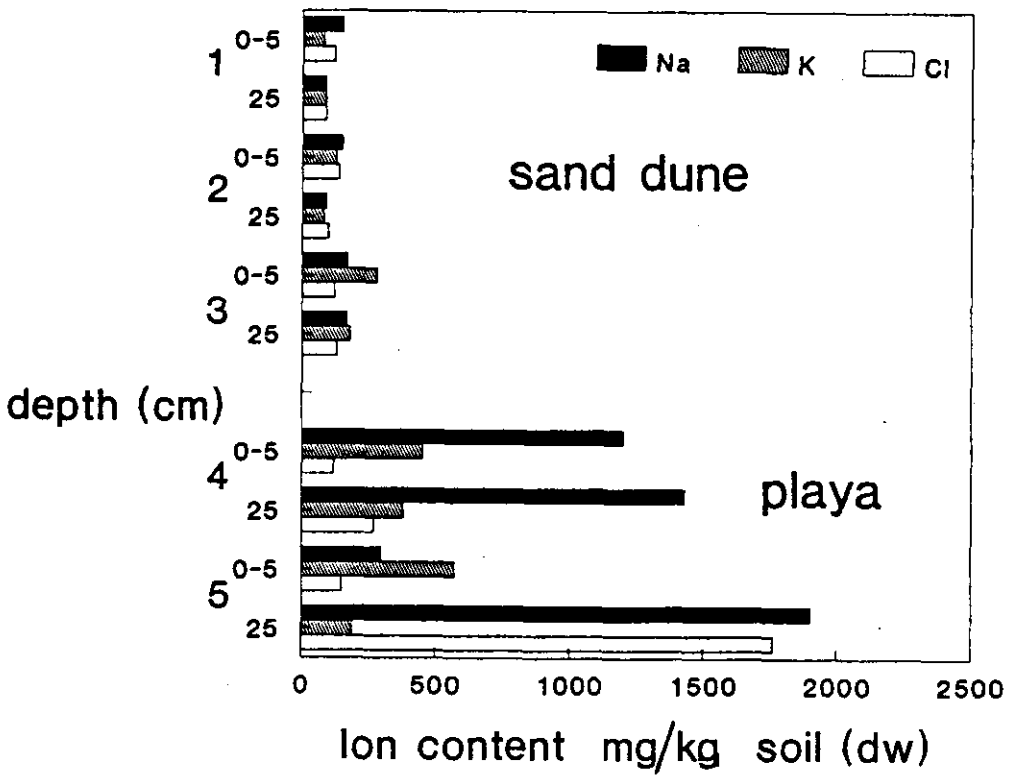

FIG 3: Ion content (Na, K, Cl) in the soil in two depths (0-5 cm, 25 cm) along a dune slope (1: upper slope, 2: mid-slope, 3: lower slope) and in a playa area (4,5).

Structure of the biological crust

A special structure in the ecosystem, which influences the function of the system is the biological crust. The dune slopes and the sandy parts of the interdune area are covered by this biological crust. The crust is build up mainly by cyanobacteria e.g. of the genus *Microcoleus*, *Nostoc*, *Schizothrix*, *Scytonema* and *Calothrix* and green algae (Danin 1989, Lange et al. 1992). On northern slopes and in the shrub surroundings where wetter conditions occur, mosses are part of the crust (Fig 4). The mosses are from the genus *Bryum* and *Brachythecium*(Lange et al. 1992). The crusts of the northern slopes cover the slopes nearly until the crest and are thicker and darker than those of the southern slopes.

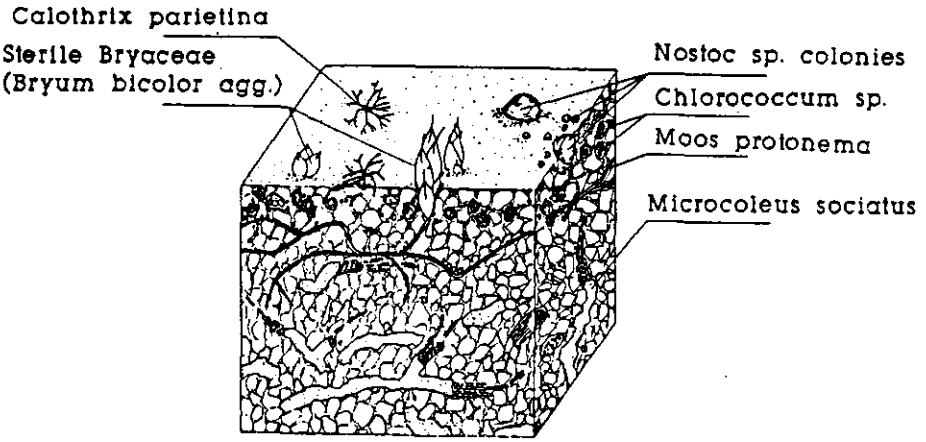

Fig 4: Schematic diagram of the biological crust (Lange et al.1992)

In the sand fields (Holot) of Alzuza and Agur 15 km north of the study site (see Fig.1) a thick crust with a dense cover of various lichens can be found. Some species of lichens have a symbiosis with nitrogen-fixating cyanobacteria (Garty, pers. comm.). This crust type does not occur either in the sand field of Nizzana nor along the transect from the coast to the inland as described by Danin et al. (1989). Whether the development of this crust type is a result of succession or of a climatical gradient between the coast and Nizzana, is still unclear. In the northern sand fields *Artemisia monosperma* is one dominant plant species, which is an indicaton of the long stability of the dunes (Danin 1991).

Function of the biological crust in the ecosystem

a) Stability and erosion

The biological crust enhances the stability of the dunes. The cyanobacteria secret polysaccharids, which stick together the grains of sand (Danin et al. 1989, Verrecchia et al. 1993). The build-up of bacteria crust prevents the saltation of sand particles and reduces the wind erosion. A change in plant species composition is a result of dune stabilization. *Stipagrostis scoparia* is a typical plant of the mobile sands and *Artemisia monosperma* will take place under stable conditions (Danin 1991). The changes in the dune morphology was described earlier.

b) Infiltration and run-off

The biological crust influences, directly or indirectly, the water flow of the dune. The infiltration of rain in the sand is reduced by the biological crust and run-off on the surface can occur (Yair 1990). After wetting the polysaccharid-sheets of the cyanobacteria swell up and reduce the infiltration through the crust (Verrechia et al. 1993). Yair (1990) induced run-off on slopes possessing a biological crust after three minutes of irrigation using a rain simulator (rain intensity 18 mm h^{-1}). To induce run-off on uncrusted sandy slopes requires a rain intensity of 53 mm min^{-1} and the run-off was observed only after 40 minutes.
The water fluxes in the sand dunes is shown in Fig. 5. The water infiltrated to a maximum depth of around 60 cm, lateral movement of water in depths of more than 2 m has been measured (Yair 1994). Transpiration by plants and evaporation from the soil are the processes of water loss in the ecosystem. Plants with tap roots e.g. *Anabasis articulata* and *Thymelaea hirsuta* are physiological active during the whole year and are able to use the water from both water layers.

c) Photosynthesis

Most of time during a year the biological crust is dry and physiological inactive. Photosynthesis can be measured after wetting of the biological crust (Fig 6, Lange et al. 1992).
Detailed studies of photosynthesis of the biological crust in nature are largely lacking. The main activity will be during the rainy season in the winter time. Fog and dewfall may play also a role for the activation of the crust as observed for lichens (Kappen et al. 1979, Lange et al. 1991). The average dewfall amount in Sede Boqer was between 0.24 and 0.34 mm (Kidron 1988). The amount will be sufficient to activate the physiological processes (Fig 6, photosynthesis), but in sunshine the crust will dry out rapidly. Only after rainfall and under cloudy conditions is the soil crust wet for several days. We measured the light intensity under such cloudy conditions. The light intensity (PPFD) was nearly identical with the saturating light conditions for photosynthesis in the laboratory experiments of Lange et al. (1992). This means that this environment conditions are optimal for the activity of the biological crust.

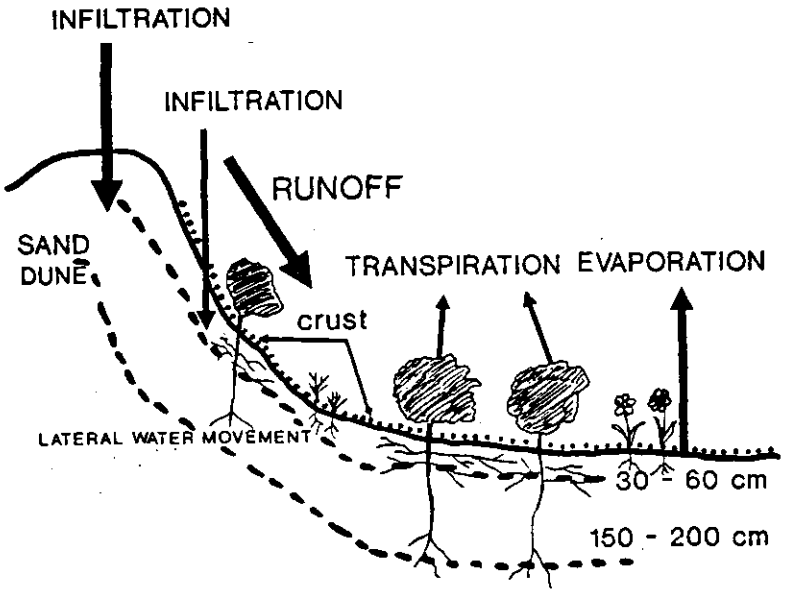

Fig 5: Schematic diagram of the water fluxes within the sand dune ecosystem

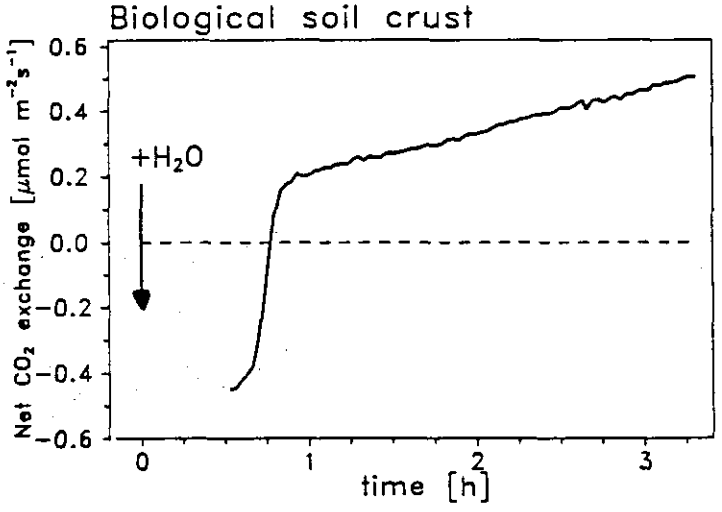

Fig 6: CO_2 exchange of a biological crust after wetting with an equal amount of 0.3 mm water
PPFD: 300 μmol m^{-2} s^{-1}, Tcuv=15 °C, rH = 90%.

d) Nitrogen fixation

Sand has a low content of nutrients for plant growth (Buckley et al. 1986). There are several indirect indications that mainly nitrogen could limit the plant growth in arid regions under good water supply (Floret and Pontanier 1979, Penning de Vries and Djiteye 1982). Some authors (e.g. Shields 1957, Shields et al. 1957, West 1990, Evans and Ehleringer 1993) mention the

important role of the biological crust in addition to the symbiontic N-fixation for the nitrogen input in desert ecosystems. Nitrogen fixing Cyanobacteria occur as free-living bacteria or in symbiosis in various lichens, and are an essential part of the biological crust. West (1990) estimated the nitrogen fixation by crusts to be between 2 and 41 kg ha^{-1} a^{-1}. Around 80% of the nitrogen in this ecosystem originated from fixation by cryptogamic crusts (West and Skujins 1977). For various desert ecosystems the N-input by crusts is listed in Table 2.

Table 2: Nitrogen input in various desert ecosystems by biological nitrogen fixation of cryptogames (after Skujins 1981, Rychert et al. 1978, van Keulen 1977 (1))

ecosystem		nitrogen input (kg ha^{-1} a^{-1})
Sonoran Desert	(USA)	12
Great Basin Desert	(USA)	13
Mohave Desert	(USA)	0.5
Central Desert	(Australia)	1.3
Semiarid regions	(1)	5.0

Most of the measurements of nitrogen-fixation by biological crust is done in the laboratory and it is still unclear if the fixation rates are relevant under natural conditions. West (1990) mentioned that the fixation rates are too high as a result of methodological problems.

This discussion of the Nizzana sand dune ecosystem shows how structures influence function and processes within a system. Only by synthesizing the knowledge of structures and functions we can analyze and understand ecosystems.

Acknowledgments

This investigation is part of the joint Israeli-German ecosystem research project "Desert Sand Dunes of Nizzana" and was carried out at the "Nizzana Research Site" of the Arid Ecosystems Research Centre (AERC, Jerusalem). The project is funded by the Bundesministerium für Forschung und Technologie - Federal Ministry of Research and Technology (DISUM 23, No. 0339495A).

We thank the AERC (Hebrew University Jerusalem) and the Department of Botany (Tel Aviv University) for their technical help and fruitful discussions.

We gratefully acknowledge EUROPCAR for their assistance with car rental.

References

Allgaier, A. (1993). Geomorphologische Untersuchungen an Längsdünen in der westlichen Negev, Israel, Dipl.Arbeit Lehrstuhl für Physische Geographie, RWTH Aachen, 84 p., unpublished.

Besler, H. (1987). Entstehung und Dynamik von Dünen in warmen Wüsten, Geographische Rundschau 39 (7/8), 422-428

Blume, H.-P., Yair, A., Yaalon, D.H. (1994). An initial study of pedogenic features along a transect across longitudinal duneareas, Nizzana region, Negev, Israel. In: Blume, H.-P. and Berkowicz, S. (eds): Arid Ecosystem Research, Adv. in GeoEcology 28, CATENA, in press

Buckley, R. (1981). Parallel dunefield ecosystems: southern Kalahari and central Australia, Journal of Arid Environments 4, 287-298.

Buckley, R., Wasson, R., Gubb, A. (1987). Phosphorus and potassium of arid dunefield soils in central Australia and southern Africa, and biogeographic implications, Journal of Arid Environments 13, 211-216.

Cooke, R., Warren, A. Goudie, A. (1993). Desert Geomorphology, UCL Press, London.

Danin, A. (1983). Desert Vegetation of Israel and Sinai, Cana Publishing House, Jerusalem.

Danin, A. (1991). Plant adaptations in desert dunes, Journal of Arid Environments 21, 193-212.

Danin, A., Bar-Or, Y., Dor, I., Yisraeli, T. (1989). The role of cyanobactera in stabilization of sand dunes in Southern Israel, Ecologia Mediterranea XV (1/2), 55-64.

Evans, R.D., Ehleringer, J.R. (1993): A break in the nitrogen cycle in aridlands? Evidence from $\delta^{15}N$ of soils, Oecologia 94, 314-317.

Floret, C., Pontanier, R.S. (1982). Management and modelling of primary production and water use in a south Tunisian steppe. Journal of Arid Environments 5, 77-90.

Goring-Morris, A.N., Goldberg, P. (1990). Late Quaternary dune migration in the southern Levant: archeology, chronology and paleoenvironments, Quaternary International 5, 115-137.

Kappen, L., Lange, O.L., Schulze, E.-D., Evenari, M., Buschbom, U. (1979). Ecophysiological investigations on lichens of the Negev Desert. VI. Annual course of the photosynthetic production of Ramalina maciformis (DEL.) BORY. Flora 168, 85-108.

Kidron, G.J. (1988). Dew variability, lichen and cyanobacterial distribution along slopes at Sde Boqer, northern Negev, Israel. Master Thesis, Hebrew University, Jerusalem (in Hebrew).

Lancaster, N. (1982). Linear dunes, Progress in Physical Geography 6, 445-504.

Lange, O.L., Meyer, A., Ullmann, I, Zellner, H. (1991). Mikroklima, Wassergehalt und Photosynthese von Flechten in der küstenahen Nebelzone der Namib-Wüste: Messungen während der herbstlichen Witterungsperiode. Flora 185, 233-266.

Lange, O.L., Kidron, G.J., Büdel, B., Meyer, A., Kilian, E., Abeliovich, A. (1992). Taxonomic composition and photosynthetic characteristics of the biological soil crusts covering sand dunes in the western Negev Desert, Functional Ecology 6, 519-527.

Otterman, J., Waisel, Y. (1974). Observation of desertification in the israeli ERTS-1 program., XIV Convegno Internazionale Technico-Scientifico Sullo Spazio, Rome, March 1974, 199-205.

Otterman, J., Waisel, Y., Rosenberg, E. (1975). Western Negev and Sinai Ecosystem: comparative study of vegetation, albedo and temperatures, Agro-Ecosystems 2, 47-59.

Penning de Vries, F.W.T., Djiteye, M.A. (1982). La Productivitié des Pâturages Sahéliens. Wageningen: Centre for Agricultural Publishing and Documentation.

Rychert, R., Skujins, J.J., Sorensen, D., Porcella, D. (1978): Nitrogen fixation by lichens and free-living microorganisms in deserts, In West., N.E., Skujins, J.J. /eds): Nitrogen in Desert Ecosystems. US/IBP Synthesis Series 9, 20-30, Pennsylvania.

Sharon, D., Berkowicz, S. (1993). Local climatic studies on dunes at the Nizzana research station, Annual Report 1992, Arid Ecosystem Research Center, Hebrew University of Jerusalem, unpublished.

Shields, L. M. (1957). Algal and lichen floras in relation to nitrogen content of certain volcanic and arid range soil. Ecology 38, 661-663.

Shields L. M. Mitchell, C., Drouet, F. (1957). Algae- and lichen-stabilized surface crusts as soil nitrogen sources. American Journal of Botany 44, 489-498.

Skujins, J.(1981): Nitrogen cycling in a arid ecosystems. In Clark, F.E., T. Rosswall (eds.) Terrestrial nitrogen cycles. Processes, ecosystem strategies and mangement impacts. Ecol. Bull. (Stockholm) 33, 477-491.

Thomas, D.S.G. (1992). Desert dune activity: concepts and significance, Journal of Arid Environments 22, 31-38.

Tsoar H., Moller, J.T. (1986). The role of vegetation in the formation of linear sand dunes. In W.G. Nickling (ed.), Aeolian Geomorphology, Allen and Unwin, Boston, 75-95.

Van Keulen, H. (1977): On the role of nitrogen in semiarid regions, Stickstoff No.20, 23-28.

Verrecchia, E., Yair, A., Ribier, J. Kidron, G. Rolko, K. (1993). Le role des cynobacteries (Cyanohyta, Cyanobacteria) dans la fixation des sols sableux désertiques: approche d'un cas dans la désert du Négev (region de Nizzana, Israel), Palynoscience 2, 255-266.

West, N.E. (1990) Structure and Function of Microphytic Soil Crusts in Wildland Ecosystems of Arid to Semi-arid Regions, Advances in Ecological Research 20, 180-223.

West, N.E., Skujins J. (1977): The nitrogen cycle in North American cold-winter semi-desert ecosystems. Oecol. Plant 12, 45-53.

Yair, A. (1990). Runoff generation in a sandy area - The Nizzana sands - Western Negev, Israel, Earth Surface Processes and Landforms 15, 597-609.

Yair, A. (1994). The Ambiguous Impact of Climate Change at a Desert Fringe: Northern Negev, Israel. In: A.C. Millington and Pye, K. (eds.) Environmental Change in Drylands. 199-227.

Bielefelder Ökologische Beiträge, Band 8 (1995) p. 97-111

Canopy Structure, Ecosystem Function and Diversity in a montane tropical primary forest in Costa Rica

Prof. Dr. S.-W. BRECKLE
Dept. of Ecology
Faculty of Biology
University of Bielefeld
Postal Box 100131
D-33501 Bielefeld
Fax: 0049-521-106-2963

Abstract

The complex structure of a tropical montane rain forest area in the Reserva Biológica de Alfredo Brenes (formerly Reserva Forestal de San Ramón) is characterized by very heterogenous canopy. The very high diversity of tree species is demonstrated by the fact that about 400 tree stems are from 94 species of trees (DBH ≥ 10cm) which occur on 1 ha. The diversity of life forms is also tremendously high with many lianas, epiphytes, hemiepiphytes, epiphyllic leaf cover etc. Around the Biological Station in the Valley of San Lorencito there are 12 different tree fern species.
Population structure of *Plinia salticola, Inga leonis* and *Pterocarpus hayesii* is given as an example of tree populations.
The dynamic functions only can be estimated. Measurements of productivity or biomass distribution as well as water budget or mineral cycling are not available. The perhumid situation and the typical tropical climate with higher daily than annual temperature fluctuations are strong reasons for the highly diverse structure and rapid growth and dynamics of this type of tropical forests.

Introduction

Land-use in Costa Rica is characterized by a rapid change. About 2 - 5 % of the forests are transferred to grazing lands and agricultural fields per year. Table 1 gives a survey on land use on Costa Rica. Tropical Forests comprise about 32.3 % of the country in 1984. Over 20% of the country's area are nationalparks (BOZA 1989). The decrease in forest cover is shown for the last 50 years in Fig. 1. In 1994 very few primary forests are left outside the national parks, which have an area of about 20% of the country's surface.
To study tropical rain forests and their unique and highly complex structure it is necessary to go in primary forests. The structures and processes going on with great variation in space and time have to be studied to understand this highly complex biological system (JANZEN 1991, TERBORGH 1992). Tropical rain forests are by far the most complex systems, when keeping in mind the complexicity levels in biological systems, starting with membranes, organelles, cells, tissues, organs, organisms, populations up to ecosystems.
In the following we will give a few remarks on structure and processes of a premontane primary rain forest. We mainly will focus on a few examples of the population structure of a few species, and on some preliminary results from other ecological studies.

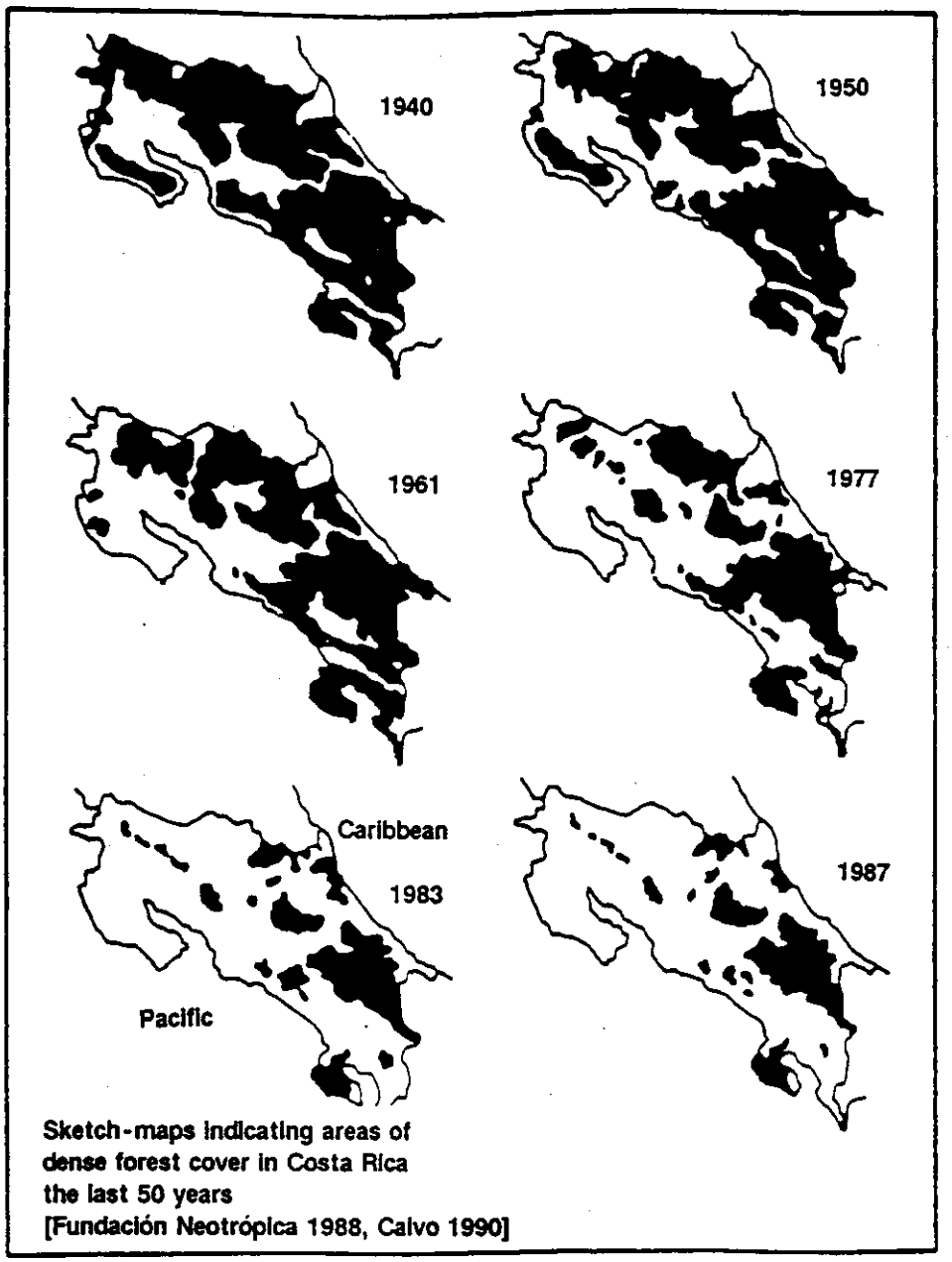

Fig. 1 : Sketch-Maps indicating areas of dense forest cover in Costa Rica since 1940. The rapid destruction of forests is obvious (Fundación Neotrópica 1988; CALVO 1990).

Table 1 : Land use in Costa Rica (Source: S.E.P.S.A. 1984)

Province-Region:	Chorotega	Huetar Norte	Huetar Atlantico	Brunca	Pacifico Central	Total	
Land use category	ha	ha	ha	ha	ha	ha	%
Urban	9.770	1.140	400	200	15.050	26.570	0.5
Agriculture	144.600	17.130	75.960	65.510	221.960	525.160	10.4
Annual Crops	109.830	1.370	18.160	30.660	39.740	199.760	3,9
Perennial Crops	34.770	15.760	57.800	34.850	182.220	325.400	6,4
Pasture	824.160	328.200	182.070	424.700	464.900	2,224.030	43,9
Forest	271.040	454.219	690.040	542.310	275.760	2,233.360	44,0
Tropical Forest	195.730	308.760	531.190	397.090	205.700	1,638.470	32,3
Other Natural Vegetation	75.310	145.450	158.850	145.220	70.060	594.890	11,7
Idle Land	3.430	2.490	5.840	0	2.080	13.840	0,3
Swamps	5.150	520	6.020	1.690	0	13.370	0,3
Waters	660	420	400	420	1.070	2.970	0,1
Other Uses	4.190	7.990	4.590	7.780	6.890	31.340	0,6
TOTAL	1,263.000	812.000	965.220	1,042.610	987.710	5,070.640	100,0

The San Ramón Biological Reserve (Alfredo Brenes)

This Reserve was founded about 1980. It comprises 80.000 ha of mostly primary forest along the Sierra de Tilaran, North of San Ramón. The Rivers Rio San Lorenzo and Rio San Lorencito drain the mountainous area to the North-East, the Caribbean side. Some ridges are remnants of volcanos. Most of the soils are derived from volcanic rocks and form andosols (VARGAS 1991).

The climate is very humid, with precipitation all year round. A slightly drier season is observed during february till april, as is shown on the preliminary constructed diagramm from a few years measurements and from relevant neighbouring meteorological stations (Fig. 2: climatic diagramm). This drier season still exhibits monthly rainfall of up to 100 mm.

The relief of the valley San Lorencito and the close vicinity of the Biological Station is shown on the contour line map (Fig. 3). Steep slopes are typical for all these valleys, the creeks are deeply cut in the slopes (BRECKLE 1993).

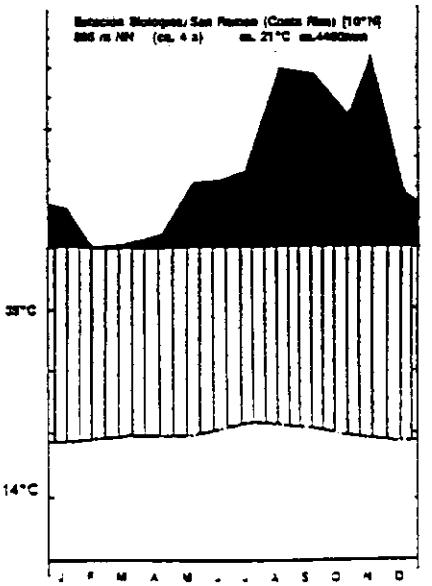

Fig. 2 : Climatic Diagramm from the Biological Station of the Reserva Biológica Alfredo Brenes, Costa Rica (drawn according to WALTER & BRECKLE 1991).

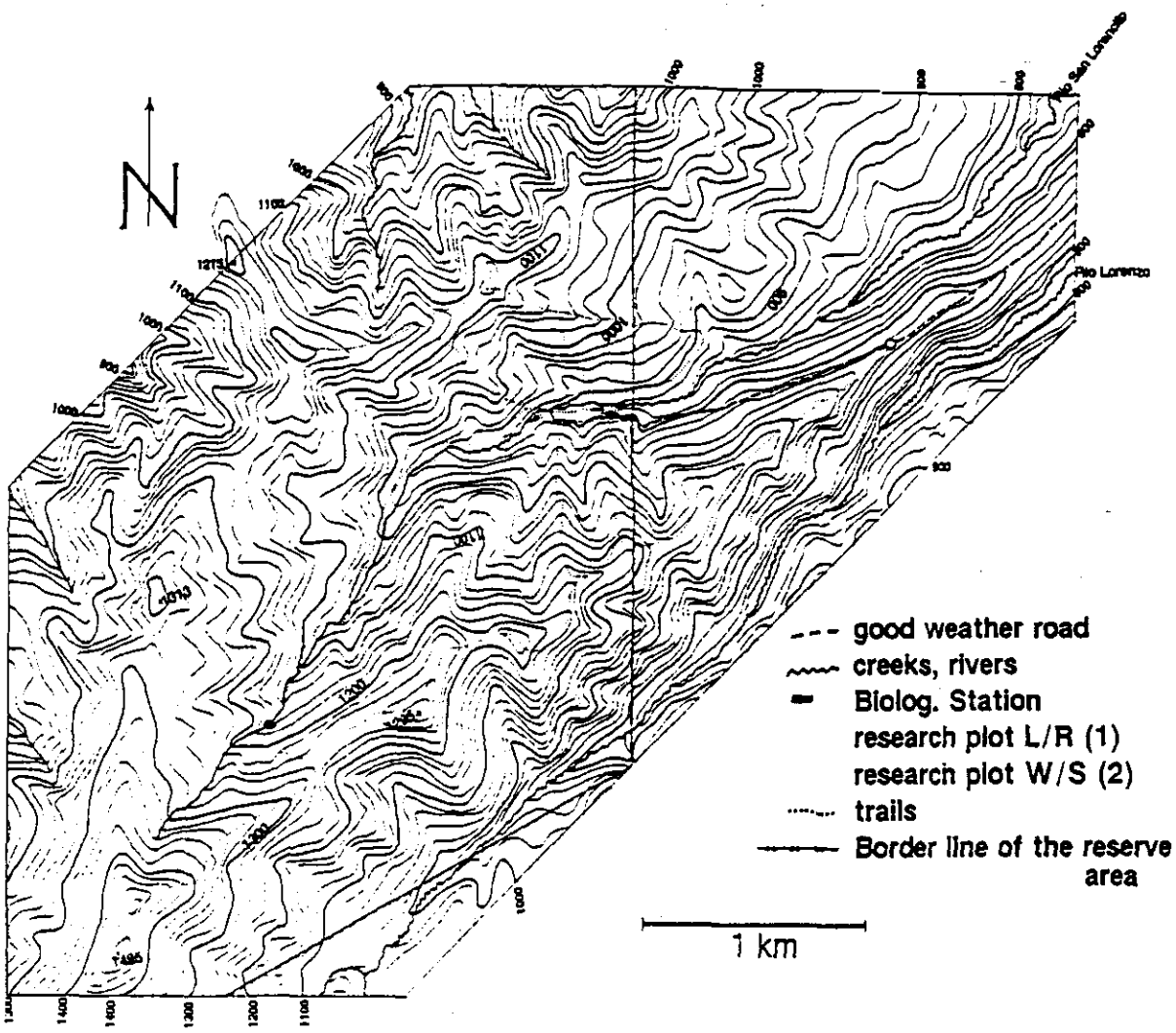

Fig. 3 : Contour line map of the San Lorencito Area within the Biological Reserve Alfredo Brenes and preliminary trail network. Southeastern part of the "Reserva", OCAD-map by H.& R.BRECKLE, source offic. map 1:50.000; contourlines 20 m.

Tree Populations

The layering of the tree crowns is almost not visible. The canopy structure of the tree crowns is very heterogenous. The various tree crown positions are described schematically by Fig. 4. Mainly the position according to light conditions is considered, since light is one of the limiting factors in primary forests.

The number of trees from the various BHD-classes is shown in Fig. 5. It clearly indicates the great majority of trees being slender. Old trees with more than 1 m BHD are only 3 individuals per hectar, which is 0.6 %. This is the case on the ridge area, on the slope area the number of tree stems is lower and there are a few very large old trees, but still the age distribution is very similar (WATTENBERG & BRECKLE 1995).

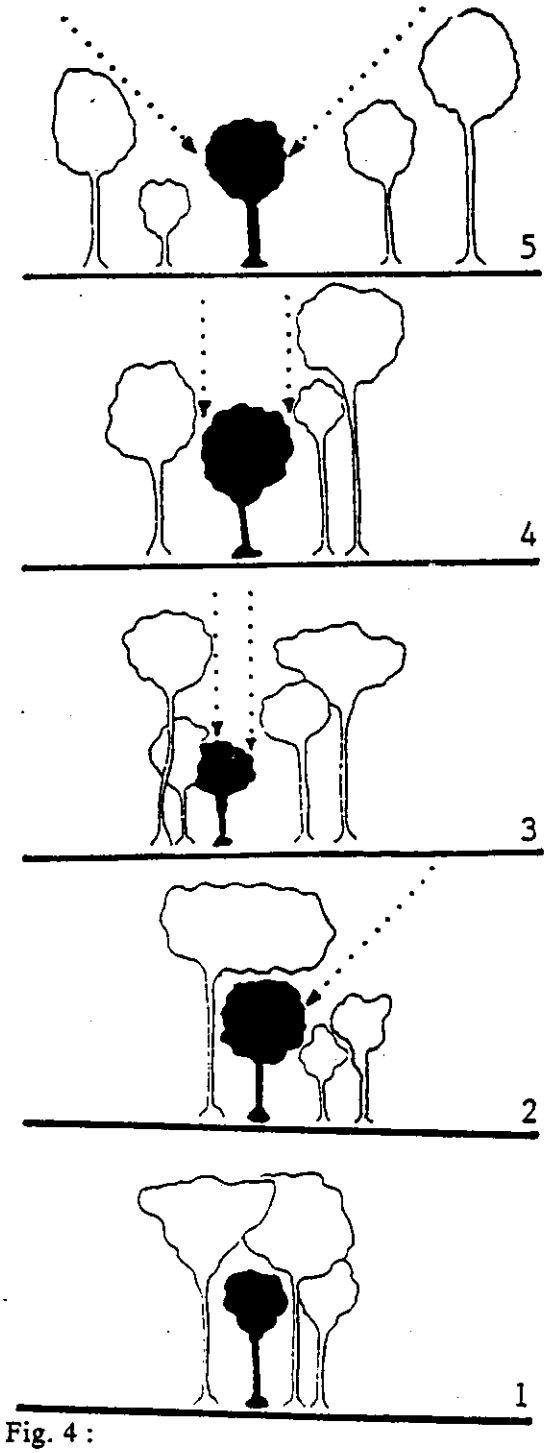

Fig. 4 :
Definition of various tree crown positions within canopy (SPRENGER 1992)

number of trees (BHD >10cm)

BHD -classes	abs. number	percentage %
10 - 19 cm	271	50,9
20 - 29 cm	125	23,3
30 - 39 cm	55	10,2
40 - 49 cm	26	5,1
50 - 59 cm	29	5,5
60 - 69 cm	8	1,5
70 - 79 cm	11	2,1
80 - 89 cm	3	0,6
90 - 99 cm	1	0,2
110 - 119 cm	2	0,4
120 cm	1	0,2
Σ	532	100

Fig. 5 :
Number of trees (>10cm BHD) of various BHD classes on 1 ha (SPRENGER 1992)

The relation between tree size and BHD gives a rough idea on the specific growth pattern of a stem and the thickness in relation to height. The subdominant endemic tree *Plinia salticola* (Myrtaceae) is rather different in this respect in comparison with *Inga leonis* (Mimosaceae) (see Fig 6. and 7.). It is obvious that *Inga leonis* (Fig. 7) stems are about 100 times larger than stem thickness, since the linear correlation is close to this function, wheras in *Plinia salticola* the stem grows thicker and thicker but tree height remains low and doesn't exceed 12 m (Fig. 6). In *Pterocarpus hayesii* these architectural structure of stem thickness and height is intermediate (Fig. 8) and even very thick, old trees grow thicker, but do not exceed about 30 m height.

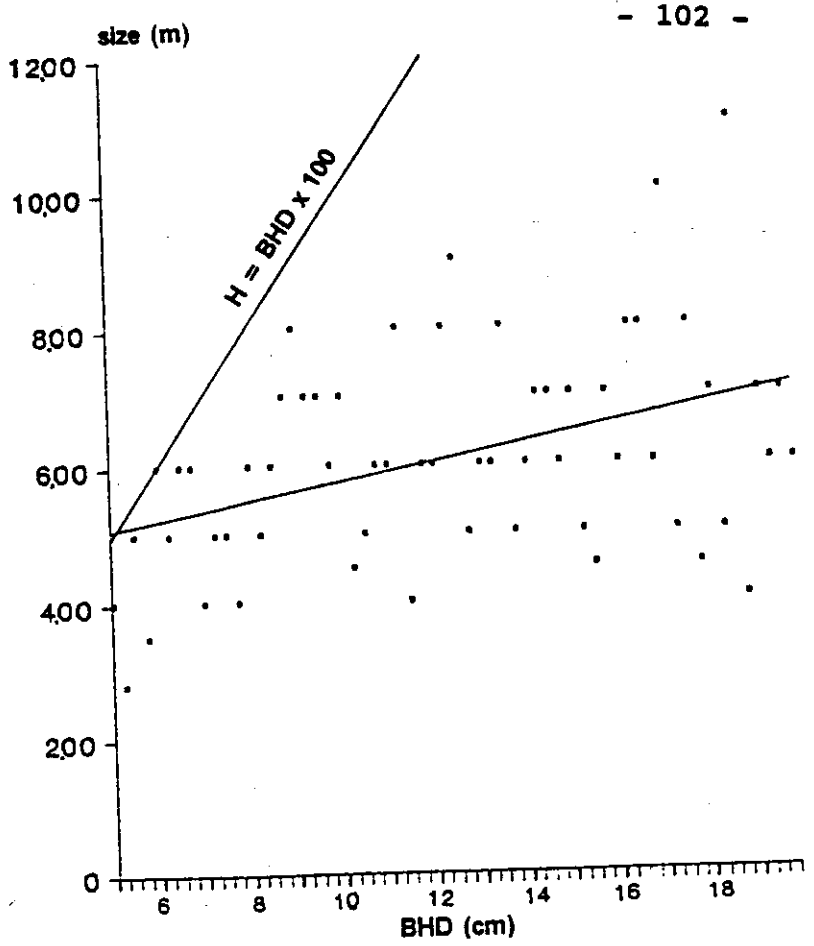

Fig. 6 :
Correlation between tree size of the subdominant *Plinia salticola* and BHD (SPRENGER 1992)

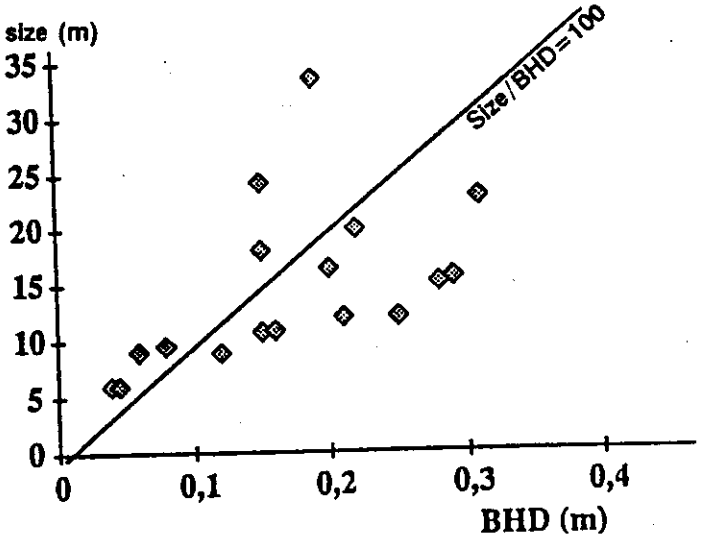

Fig. 7 :
Correlation between tree size of the dominant *Inga leonis* and BHD (RÖMICH 1993)

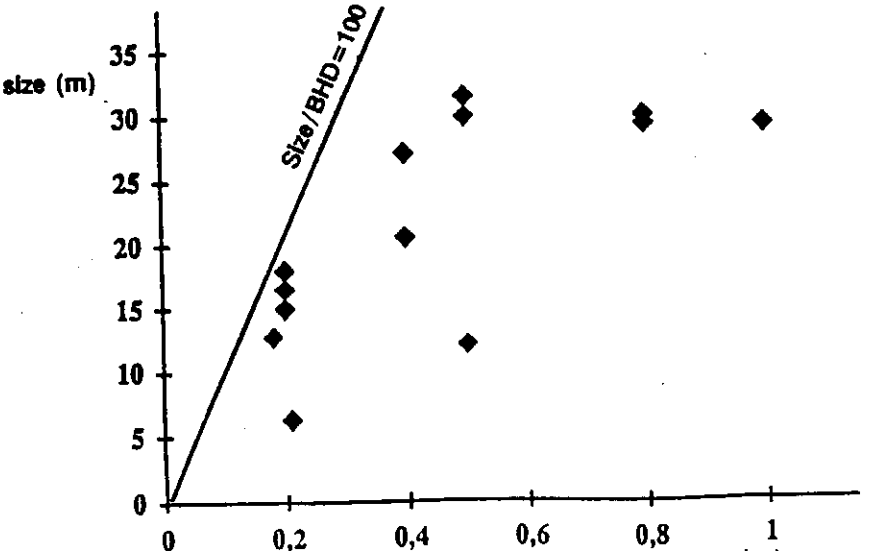

Fig. 8 :
Correlation between tree size of the dominant *Pterocarpus hayesii* and BHD (RÖMICH 1993)

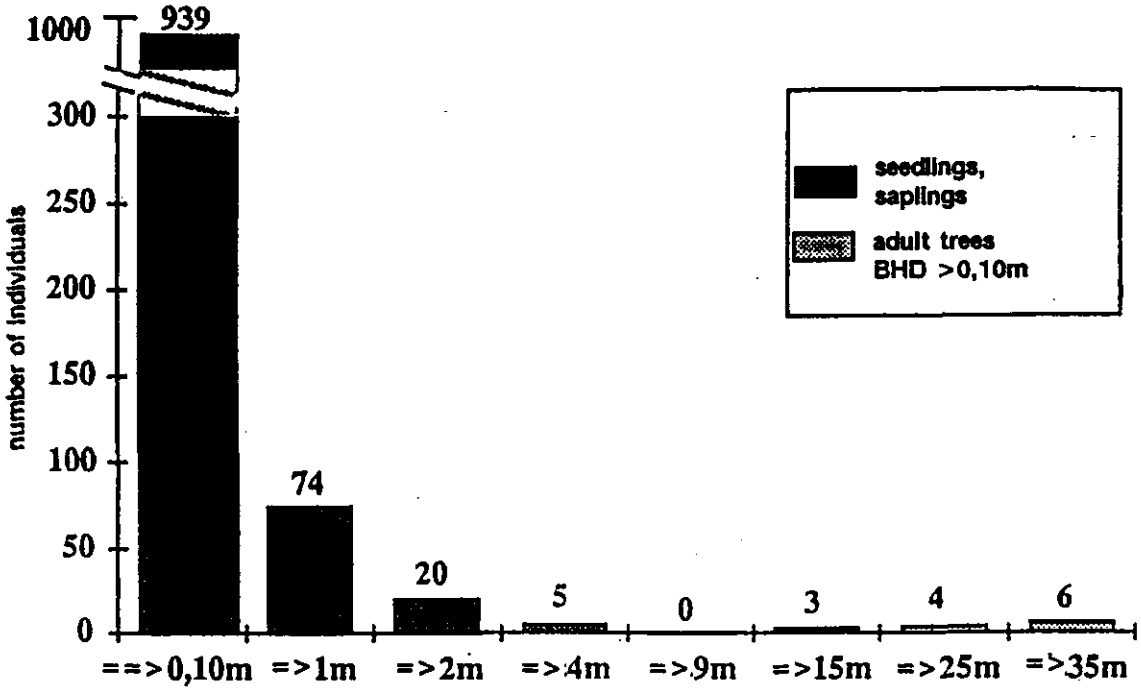

Fig. 9 :
Number of trees of various age- and size-classes of *Pterocarpus hayesii* within 1 ha (RÖMICH 1993)

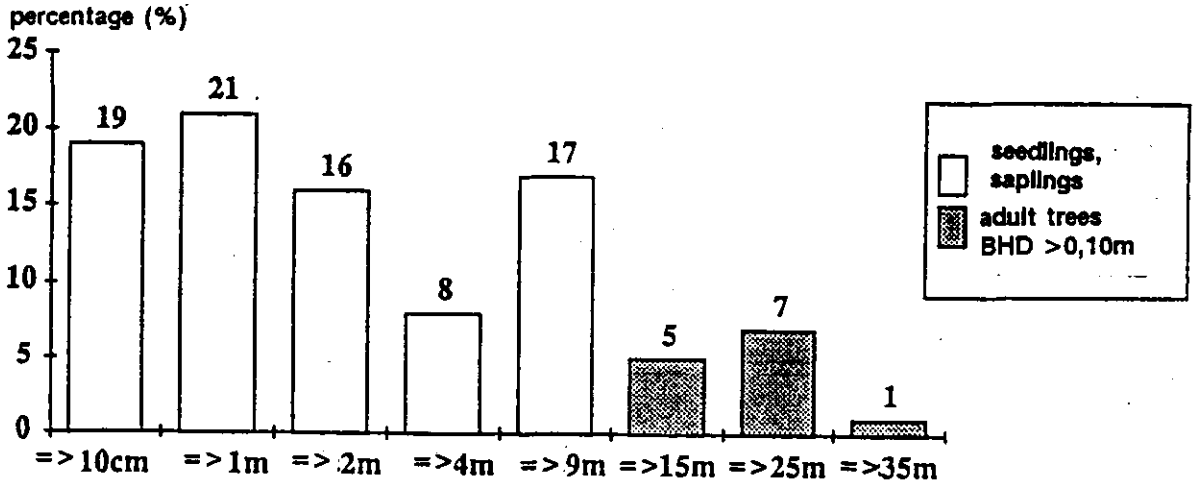

Fig. 10 :
Percentage of trees of various age- and size-classes of *Inga leonis* within 1 ha (RÖMICH 1993)

Population studies need to know the age of the various individuals of a population. It is, however, not possible to detect exact age of tree individuals in the tropics since many species do not exhibit annual xylem rings. Using height of seedlings, saplings, young and adult trees is an indirect measure of age. Such size-classes are given for *Pterocarpus hayesii* (Fig. 9). Since *Pterocarpus hayesii* is still one of the most abundant tree species with about 18 stems (≥ 10 cm DBH) it is obvious that the saplings are very common and thus easier to study in comparison to *Inga leonis* (Fig. 10) where the pattern of size classes is very different. Again this is a relatively abundant tree with 13 stems per hectare, but the seedlings and saplings are equally rare. On the other hand we always must be aware that all this census studies indicate the situation at a distinct date and thus only indicate momentum situations.

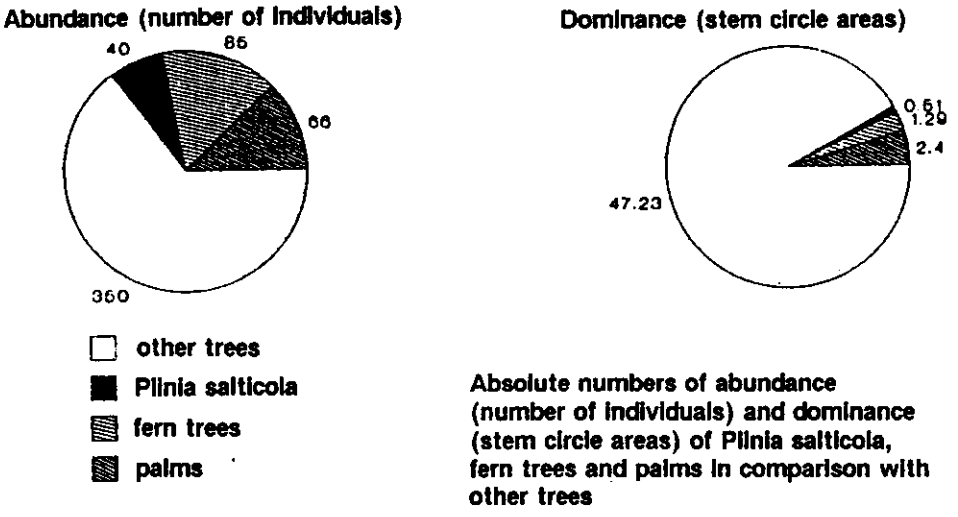

Fig. 11 : Absolute numbers of abundance (number of individuals) and dominance (stem circle areas) of *Plinia salticola*, fern trees and palm species in comparison with other trees (SPRENGER 1992)

Abundance and dominance of *Plinia salticola* is shown in comparison with palms and tree ferns in Fig. 11. There are many individuals but they are small, so abundance is relatively high but dominance is low, whereas e.g. *Elaeagia uxpanapensis* has only 3 stems per hectare but these are by far the largest trees with a stem diameter up to 2.3 m, thus dominance reaches 23 % at an abundance number of only 3 % (WATTENBERG & BRECKLE 1995). In lowland rain forest in kost examples it was shown that a few species are very abundant, but still many other species occur, as LIEBERMANN & LIEBERMANN (1978) have shown for the La Selva region, where *Pentaclethra* is very common and forms typical stands dominating canopy.

When looking for the distribution pattern of individuals it becomes important to know if the various age groups have an evenly, randomly or clumped distribution. In *Plinia salticola*, in *Inga leonis, Pterocarpus hayesii*, in the palms *Euterpe macrospadix, Iriartea deltoidea (= I. gigantea)* only seedlings and saplings exhibit a clumped distribution, older individuals are randomly distributed. However, especially in *Plinia salticola*, adult trees (≥ 8 cm DBH) have a maximum of density in regarding distance to the nearest Plinia neighbour with about 6 m, saplings are more concentrated in circles of smaller distance classes (Fig. 12). The population characteristics of the two important and rather abundant palm species *Iriartea deltoidea (I. gigantea)* and *Euterpe macrospadix* were studied by LEYERS & BRECKLE (1995). Alltogether there are some 27 palm species in the area (CHACON 1991).

It also may added here, that the phenology is controlled by the short "dry period". In *Plinia salticola* leaf shedding has a maximum in february, anthesis stops after january, fruiting time starts in february (Fig. 13). Fruits are cauliflorous and remain at the stem for a long time up to one year.

The Canopy and the Gap Mosaic

The crown canopy is very heterogenous, as it is shown by the profile (Fig. 14), as well as by a mapping of crown density of 1 hectar subdivided in 5 x 5 m plots (Fig. 15), where 8 crown density classes and their distribution is shown. There are several open spaces where crown density is less than 70 %. Smaller or larger gaps within the canopy are typical. It is not always clear whether these gaps come from trees falling apart or from old branches breaking down. Various sources of gap formation are discussed (WATTENBERG & BRECKLE 1995). The main reason is the break-down of large branches from old trees. Gaps remain open only for a few years. Successional phases seem to replace each other rapidly. Typical gap species are known, but the replacement of species is apparently very fast. The various gaps are very diffreent from each other, each gap has individual characterics, this was already shown in other areas by BRANDANI & al. (1988).

The nutrient situation was checked in some species. Most nutrients are available in sufficient concentrations from the volcanic soils of the Reserva slopes. Specific ion pattern in leaves from various species are investigated and results will come out soon.

Four *Columnea* species, which are very characteristic epiphytes on high trees were thoroughly studied by M. FREIBERG (1994), as well as the ecologcal conditions at the San Ramón Reserve, mainly microclimate of those high phorophytic trees (*Ficus jimenezii*). The microclimate has a distinct gradient from surface to the 40 m high crown of the tree. From the San Ramón Reserve some more preliminary data are available also on mineral cycling, role and distribution of nutrients (ORTIZ 1991, BULJOVCIC 1994, MOSER 1994). The epiphyllic cyanobacteria e.g. play a role in fixing of atmospheric N, which was estimated by an extrapolative calculation by E. FREIBERG (1994) to be about 2 - 7 kg N $\cdot ha^{-1} \cdot a^{-1}$. It would be interesting to know the other input and output fluxes of N of this system to have an idea of the total N-balance of this premontane rain forest ecosystem.

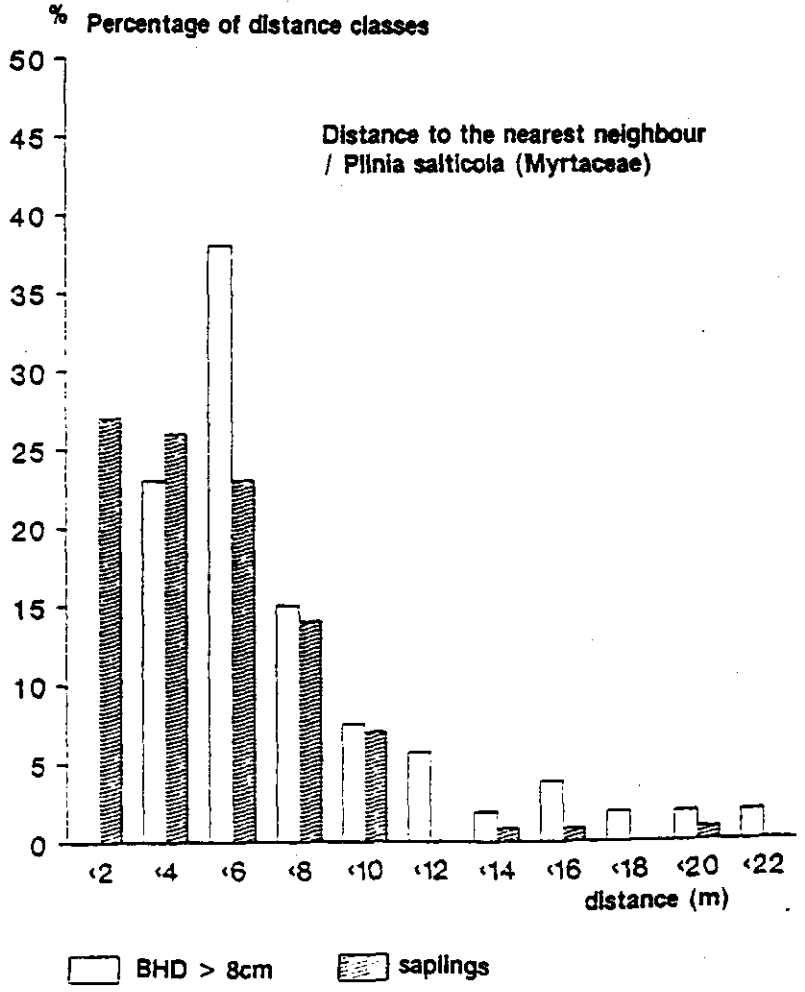

Fig. 12 : Percentage of distance classes of *Plinia salticola* seedlings and saplings (hatched bars) and adult trees (≥ 8 cm DBH) to the nearest neighbour (SPRENGER 1992)

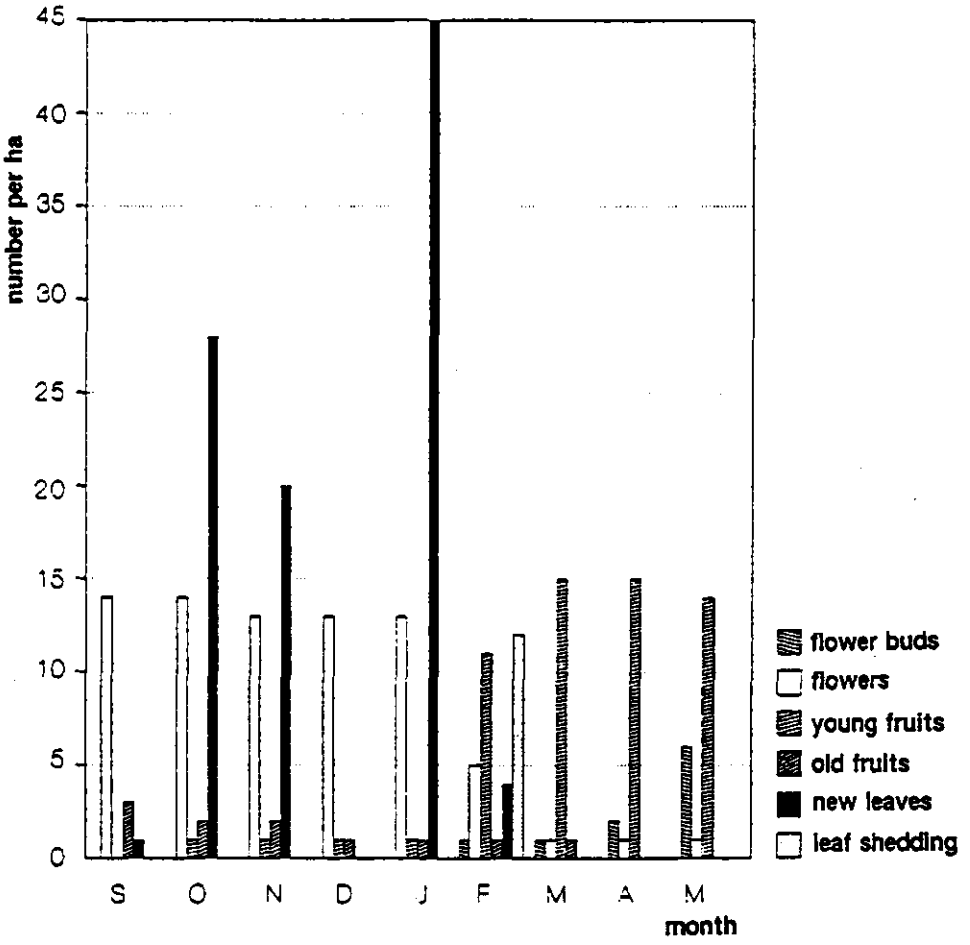

Fig. 13 : Observations on main phenological characteristics in *Plinia salticola* from september to may (SPRENGER 1992)

Fig. 14 : ==> see next page : Canopy structure shown by a profile of 40 m length (upper part) and crown pattern (lower part), *Plinia salticola* is in black (SPRENGER 1992). Numbers indicate the following species:
1: *Plinia salticola* (Myrtaceae); 2: *Iriartea gigantea* (Areaceae); 3: *Cyathea delgadii* (Cyatheaceae); 4: *Elaeagia uxpanapensis* (Rubiaceae); 5: *Elaeagia auriculata*; 6: NN (Rubiaceae); 7: *Guarea glabra* (Meliaceae); 8: *Ruagea glabra* (Meliaceae); 9: NN: (Melastomataceae); 10: *Swartzia* sp. (Fabaceae); 11: *Ouratea* sp. (Ochnaceae); 12: *Eugenia* sp. (Myrtaceae); 13: *Ocotea* sp. (Lauraceae); 14: *Virola* sp. (Euphorbiaceae); 15: *Styrax glabrescens* (Styracaceae); 16: *Coccoloba tuerckheimii* (Polygonaceae); 17: *Calatola costaricensis* (Icacinaceae); 18: NN; *: stump of *Iriartea gigantea*

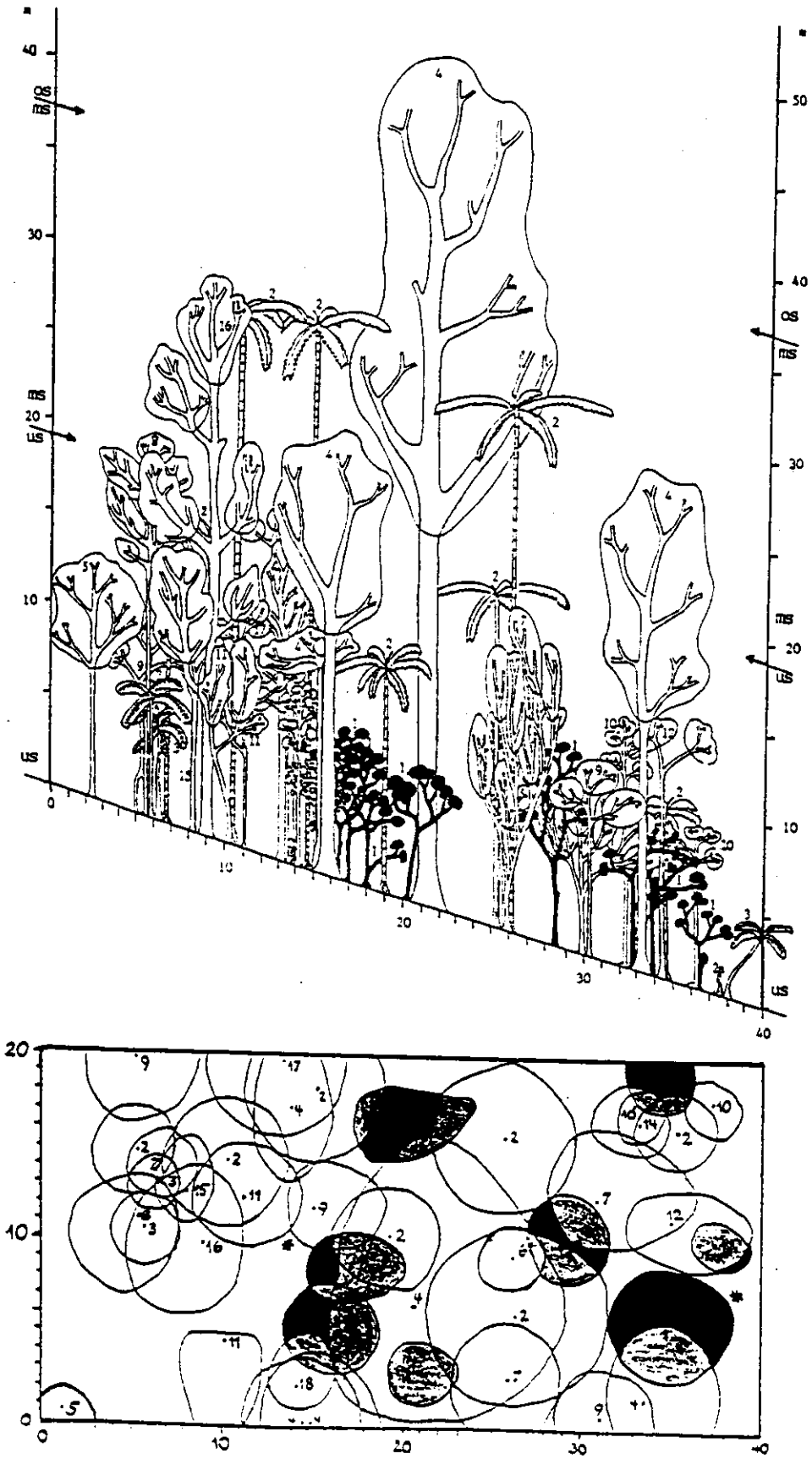

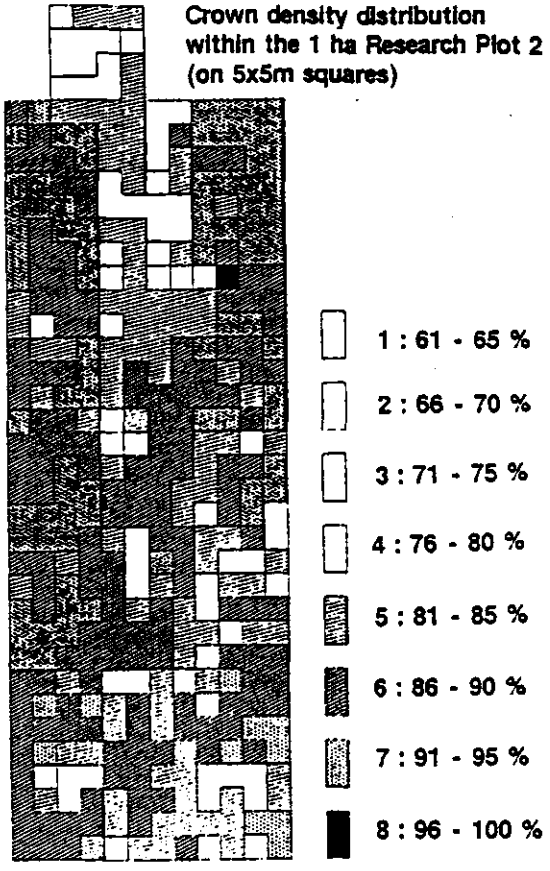

Fig. 15 :
Crown density distribution classes within 1 ha (5x5 m squares) (SPRENGER 1992)

Diversity

To characterize diversity it needs inventories of the various groups of organisms. The large trees (≥ 10 cm BHD) have about 400 - 500 stems per hectare comprising 94 species. 36 % of the tree species occur with a single stem per hectar. It is, however, very clear in regarding the species-area-relationship (WATTENBERG & BRECKLE 1995) that 1 hectar is by far not enough to have a complete inventory of tree species. The other life-forms are not yet studied in detail. From the whole area, from the Rio San Lorencito valley about 700 plant species (Angiospermae) are known at the moment (see list by GOMEZ & ORTIZ 1992), but this list is certainly still very incomplete, there might be more than 1200 species of Angiospermae, including all epiphytes, orchids etc. . Ferns are studied but a complete inventory is still lacking. There are certainly more than 100 fern species in the area (pers. comm. J.BITTNER, BITTNER & BRECKLE 1995). For Costa Rica as a whole the diversity is tremendous in comparison to more northern countries, especially on an area base (TANGLEY 1990). This is also true for species census in a lowland rain forest in Costa Rica (WHITMORE et al. 1985). This immense richness in species raises the question, how the reproductive processes, the pollination and seed dispersal is functioning in the various species, especially in those many rare species. which occur in small numbers of individuals with great distances from each other.

General and ecological conclusions

It is obvious that we know many but small details from the various organisms of the tropical rain forest. We know much less from the ecosystem functions, even we see some of the complex structure within the heterogenous canopy. The methodological difficulties in

studying tropical rain forests with tree heights of more than 40m and with a very diverse flora makes it almost impossible to do ecosystems studies to measure productivity, leaf area ratios, root turnover etc. Despite the rapid dynamics and fast turnover rates e.g. in decomposition of litter on the ground, a long time axis, long observation periods are necessary to investigate reproductive cycles or even only the faith of distinct gaps within canopy which normally play a major role in succession dynamics and replacement of trees. Reproductive strategies of the main canopy trees are almost unknown.
Growth, photosynthesis characteristics, C- allocation, water budget, nutrient cycling, food chain processes, energy turnover etc. and many other necessary processes as part of an ecosystems biology approach are almost unknown. Many of the main ecosystem processes are not measured, only speculation from qualitative observations are available, but still it is obvious that in the premontane rain forest area an almost unique ecosystem is functioning in a fascinating way.

Acknowledgements and Cooperation

The following members of the working group on "Tropical Ecology" at the Department of Ecology have contributed to the research programme and to this outline. Their help is greatly acknowledged.

Ingrid WATTENBERG (Bielefeld, Dissert. in preparation): Untersuchungen zur Populationsdynamik "dominanter" Waldbaumarten und Bedeutung der "gap"-Strukturen im tropisch montanen Regenwald der Cordillera de Tilarán im Umfeld der Biologischen Station San Ramón (Costa Rica)

Dr. Jens BITTNER (Ulm/Bielefeld): Untersuchung von Epiphytengesellschaften auf Baumfarnen in Costa Rica. Ph.D.Thesis 1994/95, 143pp.

Astrid SPRENGER (Hohenheim/Bielefeld): Populationsökologische Untersuchung von *Plinia salticola* (Myrtaceae) im prämontanen Regenwald der Cordillera de Tilarán.- Dipl. Arb. 1992, 107 pp.

Claudia LEYERS (Bielefeld): Populationsökologische Untersuchung von Palmenarten im prämontanen Regenwald der Cordillera de Tilarán im Umfeld der Biolog. Station San Ramón (Costa Rica).- Dipl. Arb. 1993, 72 pp.

Bettina RÖMICH (Bielefeld): Populationsökologische Untersuchung (*Inga, Pterocarpus*) und Floristische Bestandsaufnahme im prämontanen Regenwald der Cordillera de Tilarán im Umfeld der Biolog. Station San Ramón.- Dipl. Arb. 1993, 107 + ca.10 pp.

Zaklina BULJOVCIC (Bielefeld): Untersuchungen der Nährstoffgehalte in Blättern von Baumarten im prämontanen Regenwald der Cordillera de Tilarán im Umfeld der Biolog. Station San Ramón (C. R.).- Dipl. Arb. 1994, 92 + 14 pp.

Claudia WEBER (Oldenburg/Bielefeld): Untersuchungen der Nährstoffgehalte in Blättern der Baumfarne im prämontanen Regenwald der Cordillera de Tilarán im Umfeld der Biol. Stat. San Ramón (C.R.).- Dipl.Arb. 1994, 89 + 26 pp.

Petra MOSER (Oldenburg / Bielefeld): Untersuchungen der Nährstoffgehalte im Boden in gaps und im Bestand im prämontanen tropischen Regenwald der Cordillera de Tilarán im Umfeld der Biolog. Station San Ramón (Costa Rica).- Dipl. Arb. 1994, 48 + 24 pp.

Jens BIRKELBACH (Bielefeld): Untersuchungen der Nährstoffgehalte in Blättern von Baumarten im prämontanen Regenwald der Cordillera de Tilarán im Umfeld der Biolog. Station San Ramón (Costa Rica).- Dipl.Arb. (in preparation)

Sigrid SCHROERS (Bielefeld) and Anja SCHEFFER (Bielefeld): Dipl. Arb. 1995 in preparation

The help of the Costa Rican counterparts, Prof. Rodolpho ORTIZ, Victor, Roy and Hugo, and many others, who helped in many respects and who solved many problems to improve the infrastructure at the Biological Station in the Reserva, their help and hospitality is greatly acknowledged.

References

BITTNER,J. & BRECKLE,S.-W. 1995 : The growth rate and age of tree fern trunks in relation to habitats of the Sierra de Tilaran / Costa Rica.- Americ. Fern Journal (in press)

BOZA,M. 1989 : Parques Nacionales de Costa Rica.- Fundacion Tinker 112 pp.

BRANDANA,A., HARTSHORN,G.S. & G.H.ORIANS 1988: Internal heterogeneity of gaps and species richness in Costa Rican tropical wet forest.- J. Trop. Ecol. 4 : 759-771

BRECKLE, S.-W. 1993: Erfahrungen mit tropenökologischen Arbeiten in Costa Rica an der Biologischen Station in der Reserva Forestal de San Ramón.- in BARTHLOTT,W. et al.: "Animal-Plant-Interactions in Tropical Environments. Results of the Annual Meeting of the German Society for Tropical Ecology (Bonn, Febr. 1992), 175-180

CHACON, I. 1991 : Clave de palmas para la Reserva Forestal de San Ramón.- in: ORTIZ,R. Mem. de Investig.Reserva For.San Ramón. Universidad de Costa Rica (UCR), Coordinacion de investigacion, 37-40.

FREIBERG, E.R. 1994: Stickstoffixierung in der Phyllospäre tropischer Regenwaldpflanzen in Costa Rica.- Diss. Univ. Ulm 123 pp.

FREIBERG, M. 1994: Phänomorphologie epiphytischer Gesenriaceen in Costa Rica unter besonderer Berücksichtigung des Mikroklimas.- Diss. Univ. Ulm 146 pp.

GOMEZ,J. & R.ORTIZ 1991 Lista preliminar de plantas de la Reserva Forestal de San Ramón. in: ORTIZ,R. Mem. de Investig.Reserva For.San Ramón. Universidad de Costa Rica (UCR), Coordinacion de investigacion, 23-36.

JANZEN,D.H. (ed.) 1991: Historía natural de Costa Rica.- Edit. UCR San José, 822 pp.

LEYERS,C. & S.-W.BRECKLE : Population Studies on palm tree species in the premontane rain forest at the Biological Reserve San Ramón, Costa Rica. (in preparation)

LIEBERMANN,D. & M. LIEBERMANN 1978: Forest tree growth and dynamics at La Selva, Costa Rica (1969-1982).- J.Trop. Ecol. 3 : 347-358

ORTIZ, R. 1991 : Distribución de nitrogeno, fósforo y potasio en un bosque primario de la Reserva Forestal de San Ramón.- in: ORTIZ,R. Mem. de Investig.Reserva For.San Ramón. Universidad de Costa Rica (UCR), Coordinacion de investigacion, 49-55.

S.E.P.S.A. 1984 Land use Map 1 : 200.000

TANGLEY,L. 1990 : Cataloging Costa Rica's diversity.- BioScience 40: 633-636

TERBORGH, J. 1992 Diversity and the tropical rain forest.- The Scient. American Library. Freemann/New York

VARGAS, G. 1991 : Algunas consideraciones geográficas, geológicas y ecológicas de La Cuenca del Río Lorenzo, San Ramón, Alajuela, Costa Rica.- in! ORTIZ,R. Mem. de Investig. Reserva For. San Ramón. Universidad de Costa Rica (UCR), Coordinacion de investigacion, 17-22.

WALTER,H. & S.-W.BRECKLE 1991 Ökologie der Erde, Bd. 1 (2.Aufl.).- Fischer/Stuttgart 238p.

WATTENBERG, I. & S.-W.BRECKLE 1995 : Tree species diversity in a premontane wet forest in the Reserva Forestal de San Ramon/Costa Rica.- Ecotropica 1: ..... (in press)

WHITMORE,T.C., PERALTA,R. & K.BROWN 1985 : Total species count in a Costa Rican tropical rain forest.- J. Trop.Ecol. 1 : 375-378